CRTD/DFG – Center for Regenerative Therapies Dresden
Technische Universität Dresden
Direktor: Prof. Ezio Bonifacio, PhD

Photoreceptor transplantation into the mammalian retina
–
new perspectives in donor-host interaction

Dissertationsschrift

Zur Erlangung des akademischen Grades
Doctor of Philosophy (Ph.D.)
vorgelegt
der Medizinischen Fakultät Carl Gustav Carus
der Technischen Universität Dresden

von

MSc Sílvia Llonch Armengol

aus Barcelona

Dresden 2018

1. Gutachter: Herr. Prof. Dr. Marius Ader

2. Gutachter: Herr. Prof. Dr. Richard Funk

Tag der mündlichen Prüfung: ……14. 12……, 2018

gez.:----------

Vorsitzender der Promotionskomission

A la meva família,
especialment als meus pares, Mercè i Carles, i al meu germà Toni.

Acknowledgements

The work and effort required to bring to completion a PhD thesis involves always several people, and here I would like to thank everyone who, in one way or another, helped me to achieve this goal.

First, I would like to thank my mentor and supervisor, Prof. Dr. Marius Ader, for entrusting me and giving me the chance to work in his laboratory, encouraging me to bring my ideas to experiments and helping me to grow as a scientist. Furthermore, I would like to thank all the people who is/has been part of the Ader lab along the four years of my PhD, especially Jochen, Tiago, Oliver, Sylvia, Klaudia and Lynn. Thank you for giving me a hand with anything I needed, teaching me, discussing my experimental designs and results, giving me constructive feedback whenever I needed and helping me with all the German paperwork. But most importantly, thank you for the great working atmosphere and the daily positive mood you provided.

Second, I would like to thank my Thesis Advisory Committee, Prof. Dr. Elisabeth Knust and Dr. Mike O. Karl, for the inspiring scientific discussions and their advice on how to orient the projects I have been working on.

Next, I would like to thank all the people who supported me with the experimental work, including the Imaging Facility (especially Ruth), the FACS Facility (Anne, Katja and Erwin), and the ES/iPS Facility (Shery and Katrin). Furthermore, I would like to thank Cristina Golfieri for teaching me how to grow retinal organoids and for helping me to establish this culture technique in the lab. I would also like to thank Anne Eugster for helping me to establish the protocols for single cell analysis and Dr. Mike O. Karl for providing two of the mouse ESC lines used in this PhD thesis.

I would also like to thank the ProRetina foundation, the Deutsche Forschungsgemeinschaft (DFG) and the DIGS-BB for financially supporting me or the projects I have been involved in.

On a more personal level, I would like to thank all my friends. To the ones at home, especially Marta, Anna, Anabel, Laia(s), Gemma and Cristina, I would like to thank you for being there and to make me feel that despite the distance, nothing changed in our friendship. I really appreciate this. To the ones here in Dresden, especially Jelena (my roomie!), Cátia, Chiara, Alice, Dora and Leila. I would like to thank you all for the time we spent together, from lazy movie nights to crazy parties, and for your patience and support when I had a bad day. We have experienced together the good and dark sides of a PhD and it was great to have such a

group in which to find support during these four years. I am sure that the Dresden experience would not have been the same without you! I would also like to thank the catalan and spanish crew here in Dresden, it was a pleasure to have those nights with our beloved food, some wine and the possibility to express ourselves in our languages. I would also like to thank all the people who I met in Dresden and made those four years a very enjoyable experience, including after-work beers, barbecues, and many dancing evenings.

Finalment, vull agrair a la meva família tot el seu suport des del moment que vaig arribar en aquest món. Moltes gràcies per tota l'educació i l'amor que m'heu donat al llarg de la meva vida, que m'han convertit en la persona que sóc avui i m'han permès arribar fins aquí. Gràcies per creure en mi i fer-me costat en les decisions que he anat prenent, encara que algunes, com el fet de marxar a viure a fora, hagin representat un gran esforç per part vostra.

Abbreviations

AAV	Adeno-Assocciated Virus
AC	Amacrine Cells
AMD	Age-related Macular Degeneration
APC	Allophycocyanin
ARVO	Association for Research in Vision and Ophthalmology
β-ME	β-Mercaptoethanol
BSA	Bovine Serum Albumin
BC	Bipolar Cells
CD73	Cluster of Differentiation 73
Cpfl1	Cone Photoreceptor Function Loss 1
dapB	Dihyrdodipicolinate reductase, *B. subtilis*
DAPI	4',6-diamidino-2-phenylindole
DAPT	N-[N-(3,5-Difluorophenacetyl)-L-alanyl]-S-phenylglycine t-butyl ester
DEPC	Diethyl Pyrocarbonate
DMEM	Dulbecco's Modified Eagle Medium
DMSO	Dimethyl sulfoxide
EdU	5-Ethynyl-2'-deoxyUridine
EFTF	Eye Field Transcription Factor
eGFP	enhanced Green Fluorecent Protein
ERG	Electroretinogram
FACS	Fluorescence Activated Cell Sorting
FCS	Fetal Calf Serum
FISH	Fluorescent *in situ* hybridization
GC	Ganglion Cells
GCL	Ganglion Cell Layer
GMEM	Glasgow Minimum Essential Medium
HC	Horizontal Cells
hESC	Human Embryonic Stem Cells
IHC	Immunohistochemistry
ILM	Inner Limiting Membrane
INL	Inner Nuclear Layer
IPL	Inner Plexiform Layer
IRBP	Interphotoreceptor Retinoid-Binding Protein
IS	Inner Segments
KSR	KnockOut Serum Replacement
LIF	Leukemia Inhibitory Factor

MACS	Magnetic Activated Cell Sorting
MG	Müller Glia
mESC	Mouse Embryonic Stem Cells
mRNA	Messenger RNA
mTmG	membrane tdTomato, membrane GFP
NaPyr	Sodium Pyruvate
NEA	Non Essential Aminoacids
NR	Neural Retina
Nrl	Neural Retina Leucine zipper
OLM	Outer Limiting Membrane
ONL	Outer Nuclear Layer
OPL	Outer Plexiform Layer
OS	Outer Segments
OV	Optic Vesicles
P4	Post-natal day 4
PBS	Phosphate Buffered Saline
PFA	Paraformaldehyde
PGK	Phosphoglycerate Kinase
PhAM	Photo-Activatable Mitochondria
PI	Propidium Iodide
Polr2a	Polymerase RNA II polypeptide A
PR	Photoreceptors
PSC	Pluripotent Stem Cells
RMM	Retinal Maturation Media
RNA	Ribonucleic Acid
RP	Retinitis Pigmentosa
RPE	Retinal Pigment Epithelium
RT	Room Temperature
SRS	Sub-retinal space
SSC	Saline-Sodium Citrate

List of figures

List of tables

Abstract

Human senses are specifically designed to recognize and understand the world that surrounds us. Even though we have five senses, vision alone is responsible for at least 30 % of the sensory input to our brain. The visual process is initiated in a highly specialized cell type, the photoreceptors. These are light-sensitive cells located in the retina, a layered nervous tissue situated at the back of the eye.

Retinal degeneration diseases are a highly heterogeneous group of conditions that include mutations affecting the survival, maintenance and proper functioning of photoreceptors or the adjacent retinal pigment epithelium (RPE). Such mutations, alone or in combination with environmental factors, cause the loss of the affected cells, and therefore, impairment of the visual sense. Retinitis Pigmentosa and Age-related Macular Degeneration are typical examples of retinal degenerative diseases eventually leading to blindness. In the first one, rod photoreceptors degenerate and consequently also cone photoreceptors are lost. The second is characterized by malfunction and loss of both, RPE and photoreceptor cells.

Many current therapeutic approaches for the treatment of retinal degenerative diseases focus on slowing down the progression of the disease, rather than restoring the visual function. Currently, new therapies with the potential to recover the visual signal are under development. Some of these therapeutic strategies have already reached clinical stages, including gene therapy or retinal prosthesis. However, gene therapy approaches require the presence of remaining photoreceptors and, furthermore, particular targeting of disease-related genes. Retinal prosthesis still require improvement in terms of long-term biocompatibility and relevant visual function recovery. An alternative strategy for vision restoration is cell replacement of the lost photoreceptors, which is potentially suitable for targeting late stages of retinal degeneration diseases, independently of the inherent cause of the disease.

Human vision relies primarily on cone photoreceptors, which are the cells responsible for color and high acuity vision under daylight conditions. However, cones represent a minority of the photoreceptors within the retina, and so, due to the low availability of these cells, cone photoreceptor transplantation studies lag behind rod transplantation studies. Consequently, in this study, strategies to increase the numbers of cone photoreceptors within mouse embryonic stem cells (mESC)-derived retinal organoids, which represent a potential cell source for transplantation studies, were explored. In this regard, I manipulated developmental pathways known to be involved in retinal development, such as Notch signaling, through the addition of various compounds in the retinal organoid maturation media. However, early cone markers have not yet been definitively identified, complicating the detection and isolation of cone

photoreceptor precursors within the organoids. Therefore, a new early cone-reporter mESC line was generated in the course of this study as a valuable tool with the potential to facilitate the development of novel cone photoreceptor replacement therapies.

Equally important in the field of photoreceptor cell replacement is the understanding of how the transplanted donor cells interact with the host retina. Previous studies have shown that visual function improvement is possible after transplanting rod or cone-like photoreceptor precursors into the sub-retinal space of mouse models for retinal degeneration. For many years it has been assumed that the underlying mechanism for the observed vision improvement was the migration and structural integration of donor cells into the host outer nuclear layer, where they mature and establish synaptic connections with the host retinal circuitry. However, experiments performed in this study demonstrate, for the first time, that upon transplantation donor and host photoreceptors exchange cytoplasmic material rather than structurally integrate into the host outer nuclear layer. Furthermore, insights into the transferred cytoplasmic content are given, i.e. that mRNA, but not mitochondria are exchanged by donor and host photoreceptors. This novel way of photoreceptor-photoreceptor communication led to a paradigm change in the field of retinal transplantation, requiring a re-interpretation of former transplantation studies. In addition, the discovery of the material transfer phenomenon might serve as a starting point for the development of novel therapeutic strategies based on cell-cell support for the treatment of retinal degenerative diseases.

This study generated new knowledge in two important topics related to the development of cell therapies for retinal degeneration diseases, including the development of tools for cone transplantation studies as well as elucidating the interaction between donor and host cells upon transplantation.

Zusammenfassung

Die menschlichen Sinne sind spezifisch dafür konzipiert, die uns umgebende Welt zu erkennen und zu verstehen. Obwohl wir fünf Sinne haben, ist das Sehen allein für 30 % der sensorischen Informationen verantwortlich, die unser Gehirn erreichen. Der Prozess des Sehens wird in einem hoch spezialisierten Zelltyp initiiert – den Photorezeptoren. Dabei handelt es sich um lichtempfindliche Zellen in der Netzhaut, dem in Schichten aufgebauten Nervenzellgewebe im hinteren Bereich des Auges.

Degenerationserkrankungen der Netzhaut haben stark heterogene Ursachen, wie Mutationen die das Überleben, die Versorgung oder die korrekte Funktion der Photorezeptoren und des angrenzenden RPE beeinflussen. Solche Mutationen führen allein oder in Kombination mit Umweltfaktoren zum Verlust der betroffenen Zellen und dadurch zur Beeinträchtigung des Sehsinns. Beispiele für Degenerationserkrankungen der Netzhaut, die schlussendlich zur Erblindung führen, sind die Retinitis pigmentosa, bei der die initiale Stäbchenphotorezeptor-Degeneration in späteren Stadien ebenfalls zum sekundären Verlust der Zapfenphotorezeptoren führt, oder die altersbedinge Makuladegeneration, die durch die Fehlfunktion und den Verlust von RPE und Photorezeptorzellen charakterisiert ist.

Viele aktuelle therapeutische Ansätze zur Behandlung von Degenerationserkrankungen der Netzhaut konzentrieren sich auf das Verlangsamen des Krankheitsverlaufs, anstatt Sehfähigkeit wiederherzustellen. Momentan werden neue Therapien entwickelt, um Sehfähigkeit zurückzugewinnen. Einige dieser therapeutischen Strategien befinden sich bereits in klinischen Studien, wie gentherapeutische Ansätze oder retinale Prothesen. Allerdings setzen gentherapeutische Ansätze noch vorhandene Photorezeptoren voraus und müssen für einzelne krankheitsrelevante Gene zugeschnitten werden. Retinale Prothesen hingegen müssen noch hinsichtlich ihrer mechanischen Langlebigkeit und relevanter Verbesserungen der Sehfähigkeit optimiert werden. Eine alternative Strategie für die Wiederherstellung von Sehfähigkeit stellt der Zellersatz verlorener Photorezeptoren dar, welcher potentiell auch in späten Stadien retinaler Degenerationserkrankungen angewendet werden kann.

Das menschliche Sehen beruht primär auf Zapfenphotorezeptoren – die Zellen, die für das Farbsehen und scharfe Sehen unter Tageslichtbedingungen verantwortlich sind. Allerdings machen Zapfen nur eine Minderheit aller Photorezeptoren in der Netzhaut aus. Durch ihre geringe Verfügbarkeit müssen Transplantationsstudien mit Zapfenzellen noch zu denjenigen mit Stäbchenzellen aufschließen. Daher haben wir in dieser Studie Strategien untersucht, um die Anzahl von Zapfenphotorezeptoren in retinalen Organoiden aus murinen embryonalen

Stammzellen (mESZ) zu erhöhen, die eine potentielle Zellquelle für Transplantationsstudien repräsentieren. Zu diesem Zweck haben wir Entwicklungsbahnen durch den Zusatz verschiedener Wirkstoffe im Wachstumsmedium der retinalen Organoide manipuliert, deren Einfluss in der Netzhautentwicklung als gesichert gilt, wie dem Notch-Signalweg. Allerdings wurden bislang keine definitiven frühen Zapfenmarker identifiziert, was die Detektion und Isolation von Zapfenphotorezeptor-Vorläuferzellen innerhalb der Organoide erschwert. Daher wurde im Zuge dieser Studie eine neue mESZ-abgeleitete Zapfen-Reporterlinie generiert, die ein nützliches Werkzeug darstellt, mit dem Potential, die Entwicklung neuer Zapfenphotorezeptor-Ersatztherapien zu ermöglichen.

Im gleichen Maß wichtig auf dem Feld des Photorezeptorersatzes ist das Wissen um die Art der Interaktion zwischen transplantierten Spenderzellen mit der Empfängernetzhaut. Frühere Studien konnten eine Verbesserung der Sehfähigkeit nachweisen, nachdem Stäbchen und Zapfenartige Photorezeptorvorläuferzellen in den subretinalen Raum von Mausmodellen für Netzhautdegeneration transplantiert wurden. Viele Jahre wurde angenommen, dass der zugrundeliegende Mechanismus für die beobachteten Sehverbesserungen die Migration und strukturelle Integration der Spenderzellen in die Photorezeptorschicht des Empfängers sei, inklusive der anschließenden Reifung und dem Aufbau synaptischer Verbindungen mit dem Netzhautnetzwerk des Empfängers. Allerdings konnten Experimente der hier vorliegenden Studie zum ersten Mal demonstrieren, dass Spenderphotorezeptoren mit Empfängerphotorezeptoren nach Transplantation Zytoplasmamaterial austauschen, anstatt strukturell in die Photorezeptorschicht des Empfängers zu integrieren. Des Weiteren konnten Erkenntnisse über den Charakter des transferierten Materials gewonnen werden: mRNA, aber keine Mitochondrien werden zwischen Spender- und Empfängerphotorezeptoren ausgetauscht. Dieser neue Weg der Photorezeptor-Photorezeptor-Kommunikation hat zu einem Paradigmenwechsel auf dem Feld der retinalen Transplantation geführt und verlangt eine Neuinterpretation früherer Transplantationsstudien. Darüber hinaus könnte die Entdeckung des Phänomens des Material-Transfers als Startpunkt für die Entwicklung neuer therapeutischer Strategien dienen, die auf der Zell-Zell-Unterstützung für die Behandlung von degenerativen Netzhauterkrankungen basieren.

Diese Studie konnte neue Erkenntnisse in zwei wichtigen Bereichen der Entwicklung von Zelltherapien für retinale Degenerationserkrankungen generieren, nämlich bei der Entwicklung von Werkzeugen für Zapfen-Transplantationsstudien als auch die Aufklärung der Interaktion zwischen Spender- und Empfängerzellen nach Transplantation.

Chapter 1:

General introduction

1.1 The eye

Animals live in a world of constantly changing sensory stimulation, and therefore, developed five different senses, including vision, to capture this information. In fact, between 30 and 40 % of the cerebral cortex is dedicated to processing visual inputs. The organ responsible for vision is the eye, which is thought to have appeared for the first time around 540 M years ago, when the animal body plan began to rapidly evolve. It is thought that the vertebrate camera-like eye, like ours, evolved around 500 M years ago (Lamb et al., 2007). The eye is such a complex organ that even Darwin doubted it could have evolved through natural selection (Lamb et al., 2007; Masland, 2012). Animals that have developed an eye are not only able to detect the features of objects surrounding them, such as colors but also orientation, motion and distances.

The gross anatomy of the eye is depicted in Figure 1. The light enters the eye through the pupil, with its size regulated by the iris, a colored circular muscle. In low light conditions, the size of the pupil enlarges, allowing for more light to enter the eye, and vice versa, bright light conditions lead to a smaller pupil size. The cornea is a transparent external surface covering both, the pupil and the iris, and together with the lens, are responsible for focusing the light onto the retina, which is the sensitive neural tissue located at the back of the eye, and will be described in more detail in the next section (1.2). The lens is suspended by ligaments known as zonule fibers. Lens accommodation, i.e. change of shape due to contraction/relaxation of the suspending ligaments, is involved in sharpening the image on the retina. Between the lens and the retina lies the vitreous, a gelatinous body that helps to maintain the eye's shape. Right behind the retina, a monolayer of epithelial cells known as retinal pigment epithelium (RPE) is found. Since the RPE function is highly linked to the well-being and functioning of the retina, it will also be described in the next section (1.2). At the outermost part of the eye lies the choroid, a pigmented tissue that contains the mesh of blood vessels responsible for nourishing the outer retina. Separating the RPE from the choroid there is the Bruch's membrane, a five-layered extracellular matrix of 2 – 4µm thickness. The entire eye is surrounded by the sclera, which supports the wall of the eyeball. Between the iris and the sclera lie the ciliary body cells, which secrete fluid into the eye in order to generate the intraocular pressure necessary to maintain eye shape (Kolb et al., 1995; Rodieck, 1998; Curcio and Johnson, 2013).

In a sagittal section of the human eye it is possible to distinguish three different layers, the most external one is composed by the cornea and the sclera. The intermediate layer can be divided into anterior, containing the iris and ciliary body, and posterior, containing the choroid. The most internal layer of the eye is mainly composed of the retina. Moreover, three different

fluid chambers are present in the eye. The anterior chamber, which is delimited by the cornea and the iris, and the posterior chamber, which represents the space between the iris and the lens, are filled with aqueous humor. The largest one, the vitreous chamber, is filled with vitreous humor and occupies the space between the lens and the retina.

Two pairs of rectus muscles and one pair of oblique muscles, all together known as extraocular muscles (not depicted in Figure 1), are responsible for holding and rotating the eyeball within the orbital cavity, allowing for the image to be constantly focused on the fovea (Kolb et al., 1995).

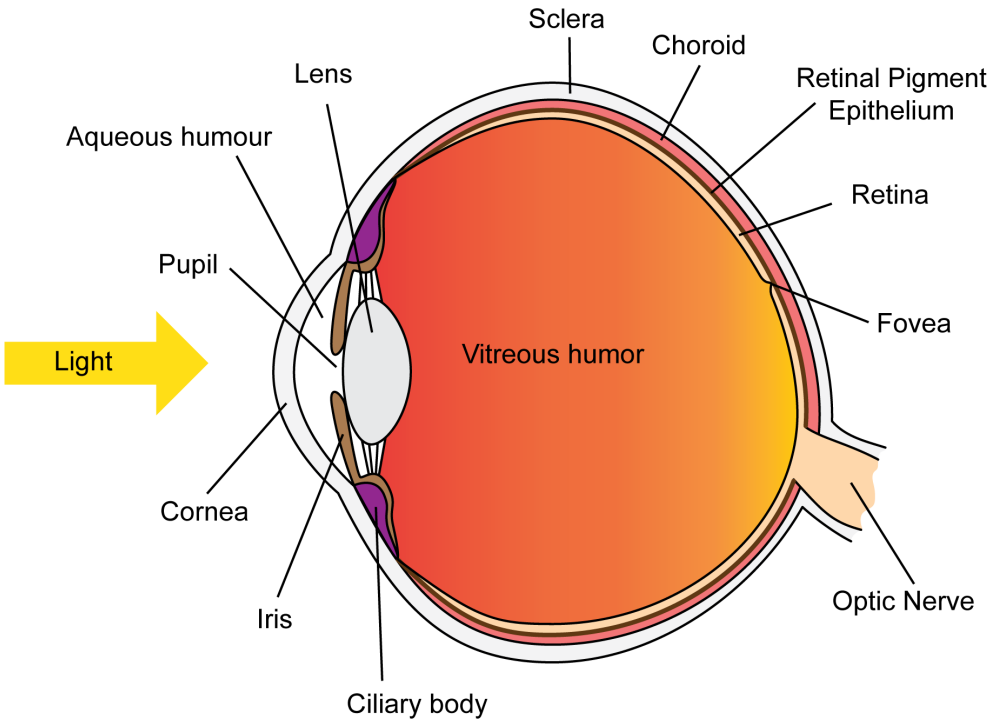

Figure 1. Schematic representation of the human eye. The light enters the eye through the pupil, which adapts its size according to the level of ambient light. Next, the lens focuses the incoming light onto the retina, where photons are captured and an electric signal is generated. This signal is collected and transported to the brain via the optic nerve.

1.2 The retina

The retina is a 0.4 mm thick nervous tissue that is localized at the back of the eye and is responsible for converting light into a visual signal that is transmitted to the visual cortex of the brain (Mustafi et al., 2009). Anatomically, it is a highly organized tissue containing six classes of neurons, including rod and cone photoreceptors, horizontal cells (HC), bipolar cells (BC), amacrine cells (AC) and ganglion cells (GC), and a type of radial glia cell, known as Müller glia

(MG) (Kolb et al., 1995). The different cell classes are organized in three nuclear layers, where cell bodies are located, and two plexiform layers, were synaptic connections between the different neurons are established (Rodieck, 1998).

The structure of the mammalian retina is represented in Figure 2. In this scheme, the retina is oriented from the innermost side (basal), which is in contact with the vitreous (bottom), to the outermost side (apical), which is in contact with the RPE (above). The nuclei of the photoreceptor cells (PR) form the outer nuclear layer (ONL). In the next nuclear layer, known as the inner nuclear layer (INL), the cell bodies of HC, BC and AC are found, together with the cell bodies of the MG cells, which give metabolic and structural support to the retina (Lamb et al., 2007). The last nuclear layer, the ganglion cell layer (GCL), contains the cell bodies of the GC. In between the ONL and the INL, lies the outer plexiform layer (OPL), in which photoreceptor cells establish their synaptic connections with the bipolar and horizontal cells. The inner plexiform layer (IPL) is found between the INL and the GCL and is where the synaptic connections between bipolar, amacrine and ganglion cells are established. On their apical processes, MG establish tight junctions with other MG cells or with PR, defining the outer limiting membrane (OLM). On the basal side, MG footplates, together with extracellular matrix (ECM) components such as collagen, glycosaminoglycan, laminin and fibronectin, compose the inner limiting membrane (ILM) (Kolb et al., 1995; Gelman et al., 2015). The space between the OLM and the RPE is named the interphotoreceptor matrix space (IPM) (Saari, 2012) or sub-retinal space (SRS) (Kolb et al., 1995). Here, specialized sub-cellular compartments of photoreceptors, the so called inner- (IS) and outer- (OS) segments, are located. The direction in which the light travels is depicted by a yellow arrow. The vertebrate retina is inverted, meaning that PRs, which are responsible for capturing the light, are located at the very end of the light path, thus, the light must pass through all retinal layers before reaching the PR outer segment, where photons are converted into a biological signal. This organization allows the metabolically very active PRs to be in close contact with the supporting RPE and the choriocapillaries, that supply nutrients and oxygen (Rodieck, 1998). Moreover, the RPE is essential for visual pigment regeneration during the visual cycle (see below).

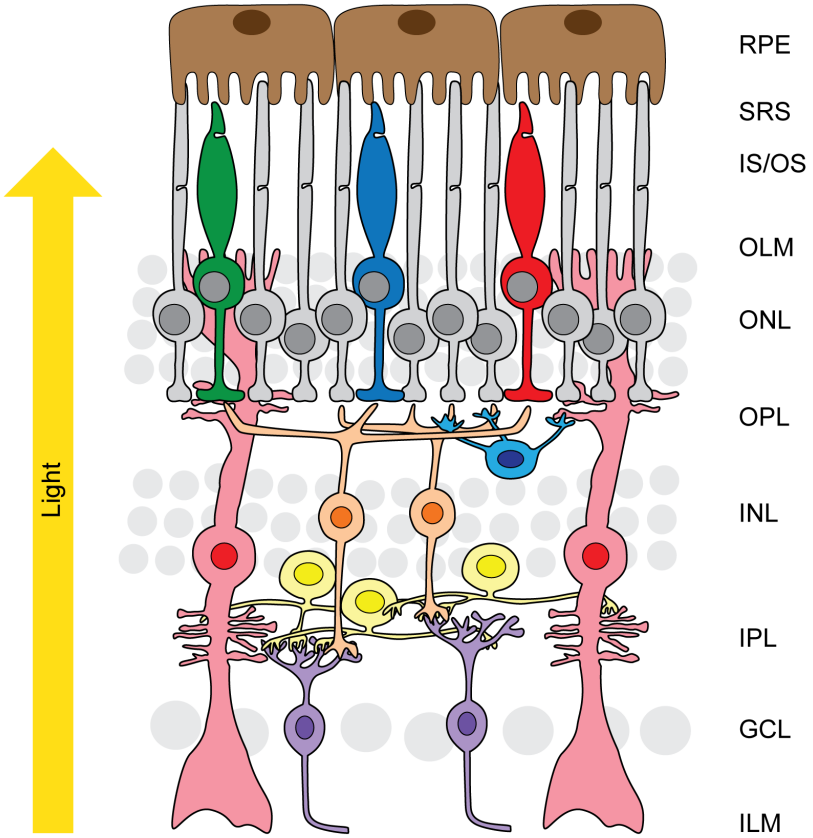

Figure 2. Schematic representation of the mammalian retina. The mammalian retinal structure is conserved across species. It consists of three nuclear layers (ONL, INL, GCL), where retinal cell bodies are located, and two plexiform layers (OPL, IPL), where synaptic connections are established. Müller glia cells delimitate the outer limiting membrane (OLM) and the inner limiting membrane (ILM). In the SRS, the photoreceptor inner and outer segments are surrounded by interphotoreceptor matrix. The light travels from the vitreous through the retina until it reaches the photoreceptor outer segments. RPE: retinal pigment epithelium, SRS: sub-retinal space, IS/OS: inner/outer segments, OLM: outer limiting membrane, ONL: outer nuclear layer, OPL: outer plexiform layer, INL: inner nuclear layer, IPL: inner plexiform layer, GCL: ganglion cell layer, ILM: inner limiting membrane.

As mentioned above, PR cells are responsible for capturing light and converting it into an electrical/molecular signal that will be transmitted to the brain via the axons of the GC. Photoreceptors are highly specialized neurons. They present an elongated shape and four distinct functional regions can be identified – the inner and outer segments, the cell body and the synaptic terminal (Figure 3, A). The outer segment (OS) contains stacks of membranes where the visual pigment is located, and it is precisely in these structures that the light is converted into an electrical signal. The inner segment (IS) contains the components necessary for photoreceptor metabolic functions, including mitochondria, ribosomes and membranes where the opsins are assembled. The IS and OS are connected by a cilium that is able to build the membranous stacks system. The cell body contains the nucleus, and the synaptic terminal is where the generated signal is transmitted to second order neurons (Kolb et al., 1995; Rodieck, 1998; Saari, 2012).

Despite having a similar basic structure, rods and cones present some differences in number (rods outnumber cones 20:1 in human and 35:1 in mouse), structure, distribution, visual pigment and connectivity that provide them with their specificity in responding to light (Mustafi et al., 2009). Rod photoreceptors are highly efficient in capturing single photons in low light conditions (scotopic vision) but saturate in high light intensities, and therefore, are responsible for vision in dim light conditions. Furthermore, rod photoreceptors have a very low spatial resolution. On the other side, cone photoreceptors have a high space resolution and, despite being less sensitive to light than rods, do not saturate at bright light conditions, and therefore, are responsible for high acuity and daylight vision (photopic vision). Recent data from Thomas Münch's laboratory, however, provides evidence against the classical concept that photopic vision is due to cone-only mediated response. They show that, in fact, rod photoreceptors are able to reverse saturation in photopic conditions and influence cone-derived responses through inhibition (Tikidji-Hamburyan et al., 2017).

In comparison to rods, for which just one visual pigment, rhodopsin, has been described, different cone visual pigments exist, each one able to capture light at a different wavelength, imparting cone photoreceptors with the ability to distinguish colors. Different species present distinct numbers and types of cone opsins, for example, most mammals are dichromatic, meaning that, besides rhodopsin (maximum sensitivity at 496 nm), they present two other types of opsin, one capturing light at long/medium wavelengths (L/M-cones) and one capturing light at short wavelengths (S-cones). Humans, instead, are trichromatic (Figure 3, C), presumably due to gene duplication, so our retinas present, besides rhodopsin, three other opsins. One has maximum sensitivity at long (red, 559 nm) wavelengths, one at medium (green, 531 nm) wavelengths and one at short (blue, 419 nm) wavelengths (Kolb et al., 1995). Morphologically, rod OS are long and thin, compared to cones, which present shorter OS in a conical-like shape. The rod membrane stacks are completely isolated from the cell membrane, while the cone membranous system is derived from invaginations of the ciliary membrane itself. Regarding distribution of photoreceptors along the retina, cone photoreceptors density is maximum at the center of the fovea (Figure 3, B). The fovea is a specialized region of the retina found in primates, including humans, that is more sensitive to detail due to a high density of cone photoreceptors, a 1:2:2 ratio of cone:BC:midget GC respectively, and a decrease of light scattering due to displacement of inner retinal layers and absence of vasculature (Bringmann et al., 2018). While other mammals also have similar retinal areas containing higher cone densities, known as area centralis or visual streak, they do not form a proper fovea. Rods density peaks at 5 mm from the fovea and then slightly decreases towards the retinal periphery. Interestingly, IS/OS of photoreceptor cells are smaller where the density is

higher, allowing a better packing of the cells (Figure 3, B) (Rodieck, 1998; Mustafi et al., 2009; Saari, 2012).

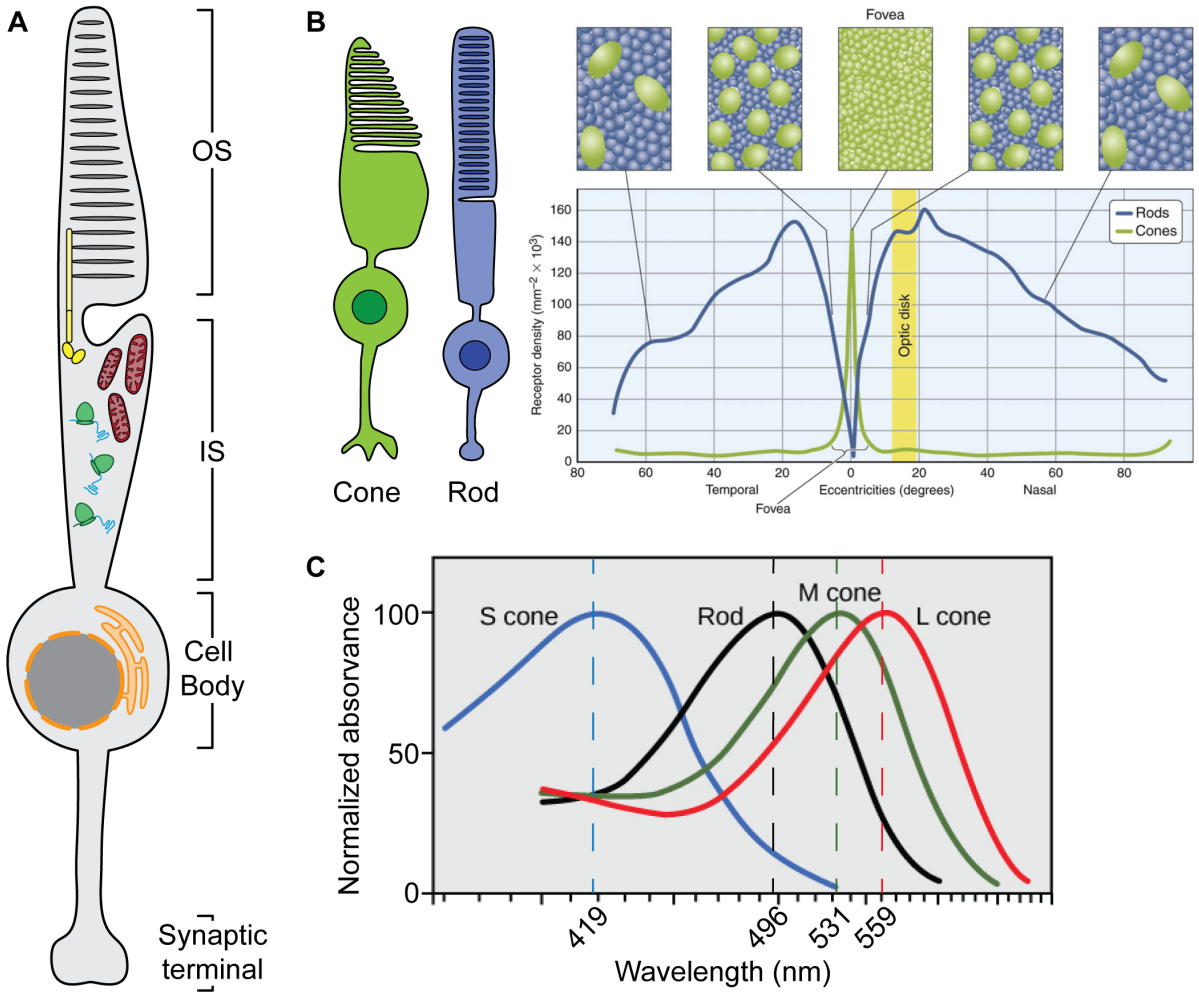

Figure 3. Photoreceptor cell structure and differences between rods and cones. A) Basic structure of a photoreceptor cell. The OS contain a stack of membranes where the visual pigments are located. The components required to satisfy the metabolic needs of the photoreceptor are found in the IS. The cell body contains the nucleus and the end of the axon represents the synaptic terminal. **B)** Structural and distribution differences between rod and cone photoreceptors. Cones (green) have shorter OS, and a thicker dimeter than rod photoreceptors (blue). The synaptic terminal of a cone cell is a large end-foot known as a cone pedicle, while the rod spherules represent an enlargement of the axon itself. Cone density peaks at the centre of the fovea, where cone diameter is smaller to allow a better packing of the cells. Rod density peaks at around 18 degrees (5 mm) from the fovea, and then decreases slowly. Rod diameter is also smaller where the density is higher (Adapted from Mustafi et al., 2009). **C)** The visual opsins of each photoreceptor cell type are slightly different in structure, allowing a maximum sensitivity at different wavelengths of the visual spectra. (Adapted from Lumen, 2013).

Functionally, the visual pigments of both rods and cones, consist of a chromophore, 11-*cis*-retinal, bound to an opsin protein through a Schiff base (Saari, 2012). The process by which photoreceptors convert light into an electrical signal is known as the phototransduction cascade and it is initiated by the isomerization of the 11-*cis*-retinal to all-*trans*-retinal due to photon absorption. This conformational change in the chromophore leads to the activation of

the opsin protein. Opsins are transmembrane proteins located within the membrane stacks of the photoreceptor OS. They comprise seven α-helical transmembrane domains and act as G-protein coupled receptors (Lamb et al., 2007). Upon activation, opsins bind to the G-protein transducin, which in turn, exchanges GDP for GTP and the α-subunit dissociates and activates a membrane-associated phosphodiesterase (PDE). PDE hydrolyses cyclic GMP (cGMP) to GMP, which leads to the closure of the cGMP-gated cation channels. Closure of these channels prevent cations (Na^+, Ca^{2+}) from entering the cell, which leads to a hyperpolarization of the photoreceptor, and in consequence, it reduces the release of glutamate neurotransmitter at the synaptic terminal. Thus, in dark conditions there is a continuous release of glutamate, which ceases upon light activation of the PR cell (Kolb et al., 1995; Mustafi et al., 2009).

For the photoreceptors to be able to respond to the subsequent incoming photons, all-*trans*-retinal must be isomerized back to 11-*cis*-retinal. Photoreceptors do not have the required enzymes for such a reaction, and therefore, the isomerization must take place somewhere else. The process of visual pigment regeneration is known as visual cycle. Briefly, all-*trans*-retinal is reduced to all-*trans*-retinol, which leaves the photoreceptor cell by an unknown mechanism. In the IPM, it is bound to the interphotoreceptor retinol-binding protein (IRBP) and transferred to the RPE. There, all-*trans*-retinol is esterified to retinyl ester and then converted to 11-*cis*-retinol by the isomerohydrolase RPE65. Next, 11-*cis*-retinol is oxidized to 11-*cis*-retinal and transported back to the photoreceptor through IRBP. Once in the photoreceptor cell, it can bind to the opsin and restore the visual pigment (Saari, 2012; Tsin et al., 2018). Regarding the visual cycle, rod and cone photoreceptors also present some differences. Rods obtain 11-*cis*-retinal exclusively from the RPE (rod visual cycle), however, cones can also replenish 11-*cis*-retinol from MG cells (cone visual cycle). The cone visual cycle is still not yet fully understood, but the possibility of obtaining recycled chromophore from both, RPE and MG, allows a faster regeneration of the visual pigment, as required in high light intensities (Saari, 2012).

Besides its critical role in the visual cycle, RPE has many other functions that make it essential in the light detection process. The RPE contains pigment granules that capture scattered light, facilitating high quality image formation. Moreover, RPE forms tight junctions in its lateral sides with other RPE cells, contributing to the blood-retina barrier. This allows a highly selective transport of substances between the choroid and the SRS and accounts, in part, for the immune privileged status of the eye. The RPE is also involved in metabolically supporting the photoreceptors and in OS renewal. Light reaching the OS initiates the process of vision, but simultaneously causes photo-oxidative damage. Therefore, daily shedding and phagocytosis of the damaged OS tips is required for maintenance of a healthy retina (Kolb et al., 1995).

The visual signal generated by the photoreceptors is processed within the retina before being transmitted to the brain. Photoreceptors transmit information to the inner retina through their synaptic endings, known as rod spherules or cone pedicles, which contact with BC and HC at the OPL. Rod spherules are small axon enlargements and are packed above cone pedicles, which are the large and flat (5-10 µm diameter) end-feet of cone PR (Figure 4). Both, rod spherules and cone pedicles present invaginations where synaptic ribbons are found. These structures serve as scaffolds for neurotransmitter-filled vesicles to accumulate. Each cone pedicle contains around 30 of these invaginating structures, each one connecting to one BC dendrite in the center and two HC dendrites in the laterals (Haverkamp et al., 2000; Masland, 2012). Therefore, the cone synapse is referred to as the cone triad. Furthermore, other types of bipolar cells that also synapse with cone pedicles establish basal synaptic connections, known as flat contacts. In contrast, each rod spherule presents only 2 ribbons, each one connecting to two central BC dendrites and 2 lateral HC processes (Kolb et al., 1995) (Figure 4).

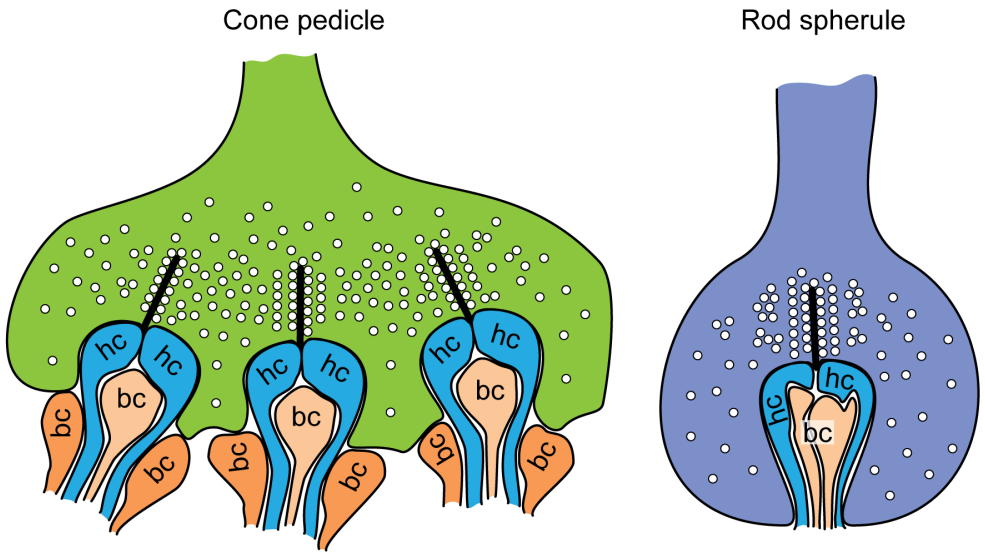

Figure 4. Schematic representation of cone pedicles and rod spherules. The synaptic terminals of both photoreceptors present ribbon synapses. However, in cone pedicles, each ribbon synapse consists of two horizontal cell dendrites and one ON-bipolar cell dendrite (light orange). OFF-bipolar cell processes (dark orange) connect with the cone pedicle in flat/basal contacts. In the rod spherule, the ribbon synapse contacts with two horizontal cell telodendritic processes and two bipolar cell dendrites. hc: horizontal cell, bc: bipolar cell.

Bipolar cells are either rod or cone specific, and therefore, the signal generated in rod photoreceptors will be processed in a rod-visual pathway, separated from the cone-generated signal, which will be processed in the more complex cone-visual pathway. There is one type of rod bipolar cell, while the number of cone bipolar cell types vary among different species. Humans, for example, present 10 cone bipolar cell types and mice have 11 different types

(Kolb et al., 1995; Rodieck, 1998; Masland, 2001, 2012). The different types of cone BC are defined regarding their shape, neurotransmitter receptors, calcium binding proteins, signaling pathways and synaptic partners, both in the OPL and IPL (Figure 5). Of particular interest are the ON and OFF cone bipolar cells. ON-bipolar cells present metabotropic glutamate receptors, such as mGluR6, which upon glutamate binding leads to the closure of the cation channel TRPM1. Thus, when light is absorbed by photoreceptors, glutamate release decreases, leading to the opening of TRPM1, and therefore, depolarization of the bipolar cell. In other words, ON-bipolar cells are activated with an increase of photons. Interestingly, ON-bipolar cells' dendrites are found in the invaginations of the cone triads and their axons are located at the inner half of the IPL. On the other hand, OFF-bipolar cells express AMPA and kainate receptors, which are actually cation channels that open with the presence of glutamate. Therefore, in response to light, which leads to a decrease of glutamate release by the photoreceptors, those channels close leading to hyperpolarization of this type of BC. Simplified, OFF-bipolar cells are active in the absence of light. As opposed to ON-bipolar cells, OFF-bipolars present flat contacts with cone PR and their axons synapse at the outer half of the IPL. ON and OFF bipolar cells are present in approximately equal numbers in the mammalian retinas, and both types can synapse with the same cone. In summary, differences in BC physiology are responsible for separating the cone output in ON and OFF channels at the first synapse, and this distinction is maintained along the entire retinal circuit (Kolb et al., 1995; Rodieck, 1998; Masland, 2001, 2012).

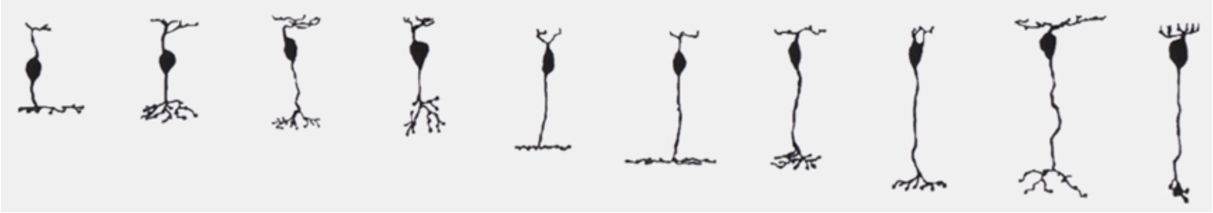

Figure 5. Bipolar cell types of a mammalian retina. The distinct bipolar cell types shown in this image are from work in the rat. Similar bipolar cells have been observed in other mammals, including rabbit, cat and monkey. Adapted from Masland, 2001.

The third cell class involved in the synaptic connections established in the OPL is the horizontal cell. Most mammalian species have two distinct types of horizontal cells (Figure 6), named HI and HII. The function of this cell class is to create the so-called center-surround effect. To do so, they extend lateral processes across the retina, receiving signals from and giving feedback to photoreceptors, thus, modifying the signal received by the BC in a process known as lateral inhibition. Moreover, each HC type is connected via gap junctions to other cells of the same type (Kolb et al., 1995). The fact that each PR establish synaptic contacts with different horizontal cells enables the transmission of information regarding spatial differences in light intensity within the image (i.e borders) (Rodieck, 1998; Masland, 2001). HI have a very long

axon that ends with a telodendritic arbor, responsible for synaptic connections with rod photoreceptors. The dendrites of HI cells contact cones (except S-cones). Due to the long axons of HI, the telodendritic arbor and the dendrites function as isolated units, so rod and cone responses are processed independently. HII establish synaptic connections with S-cones, as well as with M- and L-cones, but the influence of HII in M- and L-cones is minimum compared to HI (Rodieck, 1998).

Figure 6. Horizontal cell types. On the left, an exemplary HII horizontal cell type is represented. On the right, the morphological characteristics of an HI cell are represented, including a telodendritic arbor, a long axon and the dendrites close to the cell body. Adapted from Masland, 2001.

In the inner plexiform layer, bipolar cells synapse with amacrine cells and ganglion cells (Figure 7). The exact number of different types of both, amacrine and ganglion cells, is still under debate, however, it is estimated that there are at least 30 types of each cell class (Masland, 2012; Sanes and Masland, 2015; Baden et al., 2016). Functionally, each AC type seem to have a specific purpose, for example object motion detection. Considering that they release GABA or glycine, in general they are inhibitory to their post-synaptic partners. As for the rest of the retinal classes, amacrine cell types are distinguished according to their physiology as well as to their synaptic partners. Synaptically, AC can give feedback to BC, refining their response, contact other AC and contribute to the input signal GC require for firing. Interestingly, AC's dendritic arbors can branch in one or multiple levels of the stratified IPL. The ones presenting dendrites in different strata can actually exchange information between the ON and OFF pathways (Rodieck, 1998; Masland, 2001, 2012). The GC are the last retinal neuron before the signal is transmitted to the brain. Similarly to bipolar cells, ON or OFF ganglion cells can be distinguished, depending on the bipolar cell they synapse to. In addition, GC can also be ON-OFF, and therefore respond to both increases and decreases in light intensity. ON-OFF GC are generally responsible for distinguishing motion of a stimulus in a specific direction (Sanes and Masland, 2015). GC establish their synaptic connections with both BC and AC and therefore, their spike rate, which is the information that ultimately is transmitted to the brain, is influenced by both cell types (Rodieck, 1998; Masland, 2001, 2012).

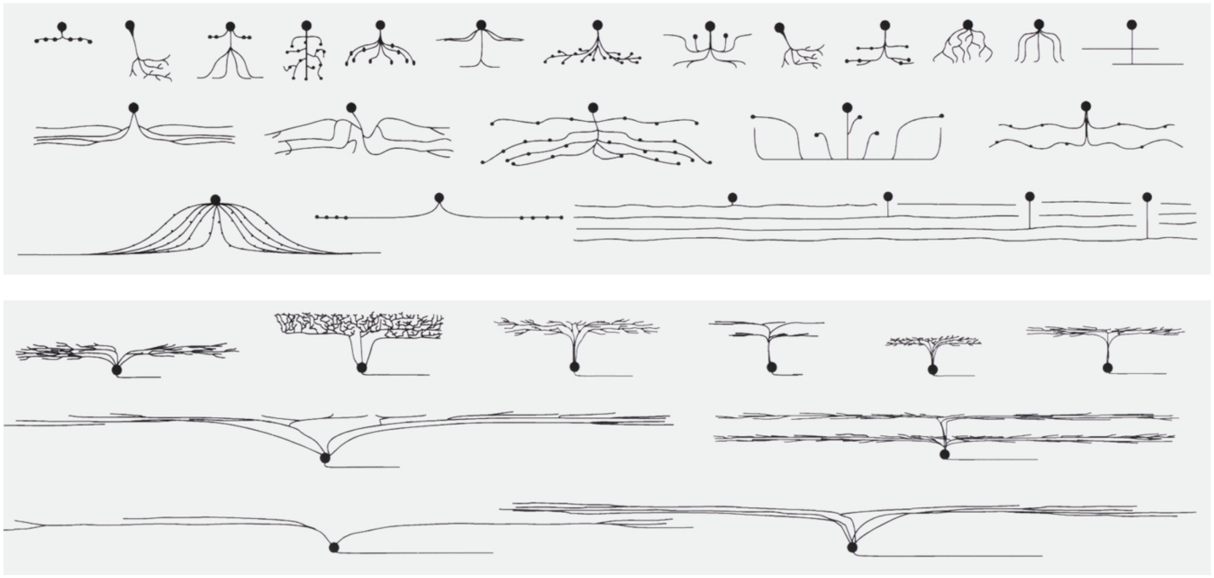

Figure 7. Amacrine and Ganglion cell types. On the upper panel distinct amacrine cell types identified from studies conducted in rabbits are shown. Each amacrine cell type present different pre- and post-synaptic partners and distinct neurotransmitters. This provide ACs with specific functions in visual signal processing, as for example dopaminergic amacrine cells adjust retina's response under dim or bright light conditions and starbust amacrine cells play a role in direction selectivity. On the bottom panel some of the ganglion cell types are presented. GC types are distinguished according to their light response and by anatomical criteria. Baden et al., 2016 for example, classify the different types of GCs according to whether these are direction-selective or not. Within these groups, ON, OFF and ON-OFF GC types are distinguished. Adapted from Masland, 2001.

In summary, signal processing at the retinal level is extremely sophisticated and complex with many interconnected cell types involved. In general terms, the rod pathway is much simpler than the cone pathway and actually takes advantage of the cone pathway to reach the GC. Briefly, rod photoreceptors synapse with one type of BC, whose signal is influenced by the telodendritic arbors of HI cells. The rod bipolar cell, in turn, connects with one type of AC (A17), which modulates the rod BC output. Another AC (AII) feeds the output of the rod BC to the cone bipolar cells, so the rod signals can reach GC (Kolb et al., 1995; Masland, 2012). In general terms, the retina has two main functions, (i) to convert light into a visual signal, which occurs in the PR, and (ii) to compare levels of neural activity in different cells, which takes place along the retinal circuitry. In a very simplified manner, vision consists on the detection of differences in light intensity (Rodieck, 1998).

1.3 Retinal development

Eye morphogenesis is a highly complex process involving a coordinated interaction between three different tissues, the neuroepithelia, the surface ectoderm and the periocular mesenchyme. This process and the genes involved are highly conserved across different species (Heavner and Pevny, 2012). In mouse, the first indication of eye development is the

formation of the optic pits. These arise from the evagination of the anterior neural plate towards the surface ectoderm, which will become the lens placode. These evaginations from the diencephalon are commonly known as optic vesicles (OV). The contact between the distal part of the OV and the surface ectoderm induces the invagination of both, leading to the formation of the optic cup (OC). The outer layer of the OC will eventually differentiate to RPE and the inner layer to the neural retina (NR) (Lamb et al., 2007; Fuhrmann, 2010; Heavner and Pevny, 2012; Reh, 2013).

At a molecular level, the genes involved in early eye morphogenesis are known as eye field transcription factors (EFTFs), and they create a feedforward network required for eye development (Heavner and Pevny, 2012; Reh, 2013). In mammals, four main EFTFs have been described: Pax6, Rax, Six3 and Lhx2. The eye field is defined as the region where the expression domains of these four transcription factors overlap (Heavner and Pevny, 2012), Rax is required at very early stages of eye development to induce the cell movements required for OV evagination (Fuhrmann, 2010) as well as to induce the expression of the rest of EFTFs (Heavner and Pevny, 2012).

During OV evagination, three distinct regions are specified: the NR at the distal part of the OV, the RPE at the dorsal part of the OV (Fuhrmann, 2010; Reh, 2013) and the optic stalk at the ventral/proximal part of the OV (Heavner and Pevny, 2012) (Figure 8). Intrinsically, NR specification is characterized by the expression of Chx10 (Vsx2), which represses the basic helix-loop-helix (bHLH) transcription factor Mitf, required for RPE specification. In turn, Mitf also represses the expression of Chx10 in the presumptive RPE. Therefore, the boundary between RPE and NR is established by the mutual repression of Chx10 and Mitf, respectively (Fuhrmann, 2010; Heavner and Pevny, 2012; Reh, 2013). The transcription factor responsible for specifying the optic stalk is Pax2. In a similar antagonistic relation as Mitf and Chx10, Pax2 and Pax6 define the boundary between the NR and the optic stalk. Lhx2 appears to coordinate all the events involved in specifying those three different regions (Figure 8) (Heavner and Pevny, 2012). Extrinsically, FGFs secretion by the lens placode is suggested to play a role in NR specification by promoting Chx10 expression (Fuhrmann, 2010; Heavner and Pevny, 2012; Reh, 2013). Moreover, canonical Wnt signaling, TGFβ and BMPs have been described as required for RPE development and Shh is involved in RPE specification on the ventral side of the OV (Heavner and Pevny, 2012; Reh, 2013). Lhx2 might play a role in transducing BMP7 signal to activate Pax2 in the ventral OV (Heavner and Pevny, 2012).

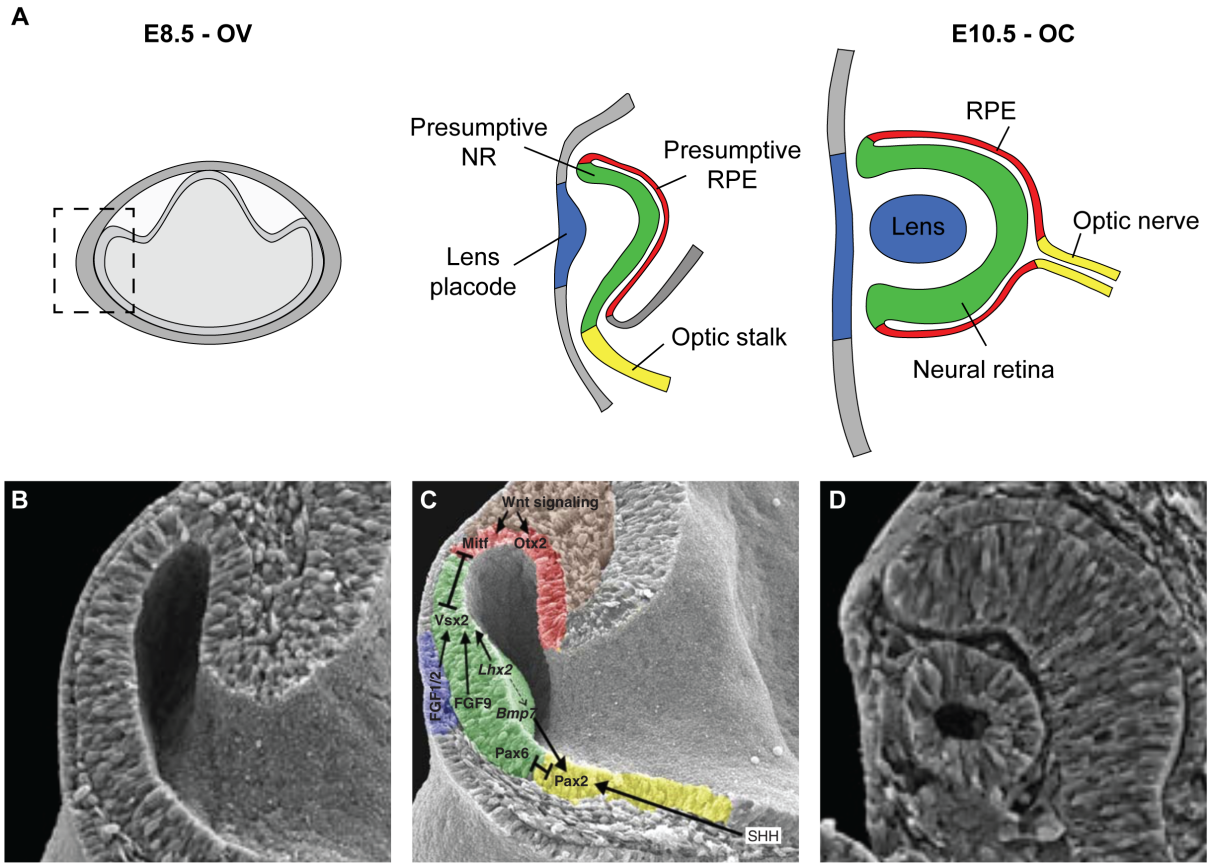

Figure 8. Eye morphogenesis. A) Schematic representation of the early steps in eye morphogenesis. At E8.5 the optic vesicles are present. From E8.5 to E10.5 invagination of the distal part of the optic vesicle (OV) together with the lens placode occurs, leading to the formation of the optic cup (OC) and lens. **B)** Optic vesicle at E.9. **C)** Transcription factors and extrinsic signalling required during optic vesicle patterning into the prospective neural retina and RPE. **D)** Optic cup and lens vesicle at E10.5. **B-D)** Adapted from Heavner and Pevny, 2012. OV: optic vesicle, OC: optic cup, NR: neural retina, RPE: retinal pigment epithelium.

Once the OC stage is achieved, in mouse around E11, retinogenesis starts. Retinal progenitor cells (RPCs) divide symmetrically to increase the number of cells within the retina, and asymmetrically to generate post-mitotic neurons (Brzezinski and Reh, 2015). Once a retinal progenitor has exited the mitotic cycle, it migrates to the corresponding retinal layer and differentiates to the specified retinal cell type. Retinal neurons are generated sequentially, yet in an overlapping manner since differentiation in the retina occurs in a central to peripheral sequence. Furthermore, the same order of retinal neuronal birth is conserved across vertebrates. In mice, early-born retinal neurons are generated in a first wave of retinogenesis occurring from E11 to E18. During this time, GC, HC and cone PR are born. The second wave of retinogenesis takes place from P0 to P7 and during this time, MG, rod PR and finally BC are born. In the case of AC, a subset of them are generated in the first wave, while the rest are generated together with the late-born neurons (Figure 9) (Lamb et al., 2007; Heavner and Pevny, 2012; Reh, 2013).

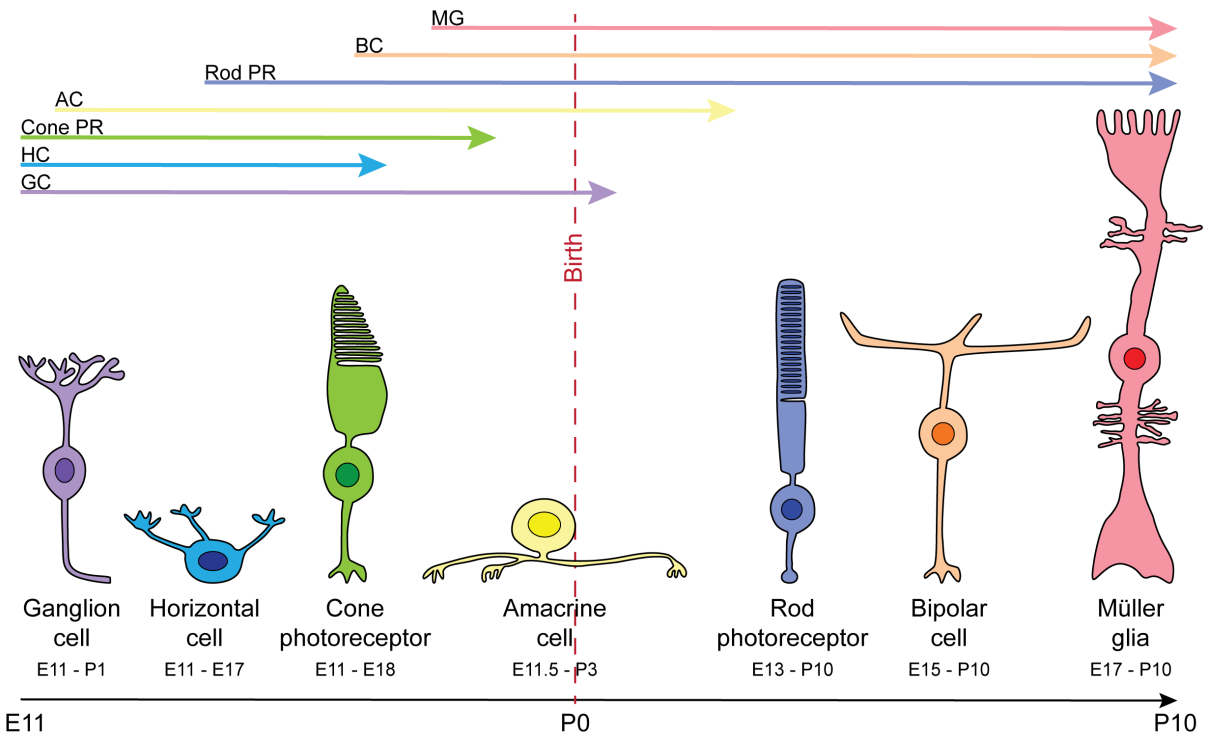

Figure 9. Retinogenesis in mammals. During embryonic development, a first wave of neurogenesis in the retina takes place. Ganglion cells, horizontal cells and cone photoreceptors are born during this time. After birth, a second wave of neurogenesis takes place. Rod photoreceptors, bipolar cells and Müller glia are born during this time. A subset of amacrine cells is generated during embryonic development, the rest are late-born neurons. Timings in this image correspond to mouse retinal development. MG: müller glia, BC: bipolar cells, PR: photoreceptor, AC: amacrine cells, HC: horizontal cells, GC: ganglion cells, E: embryonic day, P: post-natal day.

Retinal progenitor cells (RPCs) are multipotent progenitors capable of generating different retinal cell types at a given developmental stage, and the process of specification can take place during the proliferative progenitor or at the post-mitotic precursor stage (Brzezinski and Reh, 2015). Developmental studies have focused on understanding the mechanism by which RPCs change their potential to control fate specification. Two main hypothesis have been proposed: i) RPCs present intrinsic differences in terms of gene expression, that will specify them to a given cell fate, or ii) equivalent RPCs and progeny receive different extrinsic signals, which will determine their cell fate specification (Reh, 2013; Cepko, 2014). Changes in the epigenetic landscape have also been proposed as a mechanism to control cell fate (Brzezinski and Reh, 2015). Lineage tracing studies point towards an intrinsic program in the RPCs to control specification of their progeny (Cepko, 2014).

In terms of photoreceptor specification and development, six different transcription factors and the relation to one another have been identified (Figure 10). Otx2 is highly upregulated when retinal progenitors exit the cell cycle and it has been shown to be a key regulator of photoreceptor commitment, however, Otx2 alone is not sufficient for photoreceptor specification (Swaroop et al., 2010; Brzezinski and Reh, 2015). Crx acts downstream of Otx2

and plays an important role in activating the expression of photoreceptor-specific genes. The decision of rod vs. cone cell fate is taken downstream of Crx expression. Otx2 acts synergistically with Rorβ to activate Nrl expression. Nrl is a transcription factor required for rod cell fate determination. Among others, Nrl activates the expression of Nr2e3, which co-activates the expression of rod-specific genes and, at the same time, represses the expression of cone-specific genes. Thus, cells expressing Nrl and Nr2e3 are irreversibly committed to rod photoreceptor fate. Rorβ also interacts with Crx to initiate S-opsin transcription in cone photoreceptors. Therefore, Rorβ is required for the correct development of both types of photoreceptors. Photoreceptor precursors that do not express the Nrl transcription factor will follow a S-cone default pathway. Thyroid hormone, through its receptor Thrβ2, coordinates the patterning of M-opsin vs. S-opsin cones and maturation of the color vision system (Swaroop et al., 2010; Brzezinski and Reh, 2015). Rxrγ also plays a role in cone patterning (Brzezinski and Reh, 2015). Expression of Thrβ2 seems to be activated by the synergistic activity of Onecut1 and 2 and Otx2 (Brzezinski and Reh, 2015). In summary regarding photoreceptor development, it is hypothesized that photoreceptor precursors develop, by default, towards a S-cone fate, unless expression of transcription factors such as Nrl and Nr2e3 specifies rod photoreceptor fate, or expression of Thrβ2 and Rxrγ specify the cone precursor towards an M-cone cell fate (Swaroop et al., 2010).

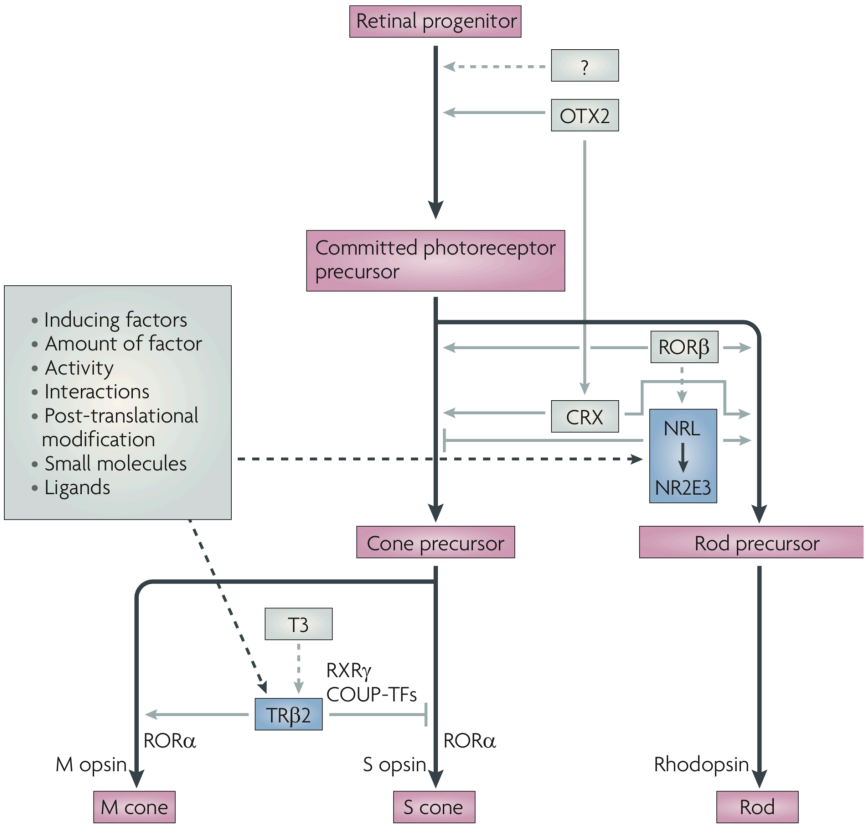

Figure 10. Transcriptional model of photoreceptor cell fate determination. From Swaroop et al., 2010.

1.4 Retinal degenerative diseases

Humans are highly dependant on vision for daily activities, therefore, vision impairment represents a significant decrease in life quality and independence and is considered an incapacitating condition (Veleri et al., 2015). In the last report of the World Health Organization (WHO) it is estimated that worldwide 253 million people are visually impaired. From those, 36 million are completely blind, with the other 217 million people ranging from moderate to severe vision impairment. Interestingly, around 81% of the visually impaired population are ≥ 50 years old. Globally, the main causes for vision loss are uncorrected refractive errors (53% of cases) and un-operated cataracts (25% of cases). Actually, over 80% of the global vision impairment can be prevented or cured (WHO, 2017).

Within the industrialized countries, however, refractive errors and cataracts are treated, leaving retinal degenerative diseases (RDDs) as the main cause of vision loss. RDDs are incurable and represent an overlapping group of highly heterogeneous genetic and clinical conditions that involve retinal neurodegeneration, especially photoreceptor cell dysfunction and death. As a consequence, the retina loses its capacity to detect light and/or transmit the resulting visual signal to the brain. Actually, primary mutations in genes involved in PR development, intracellular trafficking and cilia formation/function, phototransduction cascade, synaptic transmission and RPE integrity and/or function lead to retinal degenerative diseases. Until now, over 269 genes have been related to RDDs, however, due to the genetic heterogeneity within RDDs, it is hard to establish a one-to-one genotype-phenotype (Veleri et al., 2015; Ali et al., 2017; RetNet, 1996).

RDDs can be monogenic or multifactorial. In case of monogenic, RDDs can be subdivided, according to their Mendelian inheritance, in autosomal recessive, autosomal dominant and X-linked forms. Retinitis Pigmentosa (RP) is the most common form of inherited RDD, while age-related macular degeneration (AMD) represents the most common multifactorial RDD. Moreover, RDDs are considered non-syndromic diseases if only the retina is affected, or syndromic when also other tissues are affected, as in the case of ciliopathies, that, besides photoreceptors, might impair any other tissue or cell containing a cilium (Veleri et al., 2015).

1.4.1 Retinitis Pigmentosa

The term Retinitis Pigmentosa (RP) encompasses a subset of genetically heterogeneous diseases characterized by a progressive loss of vision due to photoreceptor cell death, as well as the degeneration of the adjacent RPE (Rodieck, 1998; Hartong et al., 2006; Ali et al., 2017). The prevalence of RP is 1:3000-7000, with a total of more than 1 million affected people

worldwide. Even though incidence of RP is equal for men and women, the X-linked form of the disease affects only males. Ethnic specificity is also not present, despite some mutations that might be found more frequently in isolated or consanguineous populations (Hartong et al., 2006; Ferrari et al., 2011).

Up to 58 different mutations affecting PR or RPE-related genes have been associated to RP, and those can be inherited in an autosomal dominant (20-25% of the cases), autosomal recessive (15-20% of the cases) or X-linked (10-15% of the cases) manner. Mutations in rhodopsin (RHO), usherin (USH2A) and retinitis pigmentosa GTPase regulator (RPGR) genes represent 30% of RP cases. RP presents non-syndromic forms, such as Leber Congenital Amaurosis (LCA) and syndromic forms, which represent 20-30% of the RP cases. Usher syndrome, which is associated with hearing loss, and Bardet-Biedl syndrome, which is associated with obesity, cognitive impairment, polydactyly, hipogenitalism and renal diseases, are examples of syndromic RP (Hartong et al., 2006; Ferrari et al., 2011; Ali et al., 2017).

The first noticeable symptoms of RP appear in young adulthood and involve night and peripheral vision loss due to rod photoreceptor cell death. With the advance of the disease, peripheral vision loss continues to the stage of tunnel vision, in which patients, thanks to cone-mediated visual response, still conserve central vision. At this middle stage, dyschromatopsia to light colors is also present. In the later stages of the disease (40-60 years old) patients experience cone-photoreceptor cell death, and thus, central vision is also lost and patients are considered legally blind. The inner retina undergoes progressive retinal remodeling mild on early stages of disease, but severe at later stages (Rodieck, 1998; Marc et al., 2003; Hartong et al., 2006; Ferrari et al., 2011; Jones et al., 2012; Ali et al., 2017).

Although RP affected patients generally do not notice vision loss until young adulthood, photoreceptor function often begins to diminish already in childhood, which can be detected using objective measures of photoreceptor function such as electroretinography (ERG) (Hartong et al., 2006). Clinically, the fundus of RP patients present pigment granules deposits (bone-spicule) starting from the periphery of the retina and advancing towards the middle with the advance of the disease (Figure 11). These pigment deposits result from the RPE invading the neural retina upon photoreceptor cell death. Moreover, the optic disc becomes pale and the retinal arterioles begin to fade and become thinner. Scotopic responses are not detectable from middle stages of the disease, and at late stages, also photopic responses disappear (Rodieck, 1998; Hartong et al., 2006; Ali et al., 2017).

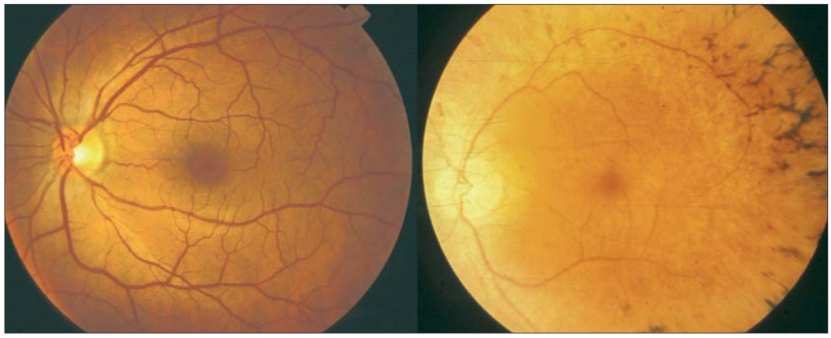

Figure 11. Healthy (left) vs. retinitis pigmentosa (right) fundus. In the image of the RP-affected fundus, the pigment deposits, thinner retinal arterioles and a paler optic disc are observed, compared to the image of the healthy fundus. From Hartong et al., 2006.

1.4.2 Age-related macular degeneration

Macular degenerations are characterized for the loss of both types of photoreceptors, rods and cones, but restricted at the macular area. Examples of macular degeneration are the early onset Stargardt disease and the complex and late (older age) onset age-related macular degeneration (AMD) (Veleri et al., 2015).

Globally, AMD represents the third largest cause of vision impairment. In fact, 4% of the moderate to severe vision impairment cases are due to AMD. In industrialized countries, however, AMD is the primary cause of vision loss (Fritsche et al., 2014; WHO, 2017). The prevalence of AMD increases steadily with age, it affects 2% of the population aged 40, but 1:4 in the elderly (around 80 years old). There exist ethnic population differences and AMD is generally more common among lightly-pigmented females (Ambati and Fowler, 2012; Fritsche et al., 2014).

Despite being a late-onset disease, AMD is a progressive neurodegenerative disease, untreatable in around 90% of the cases and driven by genetic and environmental factors. Since AMD is a complex disease, it is difficult to understand which genetic factors might be involved. The first one identified to be involved in AMD was the complement factor H (CHF). More recently, thanks to genome-wide association studies, up to 19 loci have been correlated with late AMD and they correspond to lipid metabolism, complement activation, angiogenesis and inflammation. Moreover, advanced age, family history, smoking and nutrition are known to have an impact in AMD progression (Ambati and Fowler, 2012; Bailey et al., 2013; Fritsche et al., 2014).

Within the macular region, dysregulated photoreceptor metabolism (Joyal et al., 2016) or malfunctioning of their support system, including RPE, Bruch's membrane and choroidal

vasculature, can lead to AMD. Early stages of the disease are asymptomatic and are characterized by abnormalities in the RPE and accumulation of drusen in both, the sub-retinal space and between the RPE and Bruch's membrane. Drusen are extracellular aggregates that contain lipids and various proteins, including those involved in complement regulation, TIMP3, β-amiloid, vitronectin and apolipoproteins, besides ions, such as zinc and iron. The most common forms of AMD correspond to these early stages and represent the least severe form of the disease (Ambati and Fowler, 2012; Bailey et al., 2013; Fritsche et al., 2014).

Late stages of AMD are subdivided into two different categories, known as dry and wet AMD (Figure 12). Dry AMD, also known as geographic atrophy (GA), includes cell death of the RPE and the corresponding PR, together with choroidal capillaries. It usually represents a moderate visual impairment and sometimes progresses to severe blindness. Nonetheless, dry AMD represents the most abundant and less severe of the two late stages and it is characterized by a slow progression. However, there is currently no treatment available. On the other hand, wet AMD, also known as choroidal neovascularization (CNV), represents a more severe phenotype of the disease. Fortunately, it affects only 10-15% of the patients and can be treated, though not cured, with anti-vascular endothelial growth factor (anti-VEGF) injections. If left untreated, it rapidly decreases vision, leading to blindness within months, due to edema formation and bleeding of the newly formed capillaries that invade the RPE and retina (Ambati and Fowler, 2012; Bailey et al., 2013; Fritsche et al., 2014).

Figure 12. Healthy vs. AMD fundus photographs. A) Fundus photograph of a healthy eye, presenting normal pigmentation and normal retinal blood vessels. **B)** Fundus photograph of a late stage dry AMD (geographic atrophy). RPE cells in the macula have died, therefore there is a lack of pigmentation in that region. **C)** Fundus photograph of a late stage wet AMD (choroidal neovascularization). Leaky blood vessels from the choroid are invading the retina. From Ambati and Fowler, 2012.

1.4.3 Cone dystrophies

Cone dystrophies are a genetically and clinically highly heterogeneous group of rare eye diseases in which mainly cone photoreceptors are affected. The symptoms of such diseases

include loss of visual acuity, abnormalities of color vision (achromatopsia), central scotomata, photosensitivity and a certain degree of nystagmus. Moreover, abnormal cone function is observed in electrophysiological and psychophysiological tests. Similarly to the rest of retinal degenerative diseases, cone dystrophies can be inherited in an autosomal dominant, autosomal recessive or X-linked manner.

Cone dystrophies can be subdivided into two subgroups, stationary or progressive. Stationary cone dystrophies are generally named cone dysfunction syndromes, are present from shortly after birth or infancy and show conserved rod function. Examples of cone dysfunction syndromes are complete and incomplete achromatopsia, oligocone trichromacy, blue cone monochromatism and Bornholm eye disease. Progressive cone dystrophies appear during childhood or early adulthood with cones degenerating progressively. Moreover, cone degeneration is often followed by rod degeneration at later stages of disease development, and therefore, there is some overlap between cone and cone-rod dystrophies (Michaelides et al., 2004, 2006; Veleri et al., 2015).

1.5 Therapeutic approaches

Therapeutic approaches for retinal degenerative diseases are, so far, very limited (Scholl et al., 2016). Moreover, most of the existing therapies are only able to slow down the progression of the disease, but not to cure the respective diseases or to fully restore vision. Examples of such therapies are the intake of high doses (15000 IU) of vitamin A, alone or in combination with docosahexaenoic acid (DHA), to delay rod photoreceptor cell death and decrease of cone-derived ERG responses in RP patients (Hartong et al., 2006), or treatment with anti-VEGF to prevent neovascularization and vascular leakage in wet AMD patients. This treatment has been shown to improve, or at least stabilize, vision for at least two years in the majority of cases (Ambati and Fowler, 2012; Veleri et al., 2015). Nonetheless, two thirds of patients evaluated seven years after initiating anti-VEGF treatment (SEVEN-UP study) had lost visual function (Rofagha et al., 2013). Furthermore, a significant amount of patients (around 25%) do not respond to a continuous treatment of anti-VEGF injections (Ehlken et al., 2014).

Alternative therapies such as gene replacement, optogenetics or chemical photoswitches, cell replacement and retinal prostheses are currently assessed for treating retinal degenerative diseases. Actually, several of these approaches have reached clinical trials, while the first gene supplementation therapy as well as retinal prostheses have even already been introduced to the market (Scholl et al., 2016; Fernandez, 2018).

Gene supplementation therapy consists of the delivery of a wild-type copy of a defective gene with the objective to restore its function within the cell. In the case of RDDs, this would be the approach for autosomal recessive inherited diseases (Takahashi et al., 2018). However, in autosomal dominant inherited diseases, a potential strategy might be to suppress the defective gene via silencing RNAs (Hartong et al., 2006; Ku and Pennesi, 2015) or generating indels (insertions/deletions) in the affected gene by CRISPR/Cas9 technology (Bakondi et al., 2016; Chan et al., 2017). Moreover, in some cases, it may be necessary to also introduce a wild-type copy of the affected gene. This copy can be genetically engineered in the target site for suppression and thus, be resistant to it (Farrar et al., 2012). Delivery of genetic material for retinal degenerative diseases has been mainly achieved using adeno-associated viruses (AAVs). These viral vectors are able to diffuse effectively within the nervous system, present very low immunogenicity, lack of pathogenicity and can target both, RPE and PR (Dalkara et al., 2015). Unfortunately, those viruses can accommodate genes only up to 5 kb, and therefore, alternatives for genes bigger than this are required (Veleri et al., 2015). An alternative option would be to deliver genes encoding for neurotrophic factors such as brain-derived neurotrophic factor (BDNF), ciliary neurotrophic factor (CNTF) or rod-derived cone viability factor (RdCVF) in order to preserve photoreceptor cell viability, either by preventing their death or enhancing their endogenous pro-survival mechanisms (Dalkara et al., 2015; Ku and Pennesi, 2015; Scholl et al., 2016). Delivery of AAVs can be done sub-retinally or intravitreally. When delivered sub-retinally, a small transitory retinal detachment is required, and this might cause negative effects in the recipient retina. However, when delivered in the sub-retinal space of non-human primates, rAAVs stay in place, rather than distributing to the blood and lymphatic tissue, and therefore, gene transduction in whole retinal sections results two orders of magnitude higher than when delivered intravitreally (Seitz et al., 2017; Takahashi et al., 2018). The first successful clinical example of gene therapy for RDDs is the delivery of the RPE65 gene, that encodes for a protein involved in the visual cycle, into LCA patients. Despite continued retinal degeneration (Cideciyan et al., 2013a; Bainbridge et al., 2015; Jacobson et al., 2015), these patients were reported to present an improvement in vision with no reported side effects (Bainbridge et al., 2008; Scholl et al., 2016; Veleri et al., 2015). However, discrepancies regarding the long-term visual function are reported. While Cideciyan et al., 2013 did not observe a detectable decline on visual function over long-term, both Bainbridge et al., 2015 and Jacobson et al., 2015 reported visual function decline three years after treatment. Other examples of gene therapy for RDDs that have entered clinical stage include applications for RP, Usher syndrome, achromatopsia, choroidoremia, Stargardt disease and X-linked retinoschisis (reviewed in Takahashi et al., 2018).

Optogenetic approaches represent a variation of gene replacement that aim to convert light-insensitive retinal neurons into light-sensitive cells by genetic delivery of light-dependent ion channels or pumps, which include microbial opsin proteins such as halorhodopsin or channelrhodopsin (Dalkara et al., 2015; Scholl et al., 2016). The target cells in the retina could be PR that have lost their OS, BC or GC, depending on the retinal degeneration degree. The requirements for the therapeutic use of optogenetic tools are the presence of living retinal cells, and that the target cells should be downstream of the affected retinal neurons, so the signal can be transferred to the brain through the remaining retinal circuit. Actually, the degree of vision recovery will depend on the targeted cells and on the patient's retinal degeneration stage (Dalkara et al., 2015; Ku and Pennesi, 2015; Scholl et al., 2016). Furthermore, a high light level and/or transgene expression will be required, as well as the use of external goggles to properly stimulate the targeted cells by matching the spectrum and intensity of the delivered optogenetic tools (Ku and Pennesi, 2015; Scholl et al., 2016).

Retinal prostheses are implantable medical devices able to electrically stimulate the retina, optic nerve or visual cortex, depending on the implantation site. Such electrical stimulation is meant to simulate the PR signal and create an artificial sense of vision. Some of these devices are already in the market and have shown very basic improvements in visual function in terms of detection and localization of shapes, as well as greyscale recognition in patients with end-stage retinal degeneration diseases (Stingl et al., 2017). Such visual function recovery provides a proof-of-concept for visual function recovery at late-stage of retinal degeneration. Nonetheless, the visual function recovery, so far, is limited and with a very low spatial resolution (Hartong et al., 2006; Scholl et al., 2016; Fernandez, 2018), for example, shape recognition or hand-eye coordination were not achieved (Stingl et al., 2017). Further research is required to improve such electrical devices in terms of material, architecture and biocompatibility, as well as in their capacity to provide the electrical stimuli required to create meaningful light perception, thus allowing patients to recognize objects, faces or properly orientate themselves in unfamiliar spaces (Fernandez, 2018).

1.5.1 Photoreceptor transplantation

Cell-based therapy for retinal degenerative diseases is being explored in two different directions: i) transplantation of RPE tissue, to replace the dysfunctional one and prevent further PR degeneration, ii) transplantation of PR cells in order to replace/repair the damaged or dead cells. Photoreceptor replacement represents a much more ambitious target than RPE, since the establishment of synaptic connections and the correct localization and integration of donor cells into the host tissue are required (Gaillard and Sauvé, 2007; Veleri et al., 2015; Goureau et al., 2018). This challenge is reflected in the amount of clinical trials that have been launched

to test human ESC-derived/iPSC-derived RPE transplantation for the treatment of RP and AMD patients, compared to PR replacement therapies, that have not yet reached clinical trial stages (Jones et al., 2017). For the purpose of this thesis, I will focus on PR transplantation.

Initial attempts at photoreceptor cell replacement therapy for retinal degenerative diseases were performed during the late 80s and early 90s. These initial studies took advantage of isolated embryonic rodent, porcine or human retinal tissue pieces/sheets for transplantation into the sub-retinal space of rodent/porcine models of retinal degeneration (Cerro et al., 1985; Silverman and Hughes, 1989; Del Cerro et al., 1990; Ehinger et al., 1991), proving maturation and survival of the donor tissue within the host retinas. Dissociated embryonic photoreceptors were also transplanted into murine models of retina degeneration, where they survived up to 3 months (del Cerro et al., 1988) and initial hints of functional recovery, by means of reflex inhibition studies, were achieved (del Cerro et al., 1991). Other groups studied the potential of retinal stem/progenitor cells obtained from post-natal day 0-3 and expanded *in vitro* as a cell source for photoreceptor replacement therapies. Most of these studies, however, took advantage of biomaterial scaffolds in order to improve survival, differentiation and maturation upon transplantation (Klassen et al., 2004; Redenti et al., 2008, 2009; Ballios et al., 2010; Steedman et al., 2010; Tucker et al., 2010). Moreover, concerns about using embryonic tissue were already raised during these early days of cell replacement in degenerative retinas, therefore alternative cell sources, i.e. isolated murine adult photoreceptors and RPE cells were (co-)transplanted into the SRS of rat/mouse models of fully degenerated retinas. In this case, grafts were also able to survive up to 1 month in mouse, or up to 3 months in rat (Gouras et al., 1991a, 1991b).

Enrichment of the desired cell population has evolved from a very rudimentary strategy, consisting of examining the cell suspension under a phase-contrast microscope to determine the optimal retina dissociation time in which a relatively pure photoreceptor population was obtained (Gouras et al., 1991a, 1991b, 1991c), to more sophisticated strategies. These include, for example, the use of fluorescent reporters, which allow both, to isolate specific retinal cell types/populations using fluorescence activated cell sorting (FACS), and to identify the transplanted cell population within the host retina (Klassen et al., 2004; MacLaren et al., 2006; Lakowski et al., 2010; Pearson et al., 2012; Smiley et al., 2016; Decembrini et al., 2017).

Indeed, the introduction of fluorescent reporters, such as a mouse model ubiquitously expressing GFP (Okabe et al., 1997) or under the rod-specific *nrl* promoter (Nrl-GFP, Akimoto et al., 2006) enabled the enrichment and identification of post-mitotic photoreceptor precursors, at the age of post-natal day 4 (P4), as the ideal cell source for rod photoreceptor

replacement in RDDs, in terms of survival and integration into the host ONL (MacLaren et al., 2006; Bartsch et al., 2008). Since then, most of the pre-clinical studies regarding photoreceptor transplantation have used an enriched population of young post-mitotic rod or cone-like PR precursors as donor cells (Lakowski et al., 2010; Eberle et al., 2011; Lakowski et al., 2011; Pearson et al., 2012; Barber et al., 2013; Singh et al., 2013b; Eberle et al., 2014; Santos-Ferreira et al., 2015; Smiley et al., 2016). In the case of cone photoreceptors, an equivalent developmental stage in which donor cells can be isolated and result in the maximum numbers of integration into the host retina upon transplantation, corresponds to E15.5, as has been shown in two independent studies (Lakowski et al., 2010; Decembrini et al., 2017). Nonetheless, due to the low availability of cone photoreceptors in nocturnal rodent models and the lack of early markers to identify them, the development of cone replacement therapies represents a bigger challenge, reflected in the lower number of studies addressing cell therapy for cone dystrophies.

More recently, methods based on photoreceptor-specific expression of cell surface markers have been investigated. Lakowski et al., 2011, taking advantage of the Nrl-GFP mouse model, could identify a panel of two biomarkers, CD24+, CD73+, that allows for an enrichment of young post-mitotic rod photoreceptor precursors within the donor cell population. As an alternative to FACS, which involves high rates of cell death due to the duration of the sorting, our lab established magnetic activated cell sorting (MACS) combined with CD73+ labelling to isolate young post-mitotic rod photoreceptor precursors (Eberle et al., 2011, 2012; Santos-Ferreira et al., 2015). While MACS enrichment procedures have been established for clinical applications, it would be ideal to find an alternative method to isolate photoreceptor precursors circumventing any previous labelling of the cells. This might be achieved by using inherent mechanical properties of target cells, i.e. photoreceptors, to isolate them from the rest of retinal cells, as it has been shown for different cell populations of the blood (Otto et al., 2015).

Photoreceptor delivery in the SRS can be achieved using either trans-vitreal or trans-scleral injections. The advantage of the first approach is that it is a relatively simple surgical procedure and any trained scientist is able to perform it, however, it involves puncturing, and therefore, damaging a small area of the retina. On the other side, trans-scleral injections in mouse eyes, which are relatively small, represents an increased risk of bleeding (an immune reaction) due to damage of the choroid and blood-retinal barrier. However, it is not necessary to puncture the retina, and therefore, does not involve direct retinal damage.

The use of primary rod and cone young post-mitotic photoreceptor precursors has facilitated the establishment of basic techniques for cell replacement, including retina dissociation to a

single cell suspension and enrichment of the desired cell population, strategies for photoreceptor cell delivery into the host retina and analysis of visual function recovery upon transplantation (Figure 13). Nonetheless, another interesting debate raised in some of the mentioned studies concerns the method of photoreceptor delivery into the hosts, whether it should be as a single cell suspension or as retinal sheets (Figure 13). Advantages of single cell suspensions include the possibility of transplanting a purified population, an accurate number of cells, a better contact between donor and host cells and minimal surgical intervention (del Cerro et al., 1988). Disadvantages of such a procedure include the possibility of efflux of the transplanted cells (Redenti et al., 2008; Ballios et al., 2010; Steedman et al., 2010; Tucker et al., 2010), migration of the donor cells from the transplantation site (Tucker et al., 2010), short term survival, low integration numbers (Ballios et al., 2010; Tucker et al., 2010; Assawachananont et al., 2014) and lack of graft structure (Assawachananont et al., 2014).

The main goal of sheet transplantations is to overcome the lack of graft structure after transplanting single cell suspensions by delivering photoreceptors in a more organized manner. Actually, from the very beginning of cell replacement for RDDs, several studies have focused on delivering retinal sheets isolated from neonatal rats (Silverman and Hughes, 1989), fetal (Seiler and Aramant, 1998; Radtke et al., 1999, 2002, 2004) or cadaveric (Kaplan et al., 1997) human eyes rather than cell suspensions. Besides a better structure of the graft and the possibility of delivering photoreceptors retaining their apical-basal polarity (Pritchard et al., 2010), retinal sheet offer longer graft survival, at least 6-10 months post-transplantation (Ghosh et al., 1999, 2007) compared to single cell grafts, for which survival is significantly reduced one month post-transplantation (West et al., 2010).

Regarding functionality, it remains unclear whether retinal sheet transplantation leads to systematic improvement of visual function. Transplantation of fetal neural retina, together with its RPE, into RP and AMD patients has led to a certain degree of visual improvement, but not in all the treated patients, and not to the same degree (Radtke et al., 1999, 2004, 2008). Some of the treated patients showed no visual improvement at all (Radtke et al., 2002). On the contrary, visual function recovery has been achieved in pre-clinical studies in which single cell suspensions of primary rod (Pearson et al., 2012; Barber et al., 2013; Singh et al., 2013b) or cone-like (Santos-Ferreira et al., 2015) photoreceptor precursors were transplanted.

Despite those advances in the photoreceptor transplantation field, the translation of the established procedures to clinical applications in humans would require the collection of primary cells from fetuses during the second trimester of pregnancy, which leads to insurmountable logistical, legal and ethical concerns. A seminal breakthrough in the

photoreceptor transplantation field was the possibility of obtaining photoreceptor precursors from pluripotent stem cell (PSC)-derived retinal organoids, which allows to circumvent the use of fetal primary cells. Due to their relevance for the following experimental chapter regarding organoid cultures, retinal organoids are explained in more detail in section 2.1.

Related to photoreceptor transplantation as well, it is important to understand the interaction of donor cells with the host retina upon photoreceptor transplantation. Up to date, the field has assumed that donor cells would migrate and integrate into the host retina and that this would be the underlying mechanism of visual function recovery. The basis of this line of thought lies on the detection of fluorescent reporter positive cells in the host outer nuclear layer after transplanting photoreceptor precursors labelled with such reporter. However, this concept has recently been challenged, with a pivotal contribution provided by the work described in this thesis. As such a possible alternative mechanism for visual function recovery upon transplantation has been suggested. This topic is addressed in Chapter 3 of this thesis and will be properly introduced in section 3.1.

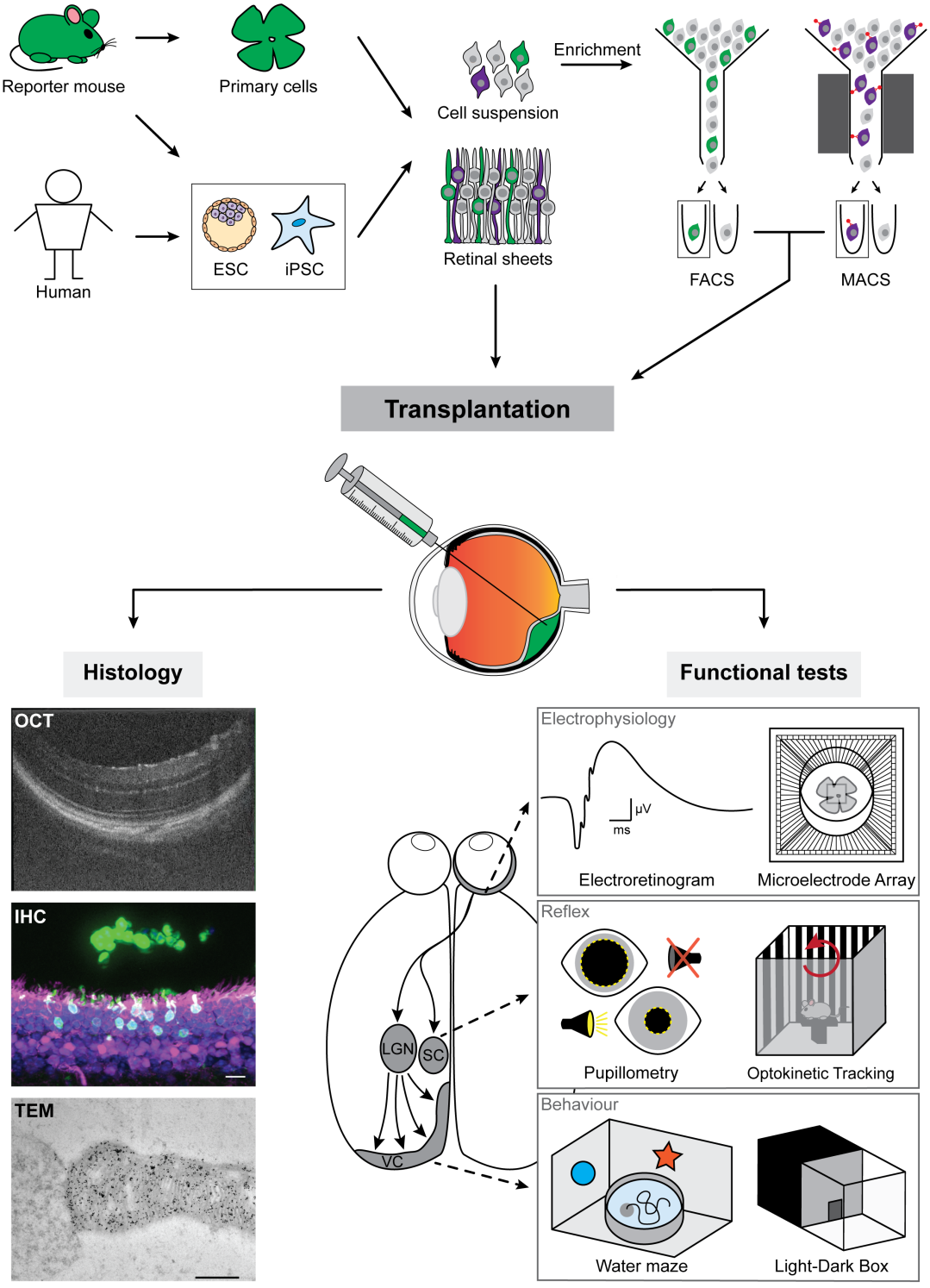

Figure 13. General overview of the photoreceptor replacement approach. Above, the different photoreceptor cell sources are represented. Photoreceptors can be delivered as a single cell suspension or as a retinal sheet. If delivered as a cell suspension, previous enrichment of the photoreceptor cell fraction is required. Following transplantation, several imaging and functional tests can be used to analyse the outcome of photoreceptor transplantation. ESC: embryonic stem cells, iPSC: induced pluripotent stem cells, FACS: fluorescence activated cell sorting, MACS: magnetic activated cell sorting, OCT: optical coherence tomography, IHC: immunohistochemistry, TEM: transmission electron microscopy, LGN: lateral geniculate nucleus, SC: superior colliculus.

1.6 Aim of the study

Cell replacement, i.e. photoreceptor transplantation, is conceived as a feasible therapeutic approach for retinal degenerative diseases. However, before photoreceptor transplantation reaches clinical stages, remaining features of this therapeutic approach have to be addressed. Here, two key aspects of photoreceptor transplantation are considered.

i) Most of the research involving photoreceptor replacement has been focused on the development of protocols and tools for rod photoreceptor enrichment and transplantation. However, humans are diurnal mammals and our vision relies mostly on cone photoreceptors. Due to the low availability of such cells, less studies have been conducted using cone photoreceptor transplantation in comparison to rod photoreceptor transplantation. Therefore, one of the aims of this study was to use the 3D retinal organoid technology to generate cone photoreceptor precursors suitable for transplantation approaches. Furthermore, considering the lack of tools to study cone transplantation approaches as a potential therapy for cone degenerative diseases, in this study a new mouse embryonic stem cell line has been generated carrying a fluorescent label in early cone photoreceptor precursors. This aspect of photoreceptor transplantation is addressed in Chapter 2 of this thesis.

ii) Structural integration and maturation of donor photoreceptors into the host retina has been assumed as the underlying mechanism for visual function recovery upon transplantation. However, recent results indicate that this assumption may be incorrect and point towards an alternative mechanism for vision restoration. In this regard, a second aim of this study was to better understand how donor and host photoreceptors interact. In Chapter 3 of this thesis it is shown that donor photoreceptors engage in cytoplasmic material exchange with host photoreceptors. Furthermore, an insight of what kind of cytoplasmic material is exchanged between donor and host cells is provided in this study.

Chapter 2:

Cell transplantation as a therapy for cone photoreceptor degeneration

2.1 Introduction

The discovery of hESC (Thomson et al., 1998) and hiPSC (Takahashi et al., 2007) resulted in a new window of opportunity for photoreceptor transplantation. PSCs represent an unlimited source of material for the generation of specific cell types suitable for cell therapy approaches. In the case of photoreceptor cell replacement, developmentally similar post-mitotic photoreceptor precursors suitable for transplantation can be obtained from PSC-derived retinal organoids.

Organoids, by definition, are three dimensional (3D) structures derived either from pluripotent stem cells (PSC) or isolated organ progenitors able to differentiate and form an organ-like tissue *in vitro*. Organoids must contain multiple cell types spatially organized similarly to the organ they resemble and be able to recapitulate, to some extent, organ-specific functions, such as excretion (renal organoids), neural activity (brain/retinal organoids) or contraction (cardiac organoids). In general, organoids also resemble at least in parts the *in vivo* development of the respective organ (Lancaster and Knoblich, 2014).

Prior to the groundbreaking discovery of retinal organoids, several efforts had been already directed to the establishment of protocols to *in vitro* differentiate cone and rod photoreceptors from mESC, miPSC, hESC and hiPSC (Zhao et al., 2002; Ikeda et al., 2005; Banin et al., 2006; Lamba et al., 2006; Osakada et al., 2008; Hirami et al., 2009; West et al., 2012). Most of these studies though, obtained neural precursors which had to be co-cultured with mouse embryonic (Ikeda et al., 2005), post-natal day 1 (Zhao et al., 2002) or adult (Lamba et al., 2006) retinal cells to achieve differentiation along the photoreceptor lineage. Osakada et al., 2008 was the first successful study in which complete *in vitro* differentiation of mouse, monkey and human ESC into photoreceptors was achieved. In order to direct stem cells to differentiate towards photoreceptors, all those studies manipulated the signaling pathways involved in retinal development by using extracellular matrix (ECM) or Wnt, Nodal and BMP antagonists, in combination with different growth factors, retinoic acid and taurine (Zhao et al., 2002; Ikeda et al., 2005; Lamba et al., 2006; Banin et al., 2006; Osakada et al., 2008; Hirami et al., 2009; Lamba et al., 2009, 2010; West et al., 2012; Boucherie et al., 2013; Barnea-Cramer et al., 2016). However, the overall efficiency of these protocols to generate cells expressing photoreceptor-specific markers was below 20% (Osakada et al., 2008).

In 2011, Gamm's team published the formation of hESC/hiPSC-derived optic vesicles able to develop towards both, neural retina and RPE (Meyer et al., 2011). In the same year, pioneering work form Sasai's lab introduced an essential break-through in the generation of photoreceptor

cells *in vitro* when, for the first time, the capability of mouse and human ESC to self-organize and generate optic cups *in vitro* was described (Eiraku et al., 2011; Nakano et al., 2012). Since then, most of the labs involved in the research and development of novel photoreceptor cell replacement therapies for RDDs have adapted the 3D retinal organoid technology for the systematic *in vitro* generation of transplantable photoreceptor precursors/retinal sheets (Gonzalez-Cordero et al., 2013; Assawachananont et al., 2014; Decembrini et al., 2014; Zhong et al., 2014a; Hiler et al., 2015; Ohlemacher et al., 2015; Chen et al., 2016a; Hiler et al., 2016; Lowe et al., 2016; Santos-Ferreira et al., 2016a; Völkner et al., 2016; Gonzalez-Cordero et al., 2017; Kruczek et al., 2017; Mandai et al., 2017; M'Barek et al., 2017) (Figure 13). A more detailed description of the different adapted protocols to generate mouse and human ESC-derived retinal organoids can be found in our recent review on organoid technology for retinal repair (Llonch et al., 2018).

Similarly, as with primary cells, methods to isolate photoreceptor cell precursors from the other cells present within the retinal organoids had to be developed. For the purpose of pre-clinical studies and proof-of-concept experiments, different fluorescent reporter lines were generated. Examples of these are *rax*-GFP (Wataya et al., 2008), *crx*-GFP (Collin et al., 2015; Decembrini et al., 2014; Kaewkhaw et al., 2015), *hPax6*-GFP (Völkner et al., 2016) and *nrl*-GFP (Phillips et al., 2018). Another strategy to fluorescently label the desired cell types within retinal organoids is to use viral vectors (lentiviruses or AAVs) containing the fluorescent reporter under the control of a specific promoter, such as *irbp*-GFP (Lamba et al., 2010), *L/M-opsin*-GFP (Gonzalez-Cordero et al., 2017; Kruczek et al., 2017; Welby et al., 2017; Waldron et al., 2018) or *rhodopsin*-GFP (Gonzalez-Cordero et al., 2013; Santos-Ferreira et al., 2016a). However, as mentioned previously, the presence of a fluorescent label is not ideal for clinical applications of hESC-derived PR. Following the strategy used for primary cells, panels of photoreceptor-specific cell surface markers were also described for the isolation of m/hESC-derived PR. Lakowski et al., 2015 found a five-cell surface marker panel, CD73+, CD24+, CD133+, CD47+, CD15-, that allowed the isolation of rod photoreceptors from mESC-derived retinal organoids. Later on, the same group described a two-cell surface marker negative selection, CD29-, SSEA-1-, to enrich photoreceptors from hPSC-derived organoids (Lakowski et al., 2018). This negative selection panel is ideal for clinical purposes since the desired cell population contains no label at all.

Cone photoreceptor isolation from retinal organoids, however, has not been properly established yet. One of the main issues to be resolved is the lack of knowledge regarding early cone markers that could be used to identify and isolate this cell population. So far, cone photoreceptors have been detected and isolated from m/hESC derived organoids by virally

labelling them using the L/M-opsin-GFP reporter (Kruczek et al., 2017; Waldron et al., 2018). However, this represents a late cone marker, thus the isolated cell population does not resemble the developmental stage that lead to optimal transplantation outcomes as observed for rod post-mitotic photoreceptor precursors (MacLaren et al., 2006; Bartsch et al., 2008). Recently, a four-cell surface marker panel, SSEA-1-, CD26+, CD133+, CD147+, has been described which leads to a relative enrichment (~50% purity) of cone photoreceptors from hPSC-derived retinal organoids (Welby et al., 2017). Furthermore, a recent publication from the Goureau team has reported that MAC-sorted CD73+ cells from D120 hiPSC-derived retinal organoids developed mostly to cone photoreceptors four weeks post-transplantation into the SRS of a rat model of retinal degeneration (Gagliardi et al., 2018). Curiously however, with longer transplantation times, the resulting cells were found to be both rods and cones. Thus, it is unclear whether CD73 is a marker for rod or cone precursors in human retinal organoids. Despite the results presented in those studies, specific early cone markers that would allow detection and isolation of post-mitotic cone photoreceptors within the retinal organoids are still missing.

Independently of the strategy used to isolate the PSC-derived photoreceptor precursors, most of the mentioned studies could show the survival and maturation of organoid derived photoreceptor precursor cells within the sub-retinal space of wild-type and retinal degeneration animal models. Hints for visual function recovery, however, have not been shown after transplanting single cell suspensions of PSC-derived photoreceptors.

On the other hand, miPSC-derived retinal sheets have also been generated and transplanted into the sub-retinal space of the fully degenerated *rd1* mouse model, where photoreceptors have been shown to mature and establish putative synaptic connections with the remaining host inner retina (Assawachananont et al., 2014; Mandai et al., 2017). Rosette formation of the graft has been described upon retinal sheet transplantation. Such rosettes might lead to the incorrect orientation of the graft, i.e. photoreceptors towards the INL and synaptic terminals towards the SRS. Nonetheless, indications of visual function recovery have been observed after transplanting miPSC-derived retinal sheets into mouse models of end-stage retinal degeneration (Mandai et al., 2017). It is worth mentioning that, in this study, the analyzed animals were supplied with 9-*cis*-retinol acetate in case the visual cycle would be impaired due to rosette formation (Mandai et al., 2017). Retinal sheets have also been derived from hESC and transplanted into two different monkey models of retinal degeneration. In this case, graft survival (for up to 5 months), maturation and integration was observed. However, visual function recovery, assessed by focal ERG, was not detected (Shirai et al., 2016). Nonetheless, visual function recovery after hESC-derived retinal sheet transplantation into rat models of

severe retinal degeneration has been recently reported in two studies from the Seiler's lab (Lin et al., 2018; McLelland et al., 2018). Moreover, long-term graft survival and light responses have been observed after transplanting hESC-derived retinal tissue into two different immunodeficient mouse models of retinal degeneration (Iraha et al., 2018).

Considering the milestones achieved within the retinal organoid field in less than 10 years, hESC-derived PR have become a highly promising cell source for photoreceptor cell replacement therapies. Nonetheless, before hESC-derived PR reach clinical trials, important issues regarding automatization, reproducibility and adaptation of the protocols to good manufacturing practices (GMPs) need to be resolved (Wiley et al., 2016). Moreover, regarding cell therapies involving hESCs and hiPSCs, adequate quality control of the hPSC-derived products should be implemented as a regular practice previous to clinical use (Lin and Xiao, 2017; Merkle et al., 2017).

Besides, as already mentioned, human vision relies mostly on cone photoreceptors and therefore, efforts in the direction of elucidating factors involved on cone cell fate specification as well as early cone markers for detection and enrichment of cone photoreceptor precursor cells are required. Hence, in this study alternative methods to manipulate retinal organoid development towards the generation of cone-enriched organoids have been evaluated. Furthermore, a new mouse embryonic stem cell line expressing a fluorescent reporter presumably in cone photoreceptors from early stages of development has been generated.

2.2 Materials and methods

2.2.1 Ethical statement

All the animal experiments were approved by the ethics committee of the TU Dresden and the Landesdirektion Dresden (24-9168.11-1/2008-33, 24-9168.11-1/2012-33 and 24-9168.11-1/2013-23, TVV 25/2018) and performed strictly following the European Union and German regulations (Tierschutzgesetz), as well as the ARVO Statement for the Use of Animals in Ophthalmic and Vision Research

2.2.2 Experimental animals

All the experimental animals used in this study were kept in the animal facility of the Center for Regenerative Therapies Dresden and bred in house. Besides the wild-type C57BL/6Rj, another mouse line was used for this study, the Cpfl1 (cone photoreceptor function loss 1, Chang et al., 2002). This mouse model has a naturally arising mutation on chromosome 19

that leads to a progressive cone degeneration. Electroretinogram of these mice show no cone response, however rod-mediated response remains normal (Chang et al., 2002).

2.2.3 mESC maintenance and mESC-derived retinal organoids generation

Different mESC lines require slightly distinct media composition for maintenance as well as for retinal organoids generation. In the next sections, the specific details for each mESC line used in this study are described.

2.2.3.1 rx-GFP mES cell line

The rx-GFP mESC line used was kindly provided by Dr. Mike O. Karl. This line was originally generated in Yoshiki Sasai's lab by knocking in the GFP gene under the Rx promoter using as recipient the EB5 (129/Ola) mESC line (Wataya et al., 2008). The line is also deposited on the RIKEN Cell Bank.

Rx-GFP mESCs were cultured in a Glasgow Minimal Essential Medium (GMEM)-based medium (Gibco, cat#11710-035) containing 1 % non-essential aminoacids (NEA, Sigma, cat# M7145), 1 % sodium pyruvate (NaPyr, Sigma, cat#S8636), 0.1 % β-mercaptoethanol (β-ME, Sigma, cat#M7522), 10 % knock-out serum replacement (KSR, Gibco, cat#10828-028) and 1 % fetal calf serum (FCS, Sigma, cat#12103C). Moreover, leukemia inhibitory factor (LIF, Millipore, cat#ESG1107) at a final concentration of 2000 U/mL, blasticidin (ThermoScientific, cat#R210-01) at a final concentration of 20 µm/mL and the MEK inhibitor PD0325901 (Axon Medchem, cat#1408) at a final concentration of 1 µM were freshly added to the medium. Medium was changed daily and cells were passaged every second day. Cells were maintained at 37 ^{o}C, with an atmosphere of 20 % O_2/5 % CO_2.

For passaging, medium was removed and cells were washed in PBS (Gibco, cat#10010-023). Cells were then dissociated by incubation in TrypLE (Gicbo, cat#12604-013) for 3 min at 37 ^{o}C. Next, cells were collected and centrifuged for 3 min at 800 rpm. Supernatant was removed and cells were resuspended in maintenance medium, counted and plated at a density of 1 million cells/10 cm in 0.1 % gelatin (Sigma, cat#G2500)-coated dishes (BD Falcon, cat#353003).

For retinal organoids generation, cells were dissociated with TrypLE as described above and 3000 cells/well were seeded (Day 0, D0) in a low adhesion 96-well U-shaped plate (Nunclon Sphera, ThermoFisher, cat#174929). At D1, Matrigel (Corning, cat#354230) was added to each well at a final concentration of 2 %. From D0 to D7, retinal organoids were cultured at 20

% O_2/5 % CO_2, in retinal differentiation medium (GMEM, 1 % NEA, 1 % NaPyr, 0.1 % β-ME, 1.5 % KSR). At D7, retinal organoids were transferred to bacterial grade petri dishes (Greiner Bio-One, cat#633181) and kept in free-floating culture in retinal maturation media 1 (RMM1, DMEM/F-12 GlutaMAX (Gibco, cat#10565-018) supplemented with 1 % N2 (Gibco, cat#17502-048) and 1 % Penicillin/Streptomycin (P/S, Gibco, cat#15140-122)). From D7 onwards, organoids were kept in a hyperoxic atmosphere (40 % O_2/5 % CO_2). At D10, the GFP+ optic vesicles/cups of the organoids were isolated and cultured in RMM2 (DMEM/F-12 GlutaMAX supplemented with 1 % N2, 10 % FCS, 1 % P/S). From D10 to D14, EC23 (Tocris Bioscience, cat#4011) at a final concentration of 0.3 µM was freshly added to the media. RMM2 media was changed every second/third day until the end of the culture (D24).

2.2.3.2 E14Tg2a/Chrnb4-eGFP mES cell lines

Considering that the Chrnb4-eGFP mESC line was generated by genetically adding a reporter into the E14Tg2a line, the ESC culture and retinal organoid media and protocols were the same for both lines.

The E14Tg2a mESC line was kindly provided by Dr. Mike O. Karl. This line is also commercially available and has the same genetic background as Rx-GFP (129/Ola).

For mESC maintenance and passaging, the procedure was exactly the same as described above (section 2.2.3.1), however, the maintenance media composition was different. For the E14Tg2a and Chrnb4-eGFP mESC lines, the maintenance media was based in Dulbecco's Modified Eagle's Medium (DMEM, Gibco, cat#21969-035). DMEM was supplemented with 1 % NEA, 1 % GlutaMAX (alternative to L-glutamine, Gibco, cat#35050-061), 0.1 % β-ME, and 15 % heat inactivated (56 °C, 30 min) FCS. LIF and the MEK inhibitor PD0325901 were freshly added to the media at a final concentration of 2000 U/mL and 1 µM respectively.

The retinal organoid protocol used for the E14Tg2a and Chrnb4-eGFP mESC lines was almost the same as the one used for the Rx-GFP mESC. The only difference was that on D10, organoids were tri-sectioned, rather than specifically isolate GFP+ optic vesicles/cups. The composition of retinal differentiation media and RMM1 and 2 were also the same as the ones described above. E14Tg2a were cultured until D24, while Chrnb4-eGFP retinal organoids were cultured only until D18.

2.2.4 Immunohistochemistry

E15.5/P4 eyes were enucleated, shortly washed in PBS and fixed in 4% paraformaldehyde (PFA, MERK, cat#1.04005.1000) for 1 h at 4 °C. Fixed eyes were cryoprotected with a 30%

sucrose (Interchim, cat#150695) solution overnight at 4 ºC. Next day, P4 eye cups were isolated by removing the extraocular muscles, cornea, iris and lens. Isolated P4 eye cups and E15.5 eyes were embedded in Neg50 (ThermoScientific, cat#6502) freezing media and deep frozen in liquid Nitrogen. Frozen samples were kept at -80 ºC until further use.

For retinal organoids, they were collected at the desired day of culture, washed in PBS and fixed in 4 % PFA for 20 min at room temperature (RT). Next, they were also cryoprotected with a 30 % sucrose solution overnight at 4 ºC. On the next day, organoids were embedded in Neg50 and deep frozen in liquid Nitrogen. Frozen organoids were also kept at -80 ºC until further processing.

For E15.5/P4 retinas, 20 µm thick sections were obtained using a Cryostat (ThermoScientific, NX70). For the retinal organoids, sections were 12 µm thick. After collecting the sections in glass slides, these were air dried for 20 min at 37 ºC and directly used or stored at -80 ºC. For immunohistochemistry, sections were air dried for 1 h at room temperature (RT) and rehydrated for 20 min in PBS. If required by the antibody, a step of antigen retrieval by sodium citrate (10 mM, pH 6, AppliChem, cat# A3901.0500) treatment (30 min, at 70 ºC) was introduced. Then, sections were incubated in blocking buffer (5 % donkey serum, [Uptima, cat#UP77719A], 1 % bovine serum albumin, BSA [Serva, cat#11926.04], 0.3 % Triton X-100 [Serva, cat#37240]) for 1 h at RT. For some of the antibodies targeting transcription factors, DNaseI (Sigma) at a 1:100 dilution was added to the blocking step (see Table 1). Next, slides were incubated with the desired primary antibody (see Table 1) one or two overnights at 4 ºC, depending on the antibody requirements. After washing, sections were incubated with the corresponding secondary antibody (see Table 1) and 4'6-diamidino-2-phenylindole (DAPI, 1:15000, AppliChem GmbH, cat#A1001) for 1h and 30 min at RT. Finally, sections were washed again and mounted using Aqua-Polymount (Aqua-Polysciences, cat#18606-20) mounting media. Slides were then air dried overnight at RT and imaged directly or stored at 4 ºC until imaging. Images were taken using Zeiss Axio Imager Z1 with ApoTome (Zeiss). The retinal organoid sections used of S-opsin positive cells quantification were taken with WF Slide scanner, Axioscan (Zeiss).

Table 1. Primary and secondary antibodies used in this study. Secondary antibodies are all from Jackson IR and used at a dilution of 1:1000.

Antibody	Company	Catalogue #	Host	Dilution	Comments	Secondary
GFP	Abcam	AB13970	Chicken	1:800	-	Anti-ch AF488
Oct4	BD	611202	Mouse	1:500	-	Anti-ms Cy2
Nanog	ReproCell	RCAB0001P	Rabbit	1:500	-	Anti-rb Cy3

Sox2	Sigma	S9072	Goat	1:200	-	Anti-gt Cy2
SSEA-1	Stemgent	09-0005	Rabbit	1:250	-	Anti-rb Cy3
Pax6	Covance	PRB-278P-100	Rabbit	1:500	Citrate	Anti-rb Cy2, 3
Chx10	Santa Cruz	sc-21690	Goat	1:600	Citrate	Anti-gt Cy2, 3
Lhx2	Santa Cruz	sc-19344	Goat	1:200	Citrate, DNaseI, 2O/N	Anti-gt Cy2, 3
Otx2	Chemicon	AB9566	Rabbit	1:200	Citrate, DNaseI, 2O/N	Anti-rb Cy2, 3
cArrestin	Millipore	AB15282	Rabbit	1:2500	-	Anti-rb Cy3
S-opsin	Santa Cruz	sc-14363	Goat	1:200	-	Anti-gt Cy2, 3, 5
M-opsin	Millipore	AB5405	Rabbit	1:5000	-	Anti-rb Cy3, 5
Rhodopsin	Sigma	RET-P1-04886	Mouse	1:1000	-	Anti-ms AF488, Cy3
Recoverin	Millipore	AB5585	Rabbit	1:5000	-	Anti-rb Cy2, 3, 5
Calbindin	Swant	300	Mouse	1:1000	-	Anti-ms AF488
Secretagoggin	Biovendor	RD184120100	Sheep	1:500	-	Anti-sh Cy3
Gad67	Millipore	MAB5406	Mouse	1:3000	-	Anti-ms AF488
Brn3a	Santa Cruz	sc-31984	Goat	1:200	-	Anti-gt Cy3
Synaptophysin	Sigma	S5768	Mouse	1:300	-	Anti ms-AF488, Cy3
Pikachurin	Wako Chemicals GmbH	011-22631	Rabbit	1:1000	-	Anti-rb Cy3

2.2.5 RNA isolation and quantitative RT-qPCR

RNA was extracted from single organoids using the Quick-RNA MiniPrep Plus kit (Zymo Research, cat# R1057). Briefly, single organoids were collected in DNA/RNA Shield and kept at -80 °C or directly processed. Next, a proteinase K treatment (55 °C, 2-5 h) was used to dissolve the retinal organoids. Samples were then treated with RNA Lysis Buffer and filtered to remove the majority of gDNA. RNA was precipitated with ethanol, treated with DNaseI (1 U/µL) to remove the rest of gDNA, washed and eluted with DNase/RNase-Free water. Isolated RNA was kept at -80 °C until further use.

cDNA of each sample was synthetized using the SuperScript III First-Strand Synthesis System (Invitrogen, cat# 18080-051). Briefly, for each sample, RNA was mixed with oligo-dT primers and dNTPs and incubated for 5 min at 65 ºC. Then, 10 µL of previously prepared cDNA synthesis mix (per 1 reaction: 2 µL 10X RT buffer, 4 µL 25 mM $MgCl_2$, 2µL 0.1 M DTT, 1 µL RNAaseOUT (40 U/µL) and 1 µL SuperScript III RT (200 U/µL)) were added to each sample and incubated for 50 min, at 50 ºC. Reactions were terminated bringing the samples to 85 ºC for 5 min. Reactions were then chilled on ice for at least 1 min and RNase H treatment for 20 min at 37 ºC was performed. Newly synthetized cDNA was kept at -20 ºC until further use.

For real time PCR, the SYBR Green Master Mix (Applied Biosystems, cat#4367659) kit was used. For each reaction, an initial amount of 800 ng of cDNA/sample were used. Each of the primers was used at a final concentration of 400 nM. The PCR program and primers used in this study are shown in Table 2 and Table 3, respectively.

Table 2. Real time PCR program used in this study. Fluorescence was measured at the end of each annealing step.

Step	Temperature	Time	Ramp rate (ºC/s):	
Denaturation	95 ºC	10 sec	4.4	
Denaturation	95 ºC	30 sec	4.4	
Annealing	58 ºC	15 sec	2.2	40x
Amplification	68 ºC	30 sec	4.4	
Melting curve	95 ºC	5 sec	4.4	
	60 ºC	1min	2.2	
	97 ºC	-	0.11	
Cooling	4 ºC	10 min	2.2	

Table 3. Primers used in this study.

Gene	Primer	
S-opsin	F	5'-TCTCTGCTACGTGCCCTATG-3'
	R	5'-CAAGCCCGGAACTGCTTATTC-3'
Rhodopsin	F	5'-CTTCACAGTCAAGGAGGCGG-3'
	R	5'-CCCTGGTGGGTGAAGATGTAG-3'
Crx	F	5'-GTTCAAGAATCGTAGGGCGAA-3'
	R	5'-TGAGATGCCCAAAGGATCTGT-3'

2.2.6 Statistical analysis

Results are presented as box and whiskers graphs. The box extends from the 25th percentile to the 75th. Whiskers represent the minimum and maximum values. Outliers were identified using the Grubbs' method (alpha: 0.05) and next ordinary One-Way ANOVA (95% confidence interval) with multiple comparisons (Dunnett test) was performed using GraphPad. In the figures is represented as P<0.0332(*), P<0.0021(**) and P<0.0002(***)

2.2.7 Chrnb4-eGFP generation

This mouse line was generated by knocking in, using the CRISPR/Cas9 technology, the eGFP reporter under the *chrnb4* promoter of the wild type E14Tg2a mESC line and it was done in collaboration with the ES/iPS Facility in the CRTD. In this section I will describe the methods of the part I did, but not what was done within the Facility.

2.2.7.1 Genomic DNA extraction

Genomic DNA was extracted from the wild type E14Tg2a as well as for the newly generated Chrnb4-eGFP clones using the Quick-gDNA Miniprep Kit (Zymo Research, cat#D3025). Briefly, 1 million cells were used as starting material. Lysis buffer was added to the pelleted cells, next samples were shortly vortexed and left at RT for 5 min. Samples were then transferred to a Zymo-Spin column, washed and eluted. Extracted gDNA was kept at -20 ^{o}C until further use.

2.2.7.2 PCR amplification

Several PCR amplifications were required during the Chrnb4-eGFP mESC line generation. For each of them, different polymerases and PCR programs were used. The primers used are presented in Table 5.

First, amplification of the target region of the E14Tg2a genome was required. For this purpose, Phusion DNA polymerase (New England BioLabs, cat#M0530S) was used. For each 50 µL reaction, the master mix contained 10 µL of 5X Phusion Buffer, each primer at a final concentration of 100nM, 1 µL of 10mM dNTPs, 40 ng of template and 0.5 µL of Phusion DNA polymerase (final concentration 1 U/50 µL PCR). The PCR program used is presented in Table 4. The product was then run in a 1% agarose gel for 1 h at 110 V and gel eluted using the Zymoclean Gen DNA Recovery Kit (Zymo Research, cat# D4008). The recovered product was brought to a concentration of 10 ng/µL and sent for sequencing to Eurofins, according to their requirements.

Table 4. Phusion DNA Polymserase PCR Program.

98 ºC	30 sec	
98 ºC	10 sec	35x
69.4 ºC	30 sec	
72 ºC	1 min 30 sec	
72 ºC	10 min	
4 ºC	∞	

Screening PCRs were performed either with HotStar Taq Plus Master Mix (Qiagen, cat#203646), to determine right and left side integration of the construct, or with LongAmp *Taq* 2X Master Mix (New England BioLabs, cat#M0287S), to distinguish between homozygous and heterozygous integration. A 25 µL PCR reaction with the HotStar Taq Plus contained 12.5 µL of HotStar Taq Plus Master Mix (2x), 2.5 µL of CoralLoad (10x), each primer at final concentration of 200 nM and 10 ng of template. The PCR program used for those reactions is shown in Table 6. A 25 µL PCR reaction using the LongAmp *Taq* 2X Master Mix contained 12.5 µL of LongAmp *Taq* 2X Master Mix, each primer at a final concentration of 200 nM and 50 ng of template. The PCR program required for this polymerase is specified in Table 7.

Table 5. Primers used for the generation of the Chrnb4-eGFP mESC line. The guide RNA used for targeting the Cas9 is also shown in this table.

Name	Primer
Chrnb-5UTR-F	5'-TCTACCTACCGCCCATCCTGTGGCCCATCAGAG-3'
Chrnb-5UTR-F1	5'-TGAAACTTAGCGTGGACCACCTAG-3'
Chrnb-Intronl1-F	5'-TCACCATCACTGACGAGTGTCTTC-3'
Chrnb-Intron1-F1	5'-CTTCCTCCCATAAAGATCACATCC-3'
Chrnb-Intron1-R	5'-AGATATGTGCTCGCTAAAGGGTGGCTGTG-3'
EGFP-Mid-R	5'-AGAAGTCGTGCTGCTTCATGTGGTCGG-3'
NTPII-F	5'- TATCGCCTTCTTGACGAGTTCTTCTG-3
sgRNA	5'-GCGTACCCCTCATGGCCGGC-3' (PAM seq – 5'-CGG-3')

Table 6. HotStar Taq Plus Master Mix PCR program.

95 ºC	5 min	
94 ºC	30 sec	35x
65ºC	30 sec	
72 ºC	2 min	
72 ºC	10 min	
4 ºC	∞	

Table 7. LongAmp *Taq* 2X Master Mix PCR program.

98 ºC	30 sec	
98 ºC	10 sec	35x
68,5ºC	30 sec	
72 ºC	5 min 30 sec	
72 ºC	10 min	
4 ºC	∞	

2.3 Results

2.3.1 Establishment of 3D retinal organoid culture

Mouse retinal organoids were first described by Eiraku et al., 2011. A modified version of the protocol described in this publication (see section 2.2.3) was used for the experiments described in this thesis.

To establish the protocol in the lab, the *rx*-GFP mESC was used. The advantage of this line is that it expresses GFP under the *rx (Rax)* transcription factor. *Rx* is an eye field transcription factor required for retinal progenitor cell specification and proliferation and, in mouse, is expressed from embryonic day 7.5 (E7.5) onwards (Mathers et al., 1997). For retinal organoids, *rx* is detected from culture day 5 (D5) (Eiraku et al., 2011), and therefore, it can be easily visualized whether mESC aggregates are developing towards eye field tissue in early stages of the 3D retinal organoids culture. Taking advantage of the fast readout for retinal tissue induction (GFP+ organoids) provided by this line, materials which are known to be critical for this step in the retinal organoid generation protocol, including the specific 96-well plates used for mESC aggregation or the Matrigel lot, were tested (data not shown).

The combination of Matrigel lot and 96-well plate that gave better efficiency for retinal organoid generation were used for the rest of experiments. Interestingly, once the mESC aggregates were properly induced towards retinal tissue, independently of the efficiency, Matrigel lot or 96-well plate used, most of them, if not all, were able to continue developing and form a retina-like structure (see Figure 14). As an example, D24 retinal organoids obtained by using two different Matrigel lots, each one used at two different concentrations, are shown here. Immunohistochemistry analysis of these organoids did not show a significantly different expression pattern when comparing established markers, including Pax6 (at this developmental stage labelling amacrine and bipolar cells), Chx10 (in late retinal development restricted to interneurons, including bipolar cells and a subset of Müller glia (Zagozewski et al., 2014)), rhodopsin (rod photoreceptors), recoverin (pan-photoreceptor marker), cone arrestin (cone photoreceptors, not detected at D24 because is, developmentally, too early) or S-opsin (short wave sensitive cone photoreceptors).

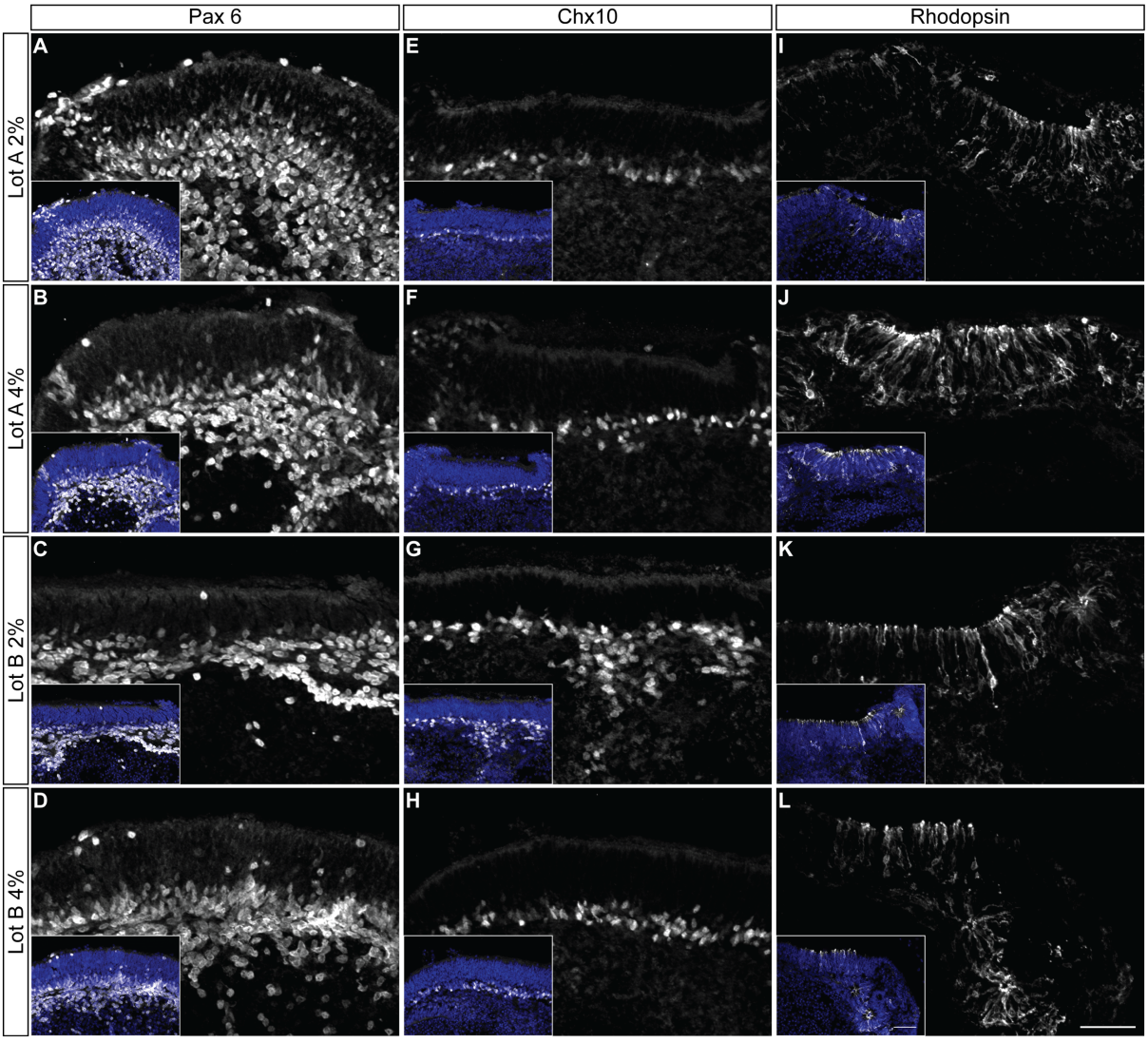

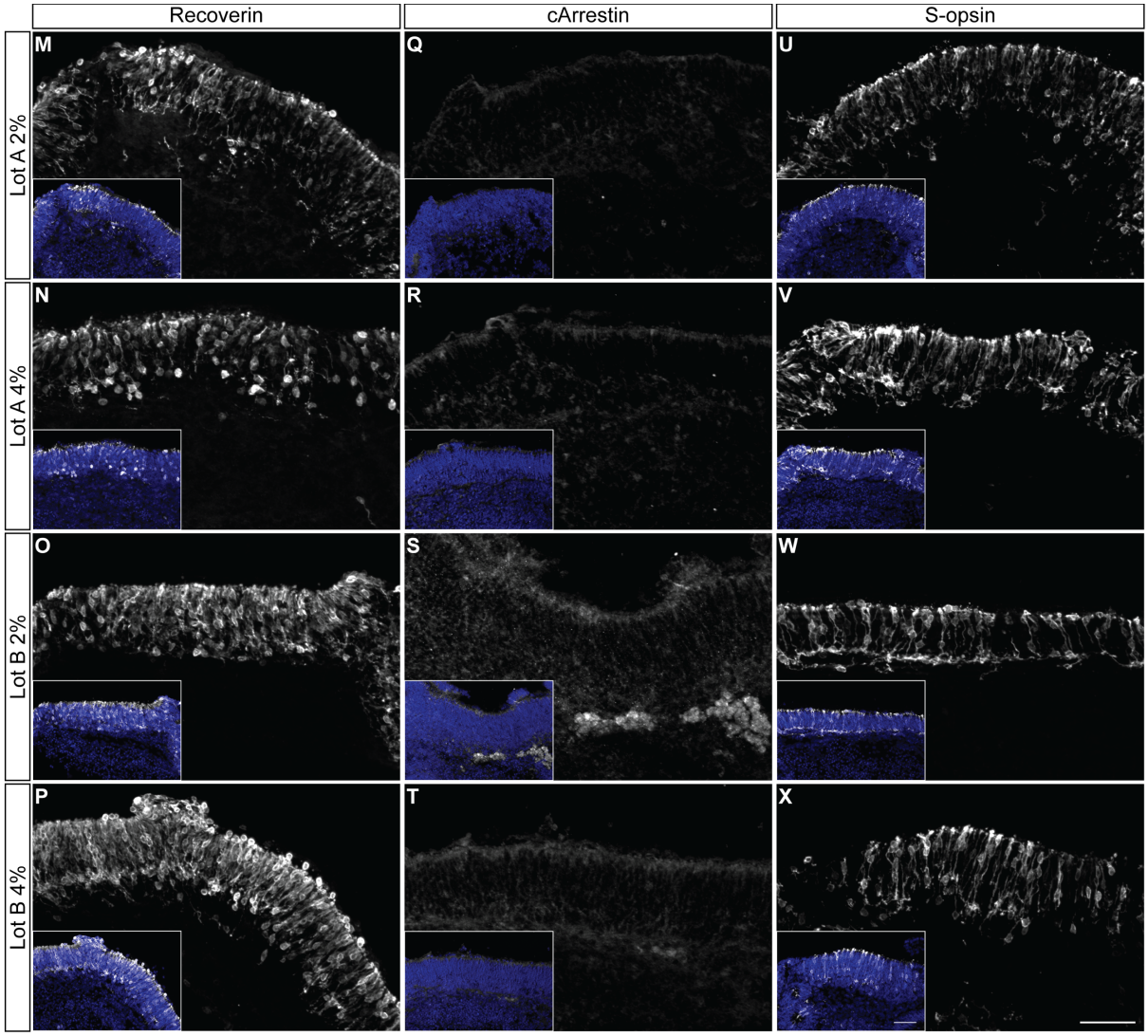

Figure 14. Establishment of 3D retinal organoid culture. Several established markers in the field were used to compare the retina-like structure of D24 retinal organoids obtained using different Matrigel lots and concentrations. At the inner-most part of the retina-like structure, Pax6 and Chx10 were detected, indicating the presence of bipolar, amacrine and ganglion cells in in this region. Photoreceptor specific markers such as rhodopsin, recoverin, and S-opsin were detected in the outer nuclear-like layer of the retinal organoids. Cone arrestin, which *in vivo* is not expressed until P9, was not detected in D24 organoids (equivalent to P4 *in vivo*). Scale bars: 50µm.

The *rx*-GFP mESC line was ideal to establish the retinal organoid culture and test several conditions. However, since GFP is expressed across the entire retinal organoid, it was not useful for the aim of this project, namely to specifically identify cone photoreceptors within the organoids. Considering that there is no mESC line available that specifically labels cone photoreceptors, I decided to generate one by adding a reporter to the wild-type E14Tg2a mESC line. Previous to generate the reporter, this line was tested for the generation of retinal organoids. As can be observed in Figure 15, cells were aggregated at D1, and upon Matrigel addition, a neuroepithelia was generated. As the organoids grew and matured, the neuroepithelia became thicker and brighter. From D18-D20 to D24, the neuroepithelia slowly became thinner and darker, indicative of retinal cells becoming post-mitotic. This could be

confirmed by IHC. It is known that Otx2 begins to be expressed in the last division of retinal progenitor cells (RPC), before they become post-mitotic (Muranishi et al., 2011). In E14Tg2a organoids, Otx2 could not be detected on D15, but it was present on D20 (Figure 16), indicating that in this period of time, cells are beginning to exit the cell cycle. Older organoids also presented a darker cell mass in the centre, which was positive for Caspase3, indicative of apoptotic cell death (data not shown). This might be due to the difficulty of nutrients to reach the centre of the organoids, which is one of the current limitations of culturing organoids for longer periods of time.

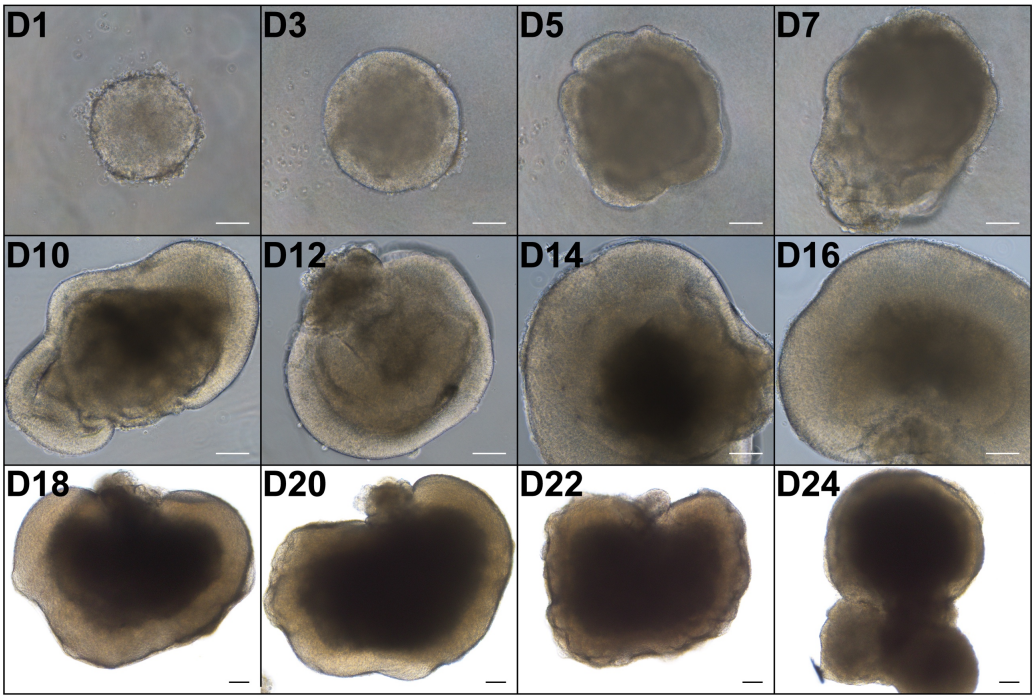

Figure 15. E14Tg2a retinal organoids development. Representative example of retinal organoid development. At D1, mESC have aggregated. From D5, a clear neuroepithelia is visible around the organoids. During growth and maturation of the organoids, the neuroepithelia becomes thicker and brighter. Once retinal progenitor cells start to exit the cell cycle and to differentiate towards their respective cell fate, the neuroepithelia starts to become thinner and darker. Scale bars: 100µm.

To assess whether these retinal organoids also recapitulated *in vivo* retinal development I compared some early and late retinal markers between embryonic retinas at E15.5 of development or post-natal day 4 (P4) retinas with organoids between D15-20 of culture and D24, respectively. The *in vivo* retinal development is described in section 1.3.

As early retinal markers (E15.5 retinas, D15-D20 organoid culture), four transcription factors were selected; three of them are key regulators of eye development (Pax6, Chx10 and Lhx2) and one of them is important for photoreceptor cell fate specification (Otx2). Since these are still expressed at later stages, i.e. P4, I also analysed their expression at later stages of retinal

organoid culture (D24). Figure 16 (A-D) shows the expression pattern, at the protein level, of those four transcription factors in E15.5 embryonic retinas, and in comparison, the expression pattern of the same genes in retinal organoids (D15 to D20). Already at D10, some cells within the organoids were positive for Pax6 (data not shown). The expression of Pax6 within the organoids increased over time; at D15 it was detected across all the neuroepithelia (Figure 16, E), and from D20 onwards its expression became restricted and localized at the basal part of the retina-like structure within the organoids (Figure 16, M). In contrast to Pax6, protein expression of Chx10, Lhx2 and Otx2 was not detected in D15 organoids. Expression of these transcription factors became detectable by IHC in organoids at D20 of culture. At that stage, Chx10 was expressed across all the retina-like structure, however, most of the Chx10+ cells were localised in the basal portion (Figure 16, F). Later in retinal organoid development (D24), a thinner layer of Chx10+ cells was detected in the basal side of the retina-like structure, similar to what is observed in P4 retinas (Figure 16, J and N). Lhx2 was expressed across all the retina-like structure at D20 and became restricted to cells within the inner nuclear-like layer of the retinal organoids at D24, resembling the expression dynamics in P4 retinas (Figure 16, C, G, K, O). At D20, Otx2 seemed to be localised on the apical side, where photoreceptor cells will be later located, while at D24, its expression was detected in the entire organoid, but in lower intensity, similar to P4 retinas (Figure 16, D, H, L, P).

As late retinal markers some of the proteins involved in the phototransduction cascade, which *in vivo* start being expressed from E18 (for example, S-opsin) onwards were selected. As a late time point, D24 of retinal organoid culture was chosen. This is the standard duration that mESC-derived retinal organoids can be kept in culture before they start to form neural rosettes within the retina-like structure and to degenerate due to lack of nutrients, especially in the centre of the organoid. As a comparison, retinas of P4 animals were used, since this is the *in vivo* time point developmentally equivalent to D24 of retinal organoid culture.

As can be observed in Figure 16, recoverin, S-opsin and rhodopsin are already detectable in P4 retinas, and these markers are localized in the outer part of the neuroblastic layer, where photoreceptors are expected to be found. S-opsin and recoverin, which are expressed from late embryonic stages, are strongly expressed, while rhodopsin, which is only expressed from P2 onwards *in vivo*, is only weakly expressed by D24 organoids as in P4 retinas. Moreover, S-opsin and recoverin at that stage are localized in the cytoplasm (cell body of the nascent photoreceptors) while rhodopsin seems to already be located at the apical most part of the photoreceptors, where the outer segments, which represent the final destination of rhodopsin, will later be generated. M-opsin cannot be detected at these early stages which is to be expected as its expression *in vivo* begins from P6 onwards. The expression pattern of these

markers in P4 retinas is mainly recapitulated in D24 retinal organoids (Figure 16). However, recoverin pattern shows more round cells in retinal organoids, rather than elongated, as observed in P4 retinas (Figure 16, Q and U). S-opsin resembles the cellular shape observed in the P4 retinas, however, far fewer S-opsin+ cells are detected within the organoids at D24 (Figure 16, S and W).

To summarize, retinal organoid development recapitulates *in vivo* retinal development, the dynamics of transcription factors such as Pax6, Chx10, Lhx2 and Otx2 are maintained in the retinal organoids, though expression is slightly delayed for some of these transcription factors compared to the *in vivo* situation. Localization of proteins belonging to the phototransduction cascade is similar when comparing P4 retinas and D24 retinal organoids.

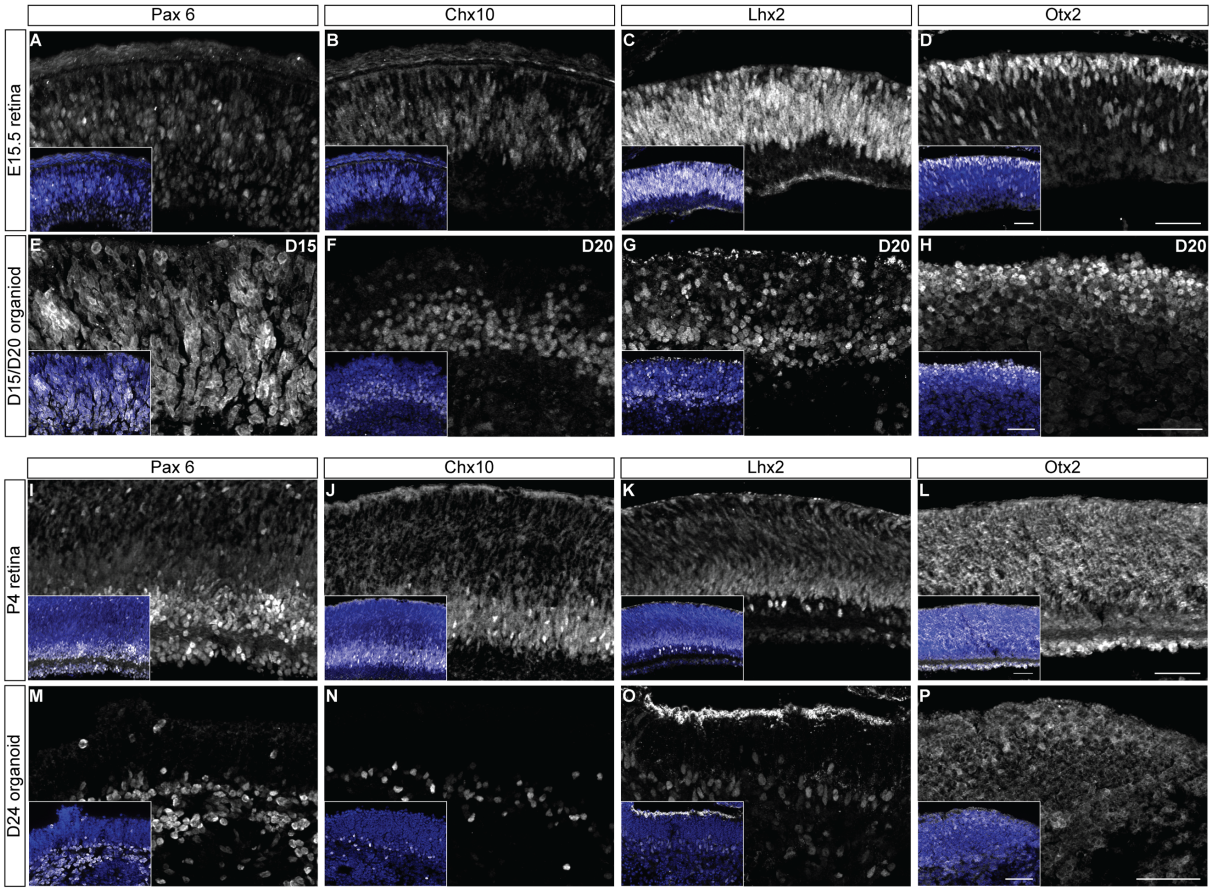

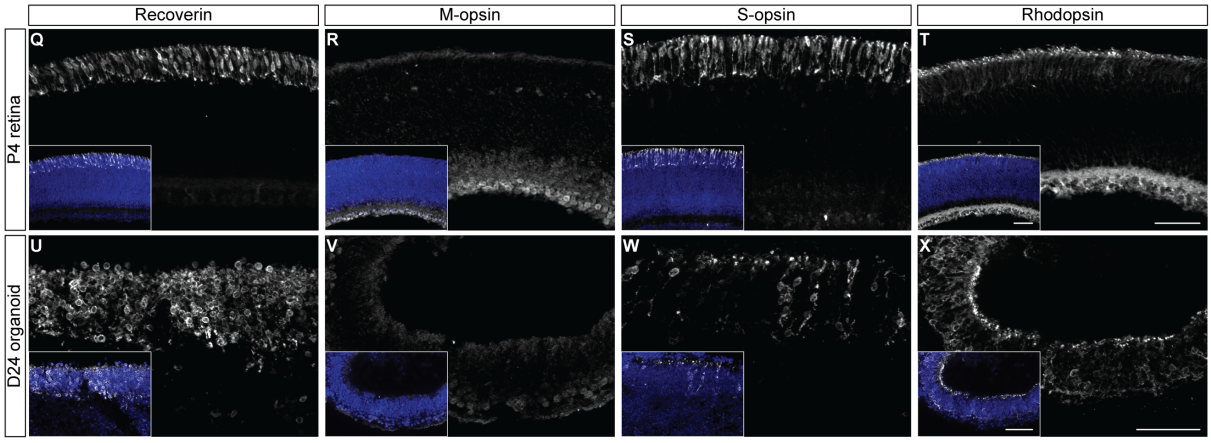

Figure 16. Organoid development recapitulates *in vivo* retinal development. Expression dynamics of the eye field transcription factors Pax6 and Lhx2, together with the transcription factors Chx10, which is important for retinal progenitor cell proliferation, and Otx2, involved in photoreceptor cell fate determination, were analysed at early (E15.5) and later (P4) developmental time points. Moreover, late retinal markers such as proteins involved in the phototransduction cascade, were analysed at later (P4) time points. **A-H)** E15.5 retinas were compared with retinal organoids at D15/D20 of culture, **(I-X)** while P4 retinas were compared to organoids at D24 of culture. At D15 of retinal organoid culture Pax6 is expressed across the developing retina-like structure, while Chx10, Lhx2 and Otx2 were not detected at that time (data not shown), but their expression at D20 resembled the E15.5 *in vivo* situation. At D24, all the markers resembled their expression pattern at P4. The different opsins analysed and recoverin presented a similar pattern in both, *in vivo* P4 retinas and D24 retinal organoids. Scale bars: 50µm.

As a last step of characterization, D24 organoids were collected and analysed by IHC for several other markers, in order to look not only for photoreceptors, but also for the presence of other retinal cell types. As can be observed in Figure 17, the organoids presented, in fact, all principle retinal cell types, and additionally showed expression of the synaptic marker synaptophysin. Both, rod and cone photoreceptors were detected in the outer nuclear-like layer within the organoids. As expected, and comparable to the *in vivo* situation (97% rods, 3% cones), rod photoreceptors (rhodopsin) were clearly more abundant than cone photoreceptors (S-opsin) within the E14Tg2a organoids. S-opsin, however, may underestimate the total number of cone photoreceptors. The ideal marker for cone photoreceptors would be cone arrestin, however as previously mentioned, cone arrestin is not expressed until later stages of development. M-opsin is also expressed later on, and therefore, is not detected in D24 organoids, as also shown in Figure 17. Nonetheless, it is important to mention that there is a high variability between organoids (see section 2.3.2) across mESC lines, and even within the same mESC line and differentiation cycle. The other main retinal cell types, including bipolar (Chx10, Secretagoggin), horizontal (Calbindin), amacrine (Gad67, Pax6) and ganglion cells (Pax6, Brn3a) were also detected within the retinal organoids.

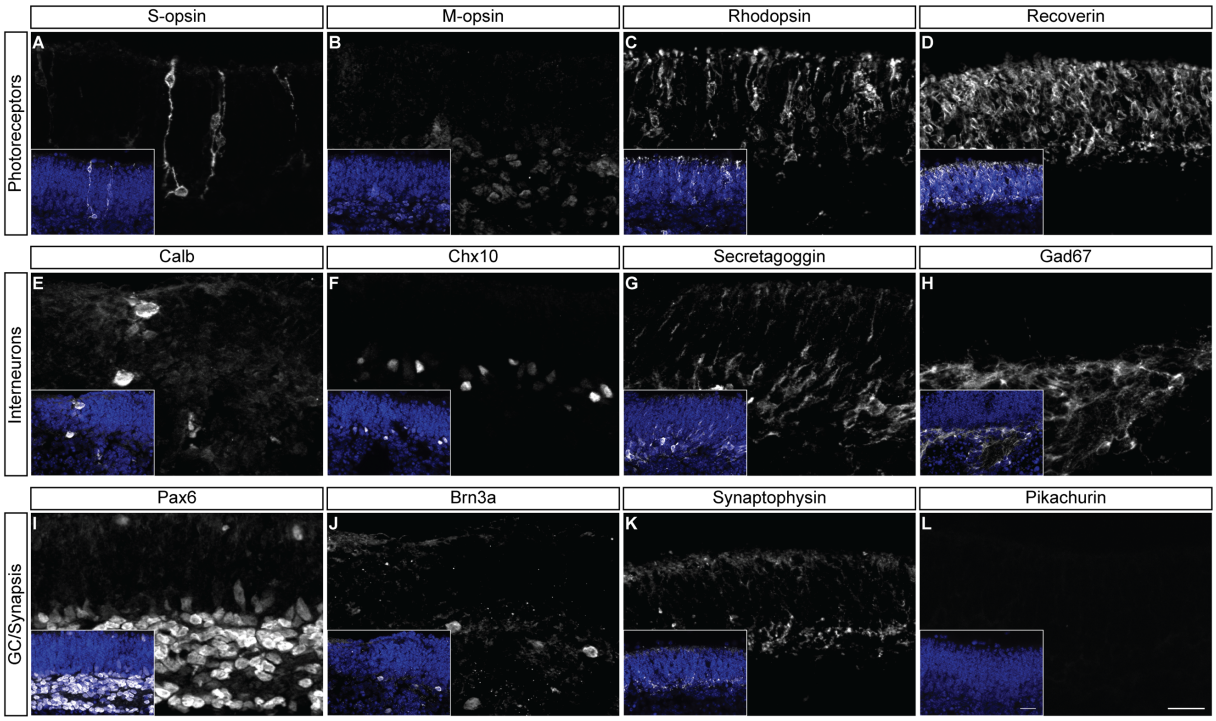

Figure 17. Characterization of D24 E14Tg2a retinal organoids. Retinal organoids at D24 were analysed for the presence of different retinal cell types: photoreceptors (S-opsin, M-opsin, Rhodopsin and Recoverin), horizontal cells (Calbindin), bipolar cells (Chx10, Secretagoggin), amacrine cells (Gad67, Pax6) and ganglion cells (Pax6, Brn3a). The presence of synaptic markers was also analysed, and synaptophysin was detected, while pikachurin was not detected. Scale bars: 20µm.

Taken together, these results indicate that the retinal organoid culture was properly established in the laboratory. Retinal organoids could develop until D24 and recapitulate early retinal development. Moreover, all major retinal cell types were found to not only be present in the retinal organoids but were also properly apically or basally located. Even though pikachurin mRNA is detected from E14.5 *in vivo* (Sato et al., 2008), no protein was detected in D24 organoids. However, detection of synaptophysin indicates that there might be synaptic connections between photoreceptors and interneurons within the retinal organoids. Nonetheless, to test this hypothesis, techniques such as calcium imaging or extracellular recordings using microelectrodes should be performed.

2.3.2 Quantification of cone photoreceptors within the mESC-derived retinal organoids

Cone photoreceptors represent a minor proportion (3%) of photoreceptors in the mouse retina, and an even lower percentage (<0.1%) within the retinal organoids (Eiraku et al., 2011). For photoreceptor transplantation approaches, high numbers of donor cells are required, and therefore, different treatments were applied to the retinal organoids with the objective of increasing the number of cone photoreceptors within them.

It has been shown that the Notch signalling pathway inhibitor N-[N-3,5-Difluorophenylacetyl)-L-alanyl]-S-phenylglycine t-butyl ester (DAPT) leads to an increase of cone or rod photoreceptors in retinal explants and organoids when applied at early (E12.5) or late (P1) developmental stages respectively (Nelson et al., 2007; Völkner et al., 2016). Moreover, it has been shown that after treating human ESC (hESC) with Dand5 (Coco protein), which simultaneously inhibits BMP, TGFβ and Wnt signalling pathways, around 60% differentiate towards S-cone photoreceptors (Zhou et al., 2015), however, this has not been yet shown in mouse organoids. IGF is also reported to increase the differentiation rate towards cone photoreceptors (Zhou et al., 2015).

For these reasons, retinal organoids obtained from the E14Tg2a mouse ESC line were treated with DAPT and COCO protein alone or in combination with IGF. The applied treatments were the following: i) DAPT from D12-14, ii) COCO protein from D10-24, iii) COCO protein from D12-14, iv) COCO protein + IGF from D10-24 and v) COCO protein + IGF from D12-14. The timing used for DAPT treatment was decided according to previous publications (Völkner et al., 2016). Regarding the treatment with COCO protein and IGF, no published data was available for mouse retinal organoids. Therefore, considering that Dand5 expression is detected from E9.5 in the mouse optic vesicle, and maintained at least until P6 in the photoreceptor layer (Zhou et al., 2015), I decided to treat retinal organoids from D10 until the end of the culture (D24) and, alternatively, as a comparison to DAPT from D12 to D14. Dimethyl sulfoxide (DMSO) - treated organoids were used as vehicle control and non-treated organoids were used as a positive control for the differentiation protocol.

Control and treated retinal organoids were analysed by IHC for the presence of S-opsin positive cells as well as by RT-qPCR for the expression of *s-opsin, rhodopsin* and *crx* transcripts.

For the IHC analysis, 7-11 organoids per condition were analysed. For each organoid, 2-3 cryosections spanning the entire organoid were stained for S-opsin and positive cells were quantified. The area of each section was calculated using the ZenBlue software. An example of a section used for quantification is shown in Figure 18, A, and the quantification results are shown in Figure 18, B. As previously shown for DAPT treatment, a statistically significant ($P < 0.05$) increase of S-opsin positive cells was obtained compared to the control organoids (Figure 18, B). None of the other conditions tested showed a significant increase of S-opsin positive cells compared to the controls. Unfortunately, sections from the organoids treated with

hCOCO+IGF (D10-24) were lost during the analysis. Similar results were obtained using rx-GFP-derived retinal organoids (data not shown).

Single retinal organoids (n=6 per condition) were used for RNA extraction and RT-qPCR analysis. Variations in the amount of *s-opsin*, *rhodopsin* and *crx* transcripts across conditions were analysed. As can be observed in Figure 18, C, no statistically significant differences in the amounts of *s-opsin* and *rhodopsin* transcripts between the differentially treated organoids were observed. Only a decrease on the total amount of photoreceptors (*crx* transcript, Figure 18, c3) was observed after treating the organoids with DAPT, compared to the other culture conditions. Similar results were obtained using rx-GFP-derived retinal organoids. The only difference being that in rx-GFP derived retinal organoids *crx* transcript did not show any statistically significant differences (data not shown).

After quantifying the amount of S-opsin positive cells within the mESC-derived retinal organoids it was estimated that in a best-case scenario, a maximum of 3500 S-opsin+ cone photoreceptor cells per organoid could be obtained. According to Ortín-Martínez et al., 2014, a mouse retina contains in total around 185000 cone photoreceptors therefore, in an ideal situation (i.e. recovering all the cone photoreceptors after organoid dissociation and cone purification) at least 50 mESC-derived retinal organoids would be required to transplant one single mouse eye. However, in a more realistic situation, in which mESC-derived cone photoreceptors would be lost during the procedure, the initial number of retinal organoids required for one complete experiment, for example, including IHC, RT-qPCR and functional analysis of the transplanted retinas, increases to a limit that makes the experiment unrealistic.

In summary, none of the treatments applied to the retinal organoids led to a sufficiently efficient increase in the number of cone photoreceptors required for transplantation approaches.

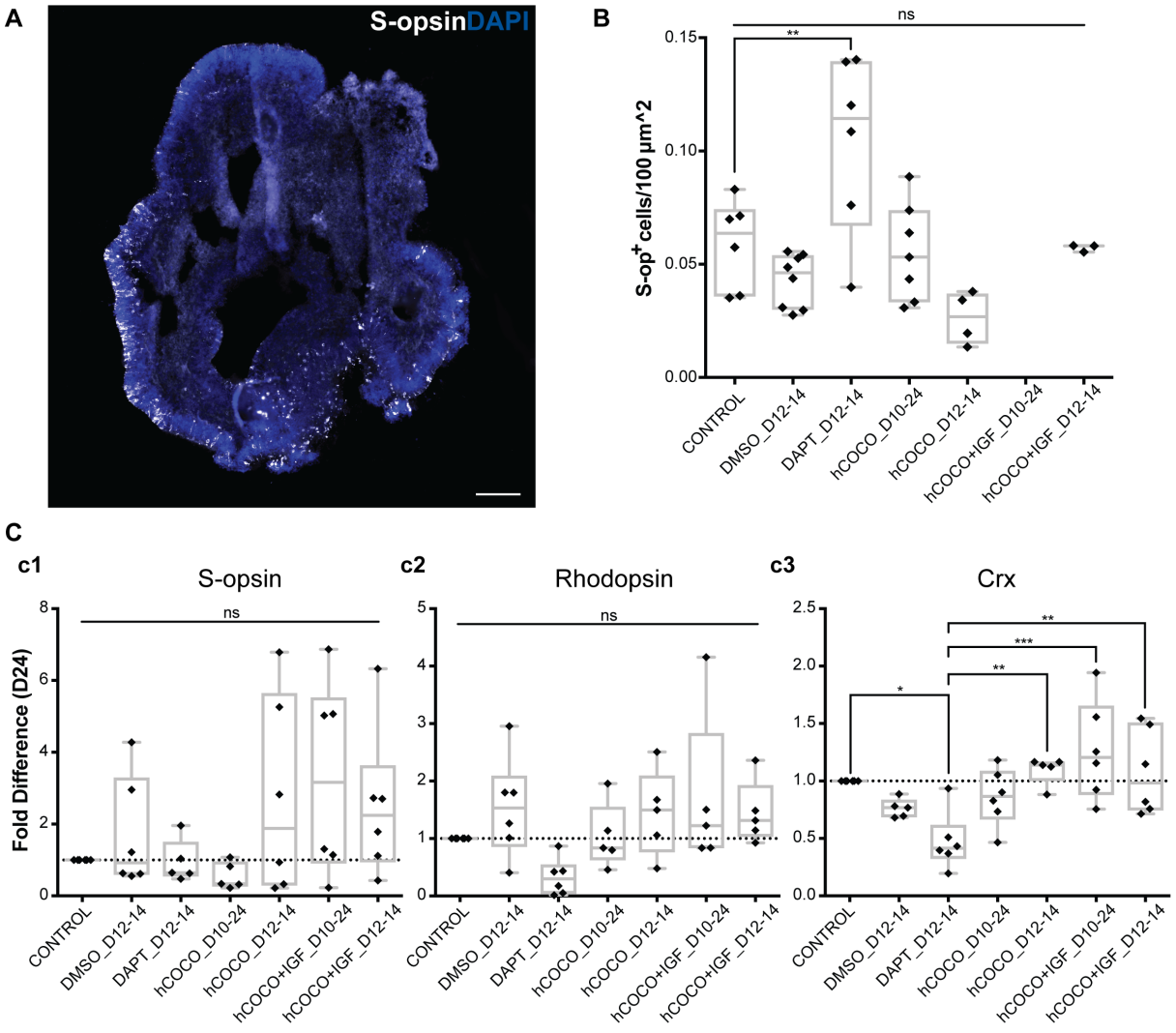

Figure 18. Quantification of cone photoreceptors within retinal organoids. A) Representative image of a retinal organoid section used for S-opsin positive cell quantification. Images were taken with WF Slide scanner, Axioscan (Zeiss) using a 40x objective. **B)** Quantification of S-opsin positive cells/100µm^2 of retinal organoid per treatment condition. **C) c1)** *s-opsin* **c2)** *rhodopsin* **c3)** *crx* transcript quantification per treatment condition (n=6 per treatment condition). Scale bar: 100µm.

2.3.3 Generation and characterization of the Chrnb4-eGFP mESC line

Thus far cone photoreceptor identification was assessed within the organoids based on the detection of S-opsin positive cells. This approach however, is not optimal. First, S-opsin labels S-cones which is not the only type of cone photoreceptor within the mouse retina therefore the total number of cones within the retinal organoids might be underestimated. Second, as previously mentioned, S-opsin is a late cone marker, so expression begins during the maturation of cone photoreceptors (E18). For the purpose of this project, though, I was interested in isolating cone photoreceptor precursors during the peak of generation which occurs around E15.5 of development.

Since early cone-specific reporter mouse ESC lines are not available in the field, I decided to generate one. Decembrini and colleagues, using the Chrnb4-GFP mouse line, reported that *chrnb4* is expressed in early retinal progenitors from E11. Later in development, from E15.5 to E18, *chrnb4* expression becomes progressively restricted to cone precursors, and therefore, they suggest that the Chrnb4-GFP mouse line traces early-born cones in E15.5 retinas (Decembrini et al., 2017). Therefore, in collaboration with the ES/iPS cell facility in the CRTD, we introduced the eGFP reporter under the control of the *chrnb4* promoter in the E14Tg2a mESC line.

First, we generated a construct containing the eGFP protein followed by an FRT floxed neomycin resistance cassette expressed under the constitutive PGK (phosphoglycerate kinase) promoter. In order to target this construct in the desired place within the E14Tg2a genome, right after the translation initiation codon (ATG) of the *chrnb4* gene, a 1000bp homology arm at each side of the described construct was cloned. To generate these homology arms, the target region of the E14Tg2a genome was used. The resulting construct was then electroporated into E14Tg2a mES cells and introduced into their genome using CRISPR/Cas9 technology. The goal was that one of the alleles of the *chrnb4* gene within the E14Tg2a mESC line genome would be disrupted by the integration of the construct, allowing the eGFP reporter to be expressed under the control of the native *chrnb4* promoter, and the other allele would remain wild type allowing the expression of the *chrnb4* gene (Figure 19).

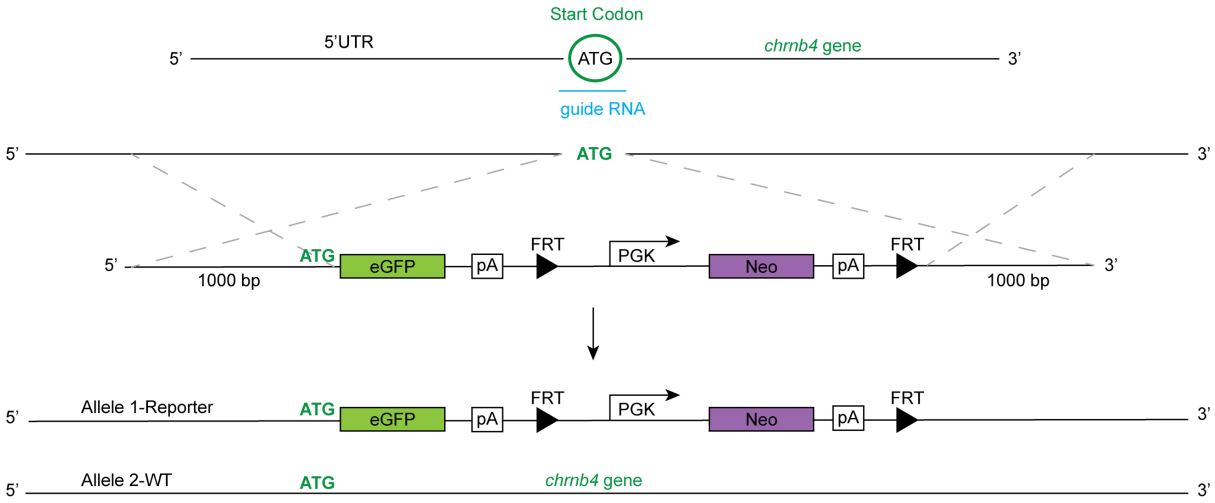

Figure 19. Chrnb4-eGFP mESC line generation. The target region of the E14Tg2a mESC line genome was amplified by PCR and used to generate the right and left homology arms of the construct. The other components of the construct were amplified from plasmids kindly provided by the ES/iPS cell facility in the CRTD. The final construct was built by joining each of the previously amplified components. Using the CRISPR/Cas9 technology, the designed construct was introduced into the E14Tg2a mESC line genome, under the control of the *chrnb4*

promoter. The goal was to have one allele containing the reporter construct, and the other allele wild type, so the *chrnb4* gene could still be expressed.

After electroporation of the construct into the E14Tg2a mESCs, cells were allowed to recover for 3 days. Then, the antibiotic G418 (aminoglycoside related to Gentamycin) was added to the media at a concentration of 450 µg/mL to select for the cells which incorporated the construct. The required concentration was previously determined by a killing curve (data not shown). After 7 days of treatment, 10 single surviving colonies were selected and expanded. Genomic DNA was extracted for each of the colonies and analysed by PCR for the correct integration of the construct. First, two different PCRs with relatively small amplicons (1355 bp /1505 bp) were used to determine the presence of the construct. One of the PCRs amplified the left side of the construct, the forward primer (Chrnb-5UTR-F) was located within the left homology arm and the reverse primers within the eGFP sequence (EGFP-mid-R). The other PCR amplified the right side of the construct, with the forward primer located within the Neomycin cassette (NPTII-F) and the reverse on the right homology arm (Chrnb-Intron1-R). The construct was detected in 4 of the selected clones (Figure 20, A). Next, the external primers (Chrnb-5UTR-F and Chrnb-Intron1-R) were used to distinguish whether those clones where homozygous (construct inserted in both alleles; one band at 5224 bp) or heterozygous (construct inserted in one of the alleles; two bands, one at 5224 bp [construct allele] and one at 2273 bp [wild type allele]). As can be observed in Figure 20, B, all the clones were found to be heterozygous as two different bands were detected after PCR amplification.

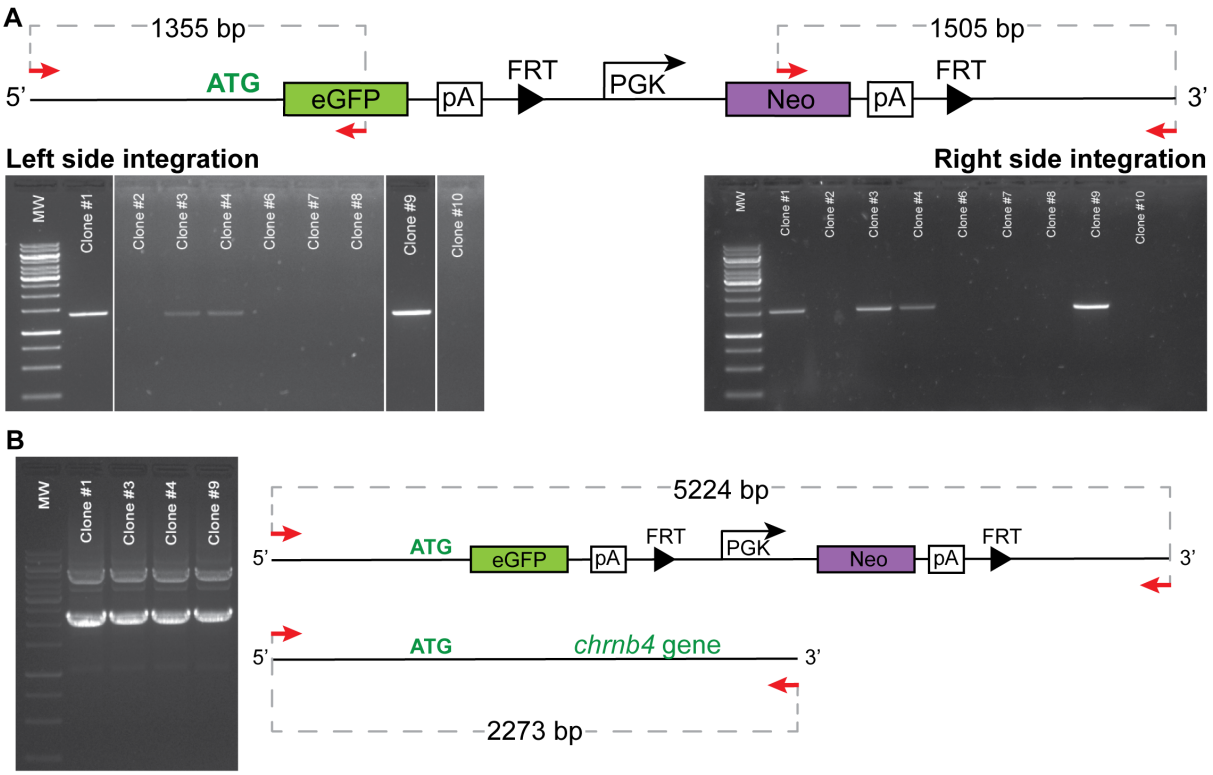

Figure 20. Screening PCRs to select for the clones that incorporated the construct. A) PCRs to analyse for the correct integration of the construct. To look for the left side integration, a primer binding on the left homology arm (Chrnb4-5UTR-F) and one on the eGFP sequence (EGFP-mid-R) were used, and a band at 1355 bp was detected in four of the analysed clones. For the right side integration, a primer binding on the Neomycin sequence (NPTII-F) and one binding on the right homology arm (Chrnb-Intron1-R) were used, and a band at 1505 bp was detected in the same four clones that presented a band for the left side integration. **B)** The four clones that presented the construct were then analysed to distinguish whether they were heterozygous (two bands, 5224 and 2273 bp) or homozygous (one band, 5224 bp). In that case, the primers binding the left (Chrnb-5UTR-F) and right (Chrnb-Intron1-R) homology arm were used. All the clones which had integrated the construct resulted to be heterozygous. MW: 250, 500, 750, 1000, 1500, 2000, 2500, 3000, 3500, 4000, 5000, 6000, 8000, 10000 bp (ThermoScientific, cat#SM0313).

Finally, for each of the clones, the wild type and the construct-containing alleles were sequenced (MPI-CBG Sequencing facility) in order to detect whether indels (insertions/deletions) had occurred due to the CRISPR/Cas9 technology within the wild type allele, and if the construct was inserted correctly within the E14Tg2a genome. Fortunately, all the clones had the correct sequences and had incorporated the construct as desired.

The clones were then expanded to generate a storage and a working cell bank to: karyotype the generated clones in order to analyse whether chromosomal integrity was maintained after genomic modification, test for the pluripotency of the cells via expression of Nanog, Oct4, Sox2 and SSEA-1, and to generate retinal organoids with the newly generated mESC reporter line. Considering that the Chrnb4-eGFP mESC line was produced on a fully characterized existing mESC line (E14Tg2a), the pluripotency characterization done in this study was only to confirm

at a basic level that the pluripotency of the cells had not been affected. As can be observed in Figure 21, Chrnb4-eGFP mESC cells kept the typical colony morphology of mESC cells, and are positive for Oct4, Nanog and SSEA-1. Sox2, which together with Oct4 and Nanog, is one of the key transcription factors regulating pluripotency, was hardly detectable.

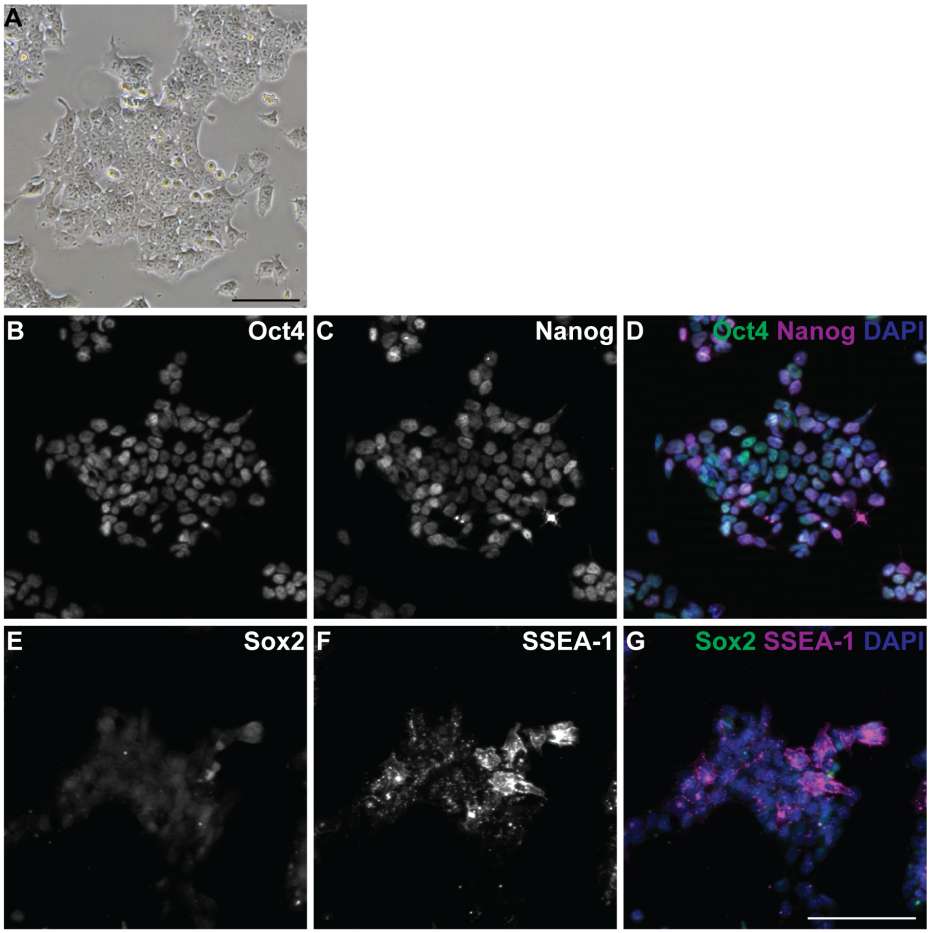

Figure 21. Characterization of the newly generated Chrnb4-eGFP mESC line. Representative example of the pluripotency characterization of the Chrnb4-eGFP mESC line. **A)** Typical morphology of a Chrnb4-eGFP mESC colony. **B-G)** Analysis of the expression of the pluripotency markers Oct4, Nanog, Sox2 and SSEA-1. Scale bars: 100µm.

The same protocol established to generate retinal organoids from E14Tg2a mESC cells was used to differentiate Chrnb4-eGFP mESC towards retinal organoids. The addition of the reporter did not affect the mESC's capacity to be induced towards the eye field and generate retinal organoids. In this case, organoids were kept in culture until D18 when they were collected for isolation and transplantation of GFP positive cells. Previous to transplantation, organoids at earlier time points were collected and characterized using the early markers Pax6, Chx10, Lhx2 and Otx2. From D9 onwards, the expression of GFP within the organoids was also analysed. Figure 22 shows the development of Chrnb4-eGFP retinal organoids and the presence of GFP.

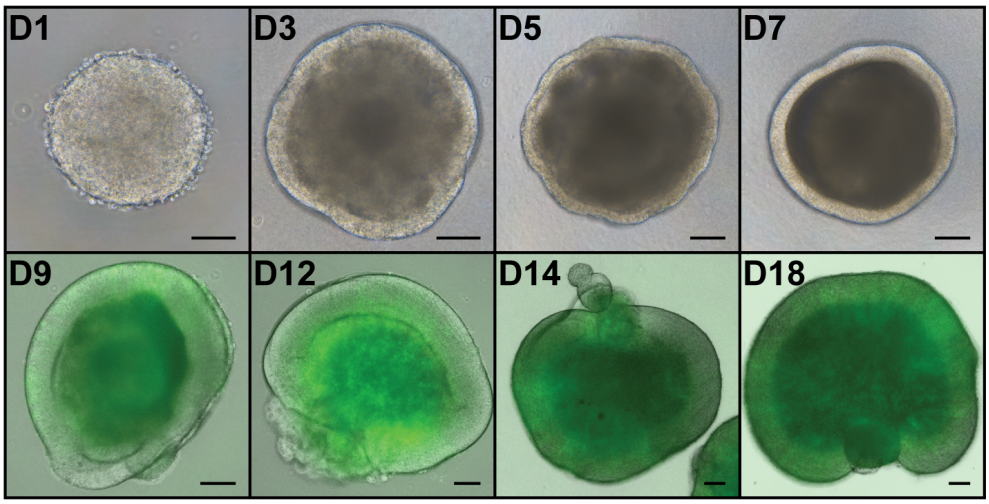

Figure 22. Chrnb4-eGFP retinal organoid development. Chrnb4-eGFP mESCs had the capacity to develop towards retinal organoids and generate a retina-like structure. Scale bars: 100µm.

Figure 23 shows part of the immunohistochemistry-based characterization of the Chrnb4-eGFP retinal organoids. Each of the earlier retinal markers, as well as the GFP reporter, are shown at D14 and D18 of organoid development, however, each marker was analysed on D9, D12, D14, D16 and D18. Pax6 was detected from D9 onwards, spanning the entire retinal-like structure of the organoids. Otx2 expression was not detected until D12-D14, in which some isolated cells within the retina-like structure were positive. Later on, as can be observed at D18 (Figure 23, L), Otx2 was mainly localized at the outer-most part of the retina-like structure. Chx10 was not detected until D14, in which a weak expression of Chx10 was detected in cells across all the retina-like structure. Later on, Chx10 became localized mostly at the inner-most part of the retina-like structure. Lhx2 was not detected until later stages. It was detected from D16, localized across the entire retina-like structure, and at D18, the external-most cells of the organoids began to downregulate Lhx2 expression.

GFP reporter expression was detected within the retina-like structure from D10-D12 in some of the organoids, however, it was not reliably detected until D14 of retinal organoid development. This developmental time in which GFP reporter is detected within the organoids resembles the *in vivo* detection of GFP under the *chrnb4* promoter (Decembrini et al., 2017). At D18, examples of double positive cells for each of the markers (i.e. Pax6, Chx10, Lhx2 and Otx2) and eGFP cells were observed (Figure 23, arrows), as well as single eGFP positive cells. Otx2/eGFP double positive cells might be potential cone photoreceptors, since Otx2 is expressed in cells that will become photoreceptors from the moment they become post-mitotic. Double positive cells for eGFP and the other markers (Pax6, Lhx2 and Chx10), however, might correspond to proliferative progenitors since these transcription factors become restricted to non-photoreceptor cells along development.

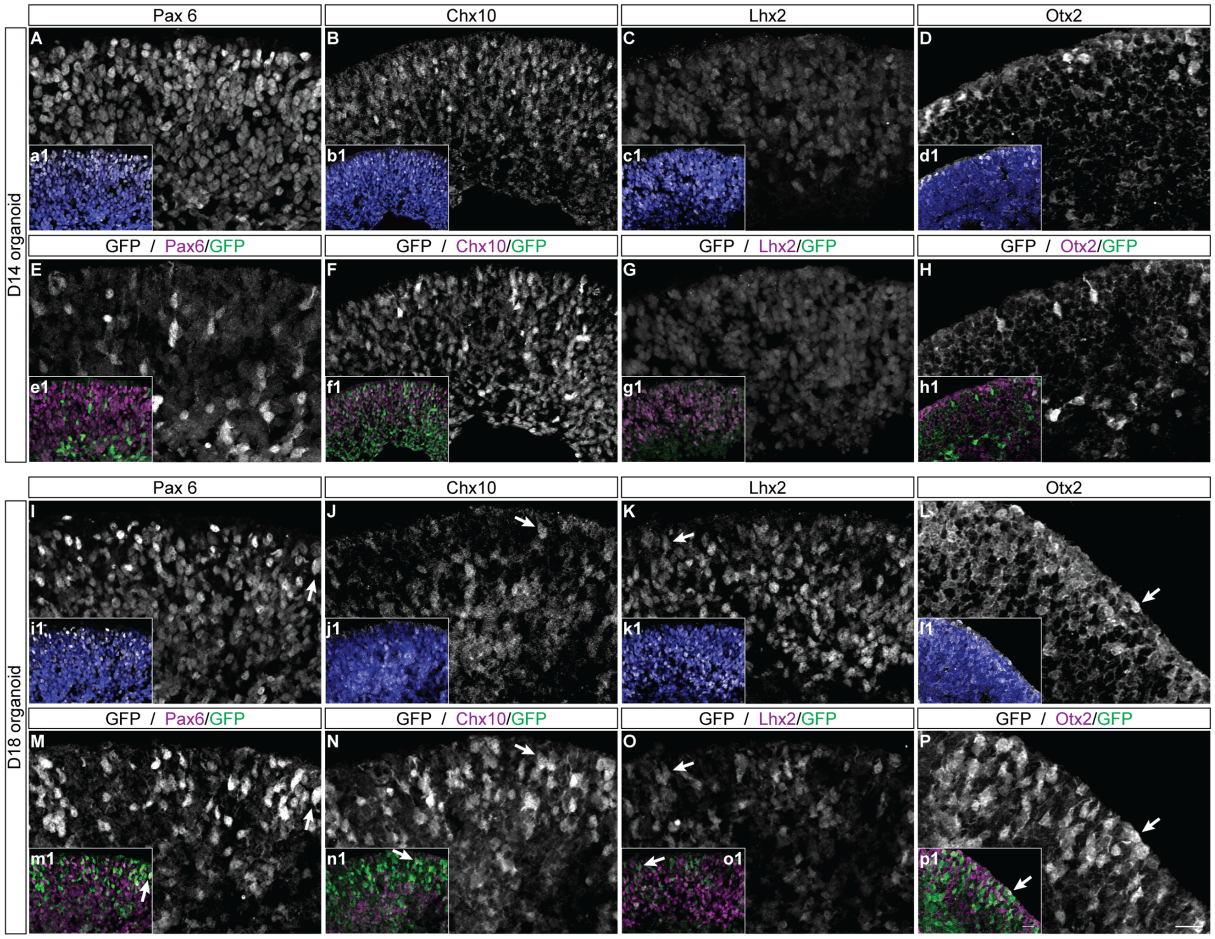

Figure 23. Immunohistochemistry characterization of Chrnb4-eGFP retinal organoids. Chrnb4-eGFP retinal organoids were analysed for early retinal markers (Pax6, Chx10, Lhx2 and Otx2) as well as for eGFP reporter. Here, two of the analysed time points are shown. The first two rows **(A-H)** correspond to D14 of retinal organoid culture, the last two rows **(I -P)** correspond to D18, time point in which organoids were collected for transplantations. **A-D, a1-d1, I-J, i1-f1)** Corresponding early retinal marker with/without DAPI. **E-H, e1- h1, M-P, m1-p1)** Corresponding early retinal marker with/without eGFP reporter. Arrows: examples of double positive cells for the corresponding early retinal marker and eGFP reporter. Scale bars: 20µm.

On D18 of culture, Chrnb4-eGFP retinal organoids were collected, dissociated to single cells and eGFP positive cells were FACS sorted and transplanted into the sub-retinal space of wild type and cone photoreceptor function loss (cpfl1) mice. The culture day in which organoids were used for transplantation was chosen as a compromise between the stage in which eGFP is restricted to cone photoreceptors only (starting progressively from E15.5 - E18 *in vivo*, (Decembrini et al., 2017)), which appears to be slightly delayed in organoids, as described above (see 2.3.1), and the post-mitotic stage that has been described as the ideal developmental stage for transplantation (See 1.5.1), which for cones corresponds to E16 *in vivo*.

After dissociation of D18 Chrnb4-eGFP organoids and FACS analysis, around 5% of the cells were positive for the eGFP reporter (See Figure 24). Wild type and cpfl1 mice were

transplanted with 100000 eGFP sorted and unsorted Chrnb4-eGFP derived retinal cells as described in section 3.2.4.

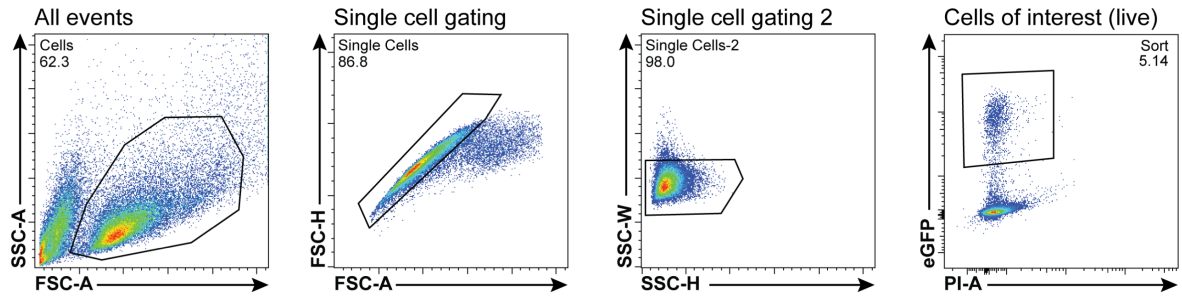

Figure 24. Gating strategy for sorting eGFP positive cells from dissociated Chrnb4-eGFP retinal organoids. A SSC-A vs. FSC-A plot was used to identify the cell population from the rest of events (debris). Two different plots (FSC-H vs. FSC-A and SSC-W vs. SSC-H) were used to gate for the single cells. To identify live eGFP positive cells, eGFP channel was ploted against PI channel. The gate shown in this plot was used to sort eGFP positive cells for transplantation. SSC-A: Side Scatter Area, SSC-H: Side Scatter Height, SSC-W: Side Scatter Width, FSC-A: Forward Scatter Area, FSC-H: Forward Scatter Height, PI: Propidium Iodide.

Three weeks post-transplantation, transplanted eyes were analysed *in vivo* for the presence of an eGFP cell mass using the MicronIV retinal imaging microscope. Next, retinas were collected and analysed by IHC for the presence of late retinal markers within the eGFP cell mass and for the presence of eGFP positive cells within the host retinas.

From the 8 eyes analysed, all of them presented a cell mass three weeks post-transplantation, indicating that the transplanted cells (FACS sorted or unsorted) were able to survive within the sub-retinal space of the host retinas. As expected, the cell mass obtained after transplanting an unsorted cell population contained mainly eGFP negative cells, and isolated clumps of eGFP positive cells (data not shown). The cell mass observed after transplanting an eGFP positive cell population contained mainly eGFP positive cells with different eGFP expression intensities (Figure 25, D, J). However, none of the transplanted retinas presented eGFP positive cells within the host outer nuclear layer, indicating that the transplanted cells do not have the capacity to interact (See Chapter 3: Cytoplasmic material transfer upon photoreceptor precursor transplantation) with the host retina.

Three weeks post-transplantation, the age of the transplanted cells should correspond to around P19 *in vivo* (18 days of culture plus 21 post-transplantation), stage in which late retinal markers such as rhodopsin, recoverin, cone arrestin, M-opsin and S-opsin should be expressed. As expected, the eGFP positive cell mass was negative for rhodopsin (Figure 25, F, f1, L, l1) as eGFP is expressed under the *chrnb4* promoter and should be restricted to cone

photoreceptors. Rhodopsin was detected only at the edge of the eGFP positive cell mass, and most likely comes from rod outer segments of the host retina that, after processing the transplanted retinas, remained attached to the cell mass.

Several recoverin positive cells were found within the cell mass obtained after transplanting eGFP positive sorted cells, however, eGFP and recoverin did not always co-localise. Both, single recoverin+ and eGFP+ cells were observed. Occasionally, some double positive (recoverin/eGFP) cells were identified (Figure 25, e1, k1). The amount of cone arrestin, M-opsin or S-opsin positive cells within the cell mass obtained following eGFP+ cell transplantation was lower than expected. Again, in most of the cases, cone arrestin, M-opsin or S-opsin did not co-localise with eGFP positive cells within the cell mass, however, examples of double positive cells for each of those late markers were also found (Figure 25, g1, h1, i1, n1, o1).

Taken together, the results indicate that sorting of eGFP+ cells from D18 Chrnb4-GFP retinal organoids allows to select a non-rod photoreceptor cell population. However, it does not seem to help to sort for a cone-only cell population, since very few cells expressing cone-specific markers were detected in the cell mass obtained after transplanting a sorted eGFP positive cell population.

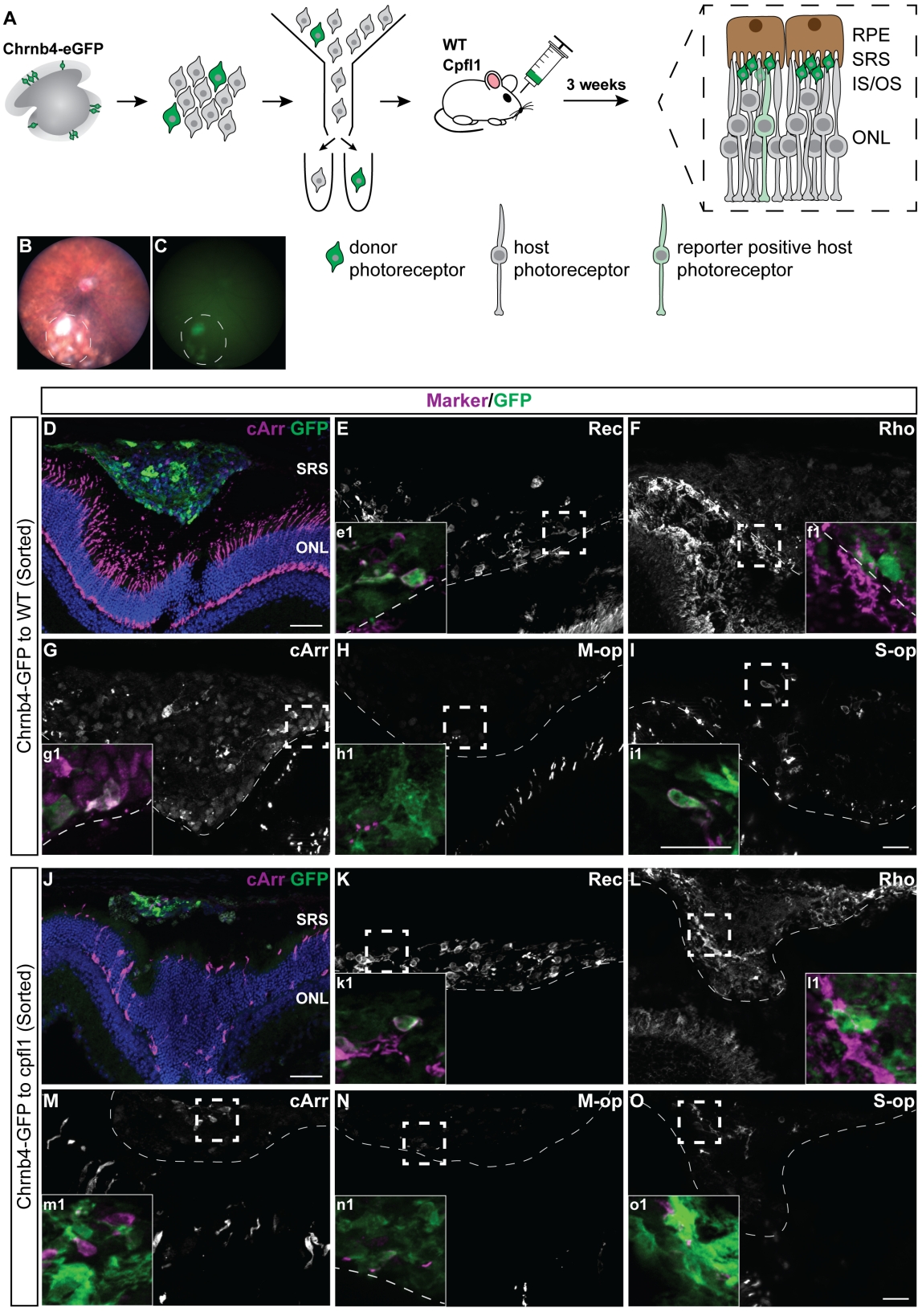

Figure 25. Analysis of transplanted retinas using as donor cells the eGFP+ cell population of D18 Chrnb4-eGFP retinal organoids. A) Schematic representation of the experimental design. Shortly, retinal organoids were obtained using the Chrnb4-eGFP mESC line. At D18 of culture, such organoids were dissociated to single cells, and the eGFP positive population was FACS sorted and transplanted into the SRS of WT and Cpfl1 mice. Three weeks post-transplantation, host retinas were analysed for the presence of mESC-derived cone photoreceptors. **B,**

C) Representative image of eye fundus of a transplanted retina obtained using MicronIV retinal imaging microscope (brightfield and GFP channel. **D-l)** Analysis for the presence of cone photoreceptors within the cell mass after transplanting the eGFP positive cell population of D18 Chrnb4-eGFP retinal organoids into the SRS of WT hosts. **e1)** Example of a recoverin/eGFP double positive cell. **f1)** Rhodopsin and eGFP do not co-localise within the eGFP positive-derived cell mass. **g1-i1)** Examples of cone-specific markers/eGFP positive cells. **J-O)** Analysis for the presence of cone photoreceptors within the cell mass after transplanting the eGFP positive cell population of D18 Chrnb4-eGFP retinal organoids into the SRS of Cpfl1 hosts. **k1)** example of a recoverin/eGFP double positive cell. **l1)** Rhodopsin and eGFP do not co-localise within the eGFP positive-derived cell mass. **m1)** Example of cone arrestin single positive cell. **n1)** Example of M-opsin/eGFP double positive cells. **o1)** Example of S-opsin/eGFP double positive cell. RPE: retinal pigment epithelium, SRS: sub-retinal space, IS/OS: inner segments/outer segments, ONL: outer nuclear layer, WT: wild type, cpfl1: cone photoreceptor function loss 1, Rec: recoverin, Rho: rhodopsin, cArr: cone arrestin, Mop: M-opsin, Sop: S-opsin. Scale bars: 50μm (D, J), 20μm (E-I, K-O, e1-i1, k1-o1)

As it is unclear which cell population is indeed GFP-labeled within the Chrnb4-eGFP mESC line-derived retinal organoids, a more detailed study of both the organoids and the resulting eGFP positive cell population should be performed. One of the possible reasons for this unexpected result is that after karyotyping of the four starting clones, the one used to perform the transplantation experiments showed an altered karyotype (see Figure 26), which might affect the differentiation and thus transplantation outcome. However, two of the Chrnb4-eGFP obtained clones presented a normal karyotype, and both of these clones have the capacity to generate retinal organoids. Therefore, in depth analysis of GFP+ cells within retinal organoids and potential transplantations should be performed using the Chrnb4-GFP mESC lines with a normal karyotype. Furthermore, it would be interesting to sort eGFP positive cells from organoids at different developmental stages, since this might influence the transplantation outcome as well.

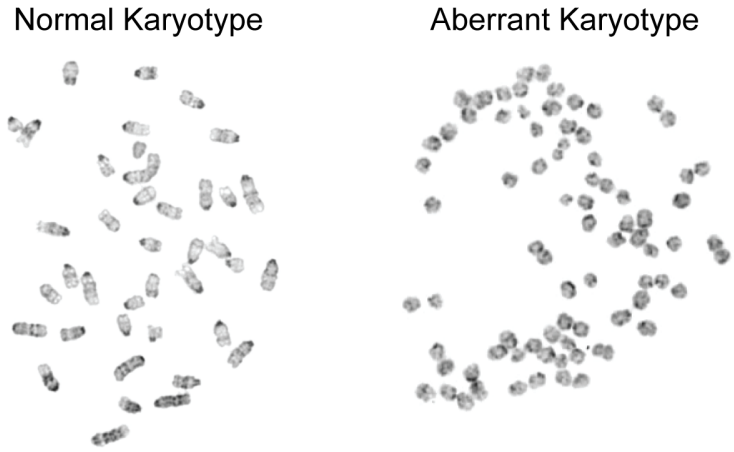

Figure 26. Karyotyping of the Chrnb4-eGFP clones obtained. On the left, an example of a normal karyotype for mESC lines, this was obtained for two of the Chrnb4-eGFP clones generated. On the right, an example of an aberrant karyotype for mESC lines, in this case corresponds to a tetraploidy. This karyotype corresponds to the mESC line used for the transplantation experiment.

2.4 Discussion

Retinal organoid cultures recapitulate *in vivo* retinal development in terms of morphogenetic events, with the generation of a neuroepithelia present from D3 of culture, OV visible from D7 onwards, and OC-like structures from D10 (Eiraku et al., 2011). In the retinal organoid cultures presented in this study, both neuroepithelia and evaginating OV were clearly observable, however, OC-like structures were generally not observed. Despite the absence of OC-like structures, retinal organoids developed a retina-like structure, with the presence of all principle types of retinal neurons. This is not surprising, since optic cup invagination and neural retina specification might be independent from each other (Fuhrmann, 2010). Actually, it seems that the optic vesicle requires contact with the pre-lens ectoderm, which is absent in the *in vitro* culture, to undergo invagination. However, if an external source of FGF signaling is provided, neural retina can be specified in the absence of pre-lens ectoderm (Hyer et al., 2003). Even though the protocol for retinal organoid generation does not require specific addition of FGFs, it does require the addition of FCS, which among other components, contains several growth factors, including FGFs, and this might be sufficient to induce neural retina specification in the three-dimensional PSC-derived retinal organoids.

Besides the morphogenetic events during retinogenesis, retinal organoids also recapitulate *in vivo* development in terms of gene expression (Völkner et al., 2016). In this study, it has also been shown that expression of eye field transcription factors such as Pax6 and Lhx2 recapitulate the expression dynamics of *in vivo* development. Both EFTS are important for eye specification and development, and their expression *in vivo* is detected from E8.5 onwards (Walther and Gruss, 1991; Porter et al., 1997). Along development, their expression becomes restricted to certain subtypes of amacrine cells. Moreover, Pax6 is also found in ganglion cells (Stanescu et al., 2007) and Lhx2 in Müller glia (Gordon et al., 2013). The retinal organoids shown in this study presented expression of Pax6 and Lhx2 across all the neuroblastic-like layer in early culture time points and later in development became restricted to cells occupying the inner-most part of the retina-like structure, where presumptive amacrine, ganglion cells and Müller glia reside. Chx10 and Otx2, which are transcription factors required during neural retina and photoreceptor specification, respectively, have also been shown to resemble their expression pattern *in vivo*. Chx10 (also known as Vsx2) is detected from E9.5 in the evaginating optic vesicle (Liu et al., 1994). In this study, expression of Chx10 was slightly delayed compared to the *in vivo* situation, however, at later stages became restricted to the inner nuclear layer – similarly to the *in vivo* situation, where it becomes restricted to bipolar cells and a subgroup of Müller glia (Rowan and Cepko, 2004). Otx2 is expressed in the neural retina from E12.5, and by day E17.5 becomes mainly restricted to the outer part of the neuroblastic layer, were photoreceptors are born. Later in development its expression is

downregulated (Nishida et al., 2003; Fuhrmann, 2010). In the retinal organoids shown in this study, Otx2 expression is also slightly delayed compared to the *in vivo* situation, and downregulation seems to occur slightly earlier, since no Otx2 expression is detected at D24 of culture.

At later stages of development, once the different retinal neurons have been specified to their corresponding cell fate and become post-mitotic, they begin to express specific markers, as for example, phototransduction cascade proteins in the case of photoreceptors, indicating their maturation. The last step of maturation involve the growth of axons and synapse formation (Swaroop et al., 2010). The retinal organoids shown in this study present all the different retinal neurons found in the *in vivo* retina and these are localized in the corresponding retinal layers, i.e. photoreceptors are located at the outer nuclear layer-like structure, bipolar cells, amacrine cells and horizontal cells are located at the inner nuclear layer-like structure and ganglion cells are located at the inner-most part of the retina-like structure within the organoids, resembling the ganglion cell layer. Moreover, late maturation markers such as cone arrestin (*in vivo* expressed from P9 onwards (Zhu et al., 2002)) or M-opsin (*in vivo* expressed from P6 onwards (Swaroop et al., 2010)) were not detected at D24 of organoid culture, which is developmentally equivalent to P4.

Another aspect in which retinal organoids resemble the retina is in their cellular composition. Most of the cells in the retina-like structure of the retinal organoids corresponds to rod photoreceptors, and cones represent a minor subpopulation (0.1 %) in the retinal organoids (Eiraku et al., 2011).

As mentioned in the introduction, organoids should be able to reproduce, at least partially, the function of the organ they resemble. Detection of pre- and post-synaptic proteins, including synaptophysin (Chen et al., 2016b; Kruczek et al., 2017; DiStefano et al., 2018), ribeye (Kruczek et al., 2017; Gagliardi et al., 2018; Ovando-Roche et al., 2018), CtBP2 (Wahlin et al., 2017), bassoon (DiStefano et al., 2018) and PSD-95 (Wahlin et al., 2017) has been used as an indication for the presence of an OPL-like layer within retinal organoids. In this regard, here, expression of synaptophysin, a protein associated to synaptic vesicles (Yoshimatsu et al., 2013), was detected correctly localized where a nascent OPL-like structure is expected within retinal organoids. Imaging of retinal organoids using electron microscopy have shown, indeed, the formation of ribbon synapses within organoids (Wahlin et al., 2017; Ovando-Roche et al., 2018). In terms of functionality, photoreceptor cells within retinal organoids have been shown to present electrical activity when analysed by patch-clamp recordings (Zhong et al., 2014b; Wahlin et al., 2017). Moreover, in larger structures, such as in brain organoids with optic cup

like structures, photosensitive cells seem to have the capacity to modulate neuronal activity (Quadrato et al., 2017).

Taken together, the available data for retinal organoids and the results presented in this study show a strong similarity in terms of morphogenesis and retinogenesis between retinal organoids and *in vivo* retinal development. Furthermore, published data indicates that photoreceptors generated in these culture conditions are able to develop their main function, i.e. responding to light. Moreover, it has been shown that, after transplanting miPSC-derived retinal sheets, visual improvement in mouse models of end-stage retinal degeneration is achieved if 9-*cis*-retinal is supplied to the host (Mandai et al., 2017). Therefore, it is reasonable to consider retinal organoids as a suitable, virtually unlimited source for transplantable post-mitotic photoreceptor precursors.

Despite the promising results described until now, and the progress done in understanding the transcriptional program required for rod photoreceptor specification, there is much less known regarding how cone photoreceptors are specified (Brzezinski and Reh, 2015). This is one of the reasons why rod photoreceptor cell replacement strategies are more advanced, compared to cone replacement therapies. However, as already mentioned, human vision relies mostly on cone photoreceptors, and therefore, a reliable source of cone photoreceptor precursors is required for preclinical studies as well as clinical applications. On that account, this study utilizes the mouse system to assess strategies for the *in vitro* generation of cone photoreceptors, since the time line for human retinal organoids is very long, and therefore prohibitive for such an investigation. The goal, nonetheless, is to eventually translate the obtained protocols to the human system.

Since cone photoreceptors represent a minor subpopulation in retinal organoids, a way to increase the number of these particular cells within the retinal organoids is required. Several studies have shown that in early steps of development, high levels of the Notch signaling pathway keep retinal progenitors in a proliferative state, however, when Notch signaling is inhibited progenitors are forced to exit the cell cycle and commit to cone or rod photoreceptors at the expense of other retinal cell types. The developmental stage in which Notch signaling is blocked determines whether cells commit to a rod or cone fate, where earlier inhibition promotes a cone cell fate (Jadhav et al., 2006; Nelson et al., 2007; Swaroop et al., 2010). This has been shown to be true also for retinal organoids (Eiraku et al., 2011; Völkner et al., 2016). However, such observations could not be fully reproduced in this study.

Retinal organoids in which Notch signaling was inhibited at the developmental stage corresponding to the peak of cone generation (D12-D14) presented an aberrant morphology (data not shown) and were significantly smaller in size, as previously described for mice retinas in which Notch1 signaling was conditionally removed at early stages (Jadhav et al., 2006). After counting the amount of S-opsin positive cells, a significant increase of cones in the treated organoids was observed, but this could not be validated using RT-qPCR as a readout. A possible explanation is that the tools currently available in the field of retinal research to quantify the number of cone photoreceptors at early stages are not appropriate. In this study, S-opsin was the only available marker for quantifying the number of cone photoreceptors within D24 retinal organoids. However, blue cones represent only between 5 and 15 % of all cones (Rodieck, 1998; Masland, 2001; Mustafi et al., 2009), and therefore, the total number of cones is likely to have been underestimated. A possibility to circumvent this limitation and identify all existing cones within the retinal organoids could be to culture them for longer, allowing cone photoreceptor cells to mature and express later cone-specific markers. One of the challenges with this approach is that, due to the lack of a circulatory system, the inside of the organoids does not receive enough nutrients leading to apoptotic cell death which has a detrimental effect on the rest of the organoid. Besides this technical problem, as mentioned previously, the most appropriate developmental stage of cone photoreceptor precursors for optimal transplantation outcome is around E15.5 (Lakowski et al., 2010; Decembrini et al., 2017), equivalent to D15-17 of culture. Therefore, culturing retinal organoids longer could allow for proper quantification of cone photoreceptors, but at the same time would lead to a decrease on the presumptive number of donor cone photoreceptors that integrate into the host retina. In other words, the transplantation outcome, in terms of efficiency, would decrease.

Interestingly, what was observed in this study is a decrease on the expression of Crx after inhibiting Notch signaling at this early stage. Since by inhibiting Notch, proliferative progenitors are forced to exit the cell cycle, the pool of potential cells to generate photoreceptors at later stages decrease, and therefore, Crx expression decreases compared to the control organoids.

Another possible explanation as to why an increase in the number of cone photoreceptors was not reproducibly observed in this study is that in general, retinal organoids present high heterogeneity. This is not only between rounds of differentiation, but also within the same differentiation round. This variability observed among retinal organoids is a general issue in the organoid field that represents a major difficulty for the comparative analysis between different treatments (Völkner et al., 2016). In this regard, to observe a reproducible significant effect after treating retinal organoids with a specific drug, the effect has to be greater than the inherent variability among organoids. Moreover, considering that Notch signaling inhibition

leads to a decrease in the size of the organoid accompanied by a reduction in the total amount of photoreceptors, the slight increase in the number of cone photoreceptors may not be sufficient to compensate for an overall decrease in photoreceptor number.

Very recently, the first publications in which ESC-derived cone photoreceptors were isolated from retinal organoids, took advantage of an AAV virus encoding the GFP reporter under the human (L/M)-cone opsin promoter for labelling the cone population (Gonzalez-Cordero et al., 2017; Welby et al., 2017; Waldron et al., 2018). The disadvantage of this approach is that the virus might not infect all the desired cell population, and therefore, cone photoreceptors may remain unlabelled and would therefore be lost during the cone enrichment procedure. Moreover, the transplanted cell population can only be obtained from D26-D30 retinal organoids (Kruczek et al., 2017) to allow for M-opsin expression. This stage is presumably too late as it is thought that the ideal developmental stage to obtain post-mitotic cone photoreceptor precursors with highest transplantation outcomes is around E15.5 (corresponding to D15-D17 in organoid culture).

In this regard, in this study a new mESC line which expresses the GFP reporter under the *chrnb4* promoter was generated. Chrnb4 is the beta-4 subunit of the acetylcholine receptor, which in adult retina is specifically expressed in cone photoreceptors, and in early stages of retinal development is expressed in proliferating retinal progenitors. Between E15.5 and E18, which is the target developmental stage for transplantable cone photoreceptor precursors isolation, Chrnb4 expression becomes progressively restricted to the retinal apical side where cone precursors undergo their terminal differentiation (Decembrini et al., 2017). Although a further characterization of the Chrnb4-GFP-derived retinal organoids themselves and the transplantation outcome of FACS-sorted GFP-positive cells derived from Chrnb4-GFP-derived organoids is required, preliminary results indicate that mESC-derived presumptive cone photoreceptors survive in the SRS of the transplanted hosts, and some of the GFP+ cells co-localize with late cone-specific markers, such as cone arrestin or S-opsin, as well as with the pan-photoreceptor marker recoverin. However, most of the GFP positive cells within the sub-retinal space do not co-localize with cone-specific markers. This might indicate that the time point chosen, D18 of culture, to isolate cone photoreceptor precursors based on their GFP expression was not adequate. A more rigorous study, in which GFP positive cells are isolated from Chrnb4-GFP retinal organoids at different developmental stages is required in order to identify the ideal culture time for organoids to generate a cone photoreceptor precursor equivalent to E15.5 stage *in vivo*. Furthermore, the experiments presented in this study should be repeated with one of the clones that presented a normal karyotype, since genetic

aberrations of the mESC-line might also account for eGFP expression in unexpected cell types within the organoids.

While GFP+ cell clusters were observed in the SRS of recipients after transplantation, in this study no GFP+ cells within the host ONL were observed (N=8), independently of the mouse model used as a host (wild-type and Cpfl1). Actually, in general, cone transplantation outcomes in terms of the number of GFP+ cells within the host ONL is much lower in comparison to transplantation of cone-like or rod photoreceptor precursors. Rod transplantations normally result in around 1,000 – 20,000 GFP+ cells/ONL, depending on the injection procedure and retinal environment of the host (Pearson et al., 2012; Barber et al., 2013; Santos-Ferreira et al., 2015). Furthermore, it has been described that after transplanting cone photoreceptor precursors into wild-type animals, a high transplantation failure rate (absence of a cell mass in the SRS of the transplanted eyes) is observed (Waldron et al., 2018). However, in the animals successfully transplanted between 350 and 400 GFP+ cells/ONL were observed (Waldron et al., 2018). These numbers are considerably reduced to around 55 GFP+ cells/ONL when transplanting hESC-derived cone photoreceptors into murine models of retinal degeneration (Gonzalez-Cordero et al., 2017). In that study, such a decrease in the number of GFP+ cells within the host ONL might be due to the xenotransplantation condition (human into mouse).

A mESC reporter line like the one generated in this study, together with techniques to quantify single organoid fluorescence *in vivo* (Vergara et al., 2017) might facilitate the study of transcriptional networks required for cone photoreceptor cell fate specification, since it offers a direct readout for cone generation (GFP fluorescence). A better knowledge of cone fate specification will be vital in the development of cone replacement therapies in terms of improving PSC-cone derivation protocols. Moreover, the isolation of early cone photoreceptor precursors at different time points of retinal organoid vs. *in vivo* development and a comparative analysis of gene expression could help to unravel cell surface markers to isolate the desired cell population, and therefore avoid a fluorescence targeting of the transplantable cone photoreceptor precursors. A similar approach has recently been performed by isolating virally labelled cone photoreceptor precursors from hESC-derived retinal organoids and foetal human retinas. A four-biomarker panel (SSEA1-, CD133+, CD26+, CD147+) was identified to enrich cone photoreceptors (55.1% ± 30.7% of cArr/Crx double positive cells), compared to unsorted populations (8.4% ± 3.1%) (Welby et al., 2017). The team of Olivier Goureau has recently published a study in which, by using the CD73 cell surface marker on D120 organoids, an enrichment on Crx/Recoverin double positive cells was achieved (66% ± 15%). Four weeks after transplantation, characterization of the grafted CD73+ cell population revealed a high

enrichment in cones, detected by specific staining for human cArr. However, at longer post-transplantation times (10 weeks) the transplanted mass was also positive for rhodopsin, indicating the presence of rods (Gagliardi et al., 2018). These studies support the feasibility of obtaining donor cone photoreceptors from retinal organoids, however, the sorting of these cells is performed at late stages of cone development when L/M-opsin or cone arrestin are already expressed. Therefore, there is still room for improvement of cone enrichment strategies, especially at early stages of development, prior to transplantation.

Retinal organoids have been widely exploited since their discovery and they represent an attractive source for transplantable photoreceptor precursors. Nonetheless, remaining milestones need to be achieved before PSC-derived photoreceptor cells reach the clinics. First, retinal organoids are known to be highly heterogeneous, as has been also shown in this study. Such variability can lead to a lack of reproducibility from batch to batch, which is unacceptable in clinical applications. Some research groups have started to develop retinal organoid protocols compliant with good manufacturing practices (GMP), in which animal products are eliminated from the culture (Wiley et al., 2016; Reichman et al., 2017; Zhu et al., 2018). Other groups have been focusing on increasing the robustness of the protocols for generating retinal organoids by standardizing some of the steps in the protocol and scaling them up through the use of bioreactors (DiStefano et al., 2018). Furthermore, due to the duration of the protocols to obtain hESC/hiPSC-derived transplantable photoreceptors (at least 4 months), other groups are studying the possibility to freeze down retinal organoids to have a readily available stock of donor cells (Reichman et al., 2017; Gagliardi et al., 2018).

Another important issue to consider when using PSC-derived photoreceptors, and, in general, any cell type derived from hESC or hiPSC is that a rigorous quality control of the final product should be performed. Expansion of PSC *in vitro* and reprogramming of adult somatic cells to PSC might be a source for the acquisition of teratogenic mutations or karyotype aberrations that remain in the differentiated products, and these should not be transplanted into patients (Laurent et al., 2011; Lin and Xiao, 2017; Merkle et al., 2017). Actually, karyotyping of the different Chrnb4-GFP clones generated in this study revealed that 2 of the 4 clones obtained carried genetic aberrations.

In summary, in this study an established protocol to differentiate mESCs towards retinal organoids has been adapted with the objective to increase the amount of cone photoreceptors in such 3D structures. However, none of the assessed protocol modifications resulted in a satisfactory outcome in terms of increasing the cone photoreceptor number within retinal organoids. Considering the high variability among organoids and the lack of reliable tools to

accurately assess the number of cone photoreceptors within the retinal organoids, a novel early cone reporter mESC line, Chrnb4-eGFP, has been generated to circumvent such limitations. However, a more detailed analysis of the Chrnb4-eGFP organoids before and after transplantation is required to determine the eGFP labeled cell population.

Chapter 3:

Cytoplasmic material transfer upon photoreceptor precursor transplantation

Part of this chapter has been already published in Santos-Ferreira T*, **Llonch S***, Borsch O* et al. 2016. Retinal transplantation of photoreceptors results in donor-host cytoplasmic exchange. *Nat. Comms* 7:13028.

3.1 Introduction

In pre-clinical studies for any kind of cell therapy it is important to develop strategies for tracking the cells upon transplantation. In the field of photoreceptor transplantation, different labelling methods have been applied during the development of the photoreceptor transplantation approach as we know it today (Nickerson et al., 2018). Some of these labelling strategies include pre-labelling of the donor cells with dyes such as Fast Blue or DiI (del Cerro et al., 1988; Silverman and Hughes, 1989), co-transplantation of RPE cells with photoreceptors, using the pigments of the RPE to localize the graft (Gouras et al., 1991a) and pre-labelling of donor cells with ^{3}H-thymidine or with a genetic reporter, such as *lacZ* (Gouras et al., 1991b, 1991c). More recently, cell type-specific fluorescent reporters, such as the Nrl-GFP mouse (Akimoto et al., 2006), which specifically labels rod photoreceptors, have been developed. The availability of such reporter lines have facilitated on one side the isolation of a specific cell type, for example by using FACS, and on the other side the identification of donor cells upon transplantation, since no staining or additional processing is required for detection (Nickerson et al., 2018).

In the field of photoreceptor transplantation, the use of fluorescent reporter lines, such as the Nrl-GFP, Crx-GFP (Samson et al., 2009), Chrnb4-GFP (Siegert et al., 2009) or the ubiquitous GFP reporter (Okabe et al., 1997) mouse lines, enabled the identification of post-mitotic photoreceptor precursors as the cell source for favourable transplantation outcome (MacLaren et al., 2006; Bartsch et al., 2008; Lakowski et al., 2010; Decembrini et al., 2017). Taking advantage of this specific cell population, some visual function restoration has been achieved after transplanting single cell suspensions of primary post-mitotic rod (MacLaren et al., 2006; Pearson et al., 2012; Barber et al., 2013; Singh et al., 2013b) or cone-like photoreceptor precursors (Santos-Ferreira et al., 2015) into different mouse models of retinal degeneration.

In these studies, transplantation success was assessed by the number of GFP+ cells within the ONL. The morphology of these GFP+ cells revealed the presence of structures characteristic of mature photoreceptors, such as outer- and inner-segments and axonal protrusions within synaptic terminals. These observations led researchers in the field to assume that the underlying mechanism for vision restoration upon photoreceptor transplantation was the structural integration and maturation of donor photoreceptors within the host ONL and subsequent ability to establish synaptic connections with second order retinal neurons present in the host INL (Nickerson et al., 2018). However, in other studies it has been previously shown that relying on reporter expression to identify transplanted cells can be misleading. For example, based on reporter expression it was reported that bone

marrow-derived cells have the potential to transdifferentiate into neuronal cell types. This was later discovered to be a result of fusion between the two cell types (Terada et al., 2002; Ying et al., 2002; Alvarez-Dolado et al., 2003; Kemp et al., 2014).

The possibility of cell fusion between donor and host cells in the field of photoreceptor transplantation, however, was ruled out in two independent studies (MacLaren et al., 2006; Bartsch et al., 2008). There were two main strategies used to discard the possibility of cell fusion. Firstly, fluorescently labelled donor photoreceptors were transplanted into host animals expressing a different fluorescent reporter. In case of fusion, cells positive for the two fluorescent reporters should have been detected within the host retina, however this was not reported. Second, one of the characteristics of classical cell fusion is the presence of two nuclei per cell instead of one. In the two mentioned studies, no cells with more than one nucleus were detected within the host outer nuclear layer following transplantation. Taken together, these results discarded the possibility of fusion between donor and host cells upon photoreceptor transplantation. A major drawback of these studies, though, is that only examples of non-double fluorescent or single nucleated cells were shown and no quantifications were performed. This together with the fact that GFP+ cells within the host retina presented mature photoreceptor morphology consolidated the hypothesis of structural integration and establishment of synaptic connections with host interneurons as the underlying mechanism of visual function recovery upon photoreceptor transplantation.

In 2014, the group of R. MacLaren reported the co-localization of donor-derived fluorescent reporter in host photoreceptors expressing a different reporter, and therefore, re-opened the possibility of fusion between donor and host cells (Singh et al., 2014). Moreover, a recent study from V. Wallace laboratory also described the presence of fluorescent reporter-positive cells with a rod-like morphology in the host retina after transplanting cod (cone-like photoreceptors, isolated from an $Nrl^{-/-}$ animal)-GFP positive cells. GFP+ cells found within the host retina were single nucleated, which would argue against classical cell fusion, however, they did not express mature cone markers and presented a rod-like heterochromatin pattern. Therefore, the authors could not rule out fusion as responsible for the presence of reporter positive cells in the host retina (Smiley et al., 2016). Moreover, in our laboratory we observed that after transplanting photoreceptor precursors double labelled with EdU (nuclear labelling) and GFP (cytoplasmic labelling) into wild type hosts, GFP+ cells within the host ONL were lacking the EdU labelling. This observation questioned the integration of donor photoreceptors into the host ONL. Together with the published results from the MacLaren and Wallace laboratories, these results indicate that further investigation was required to understand the interaction between donor and host photoreceptors upon transplantation.

Due to the presence of donor-derived fluorescent reporter in host photoreceptors, together with the fact that neither nuclear labelling such as EdU or double nucleated cells were identified among the reporter-positive cells within the host retina, we hypothesized that donor and host photoreceptors engage in cytoplasmic material transfer. Here, experiments aiming to distinguish between structural integration of donor photoreceptors and cytoplasmic material transfer are performed.

3.2 Materials and methods

3.2.1 Ethical statement

All the animal experiments were approved by the ethics committee of the TU Dresden and the Landesdirektion Dresden (24-9168.11-1/2008-33, 24-9168.11-1/2012-33 and 24-9168.11-1/2013-23, TVV 25/2018) and performed strictly following the European Union and German regulations (Tierschutzgesetz), as well as the ARVO Statement for the Use of Animals in Ophthalmic and Vision Research.

3.2.2 Experimental animals

All the experimental animals used in this study were kept in the animal facility of the Center for Regenerative Therapies Dresden and bred in house. Several transgenic mouse lines were used for this part of the thesis, besides the wild-type C57BL/6Rj:

- Nrl-eGFP: This mouse line has a construct that drives eGFP expression under the *nrl* promoter (Akimoto et al., 2006). Nrl is a transcription factor specifically expressed in rod photoreceptors and is critical for their development and function. Therefore, in this mouse line, all rod photoreceptors are labelled with the eGFP reporter.
- PhAM: This mouse line has a construct that drives the expression of Dendra2 and localises it to the mitochondria (B6; 129S-Gt(ROSA)26Sor<tm1.1(CAG-COX8A/Dendra2)Dcc/J) (Pham et al., 2012). Dendra2 is an irreversible photo-convertible protein, that upon activation can change from green to red colour. For the purpose of this thesis, the property of being photo-convertible is irrelevant, what is interesting is that this line represents a good mitochondrial reporter.
- mTmG: This mouse line is a double fluorescent Cre recombinase reporter (Muzumdar et al., 2007). It contains a construct which encodes for the membrane tagged tdTomato, flanked in between two *loxP* sites. Upon Cre recombination, this part of the construct is removed, allowing for the expression of the encoded membrane tagged GFP protein. For the experiments described in this thesis, the interesting characteristic of this mouse is the membrane tagged tdTomato.

3.2.3 Isolation of primary post-mitotic photoreceptor precursors

Photoreceptor precursors were obtained from donor animals at the age of post-natal day 4 (P4). Eyes were enucleated and retinas were isolated and enzymatically dissociated to a single cell suspension. The dissociation was performed using the Papain Dissociation Kit (Worthington, cat# LK003150). Briefly, after cutting isolated retinas into small pieces, papain solution (2 U/mL) containing 10 µg/mL of DNaseI (Sigma) was added to the tube. Retinas were incubated in such solution for 30-45 min at 37 ^{o}C, mixing manually every 10 min. Papain digestion was stopped by transferring the solution to an ovomucoid inhibitor solution. Next, the sample was centrifuged for 5 min at 300 g. Retinal cells were re-suspended into MACS buffer and stained against the surface marker CD73 using as primary antibody rat anti-CD73 (BD Pharmingen, cat#550738) and as secondary goat anti-rat IgG microbeads (Miltenyi, cat#130-048-501). The labelled cells were loaded to an LS column (Miltenyi, cat#130-042-401) standing on a MACS (Magnetic Activated Cell Sorting) sorter (Miltenyi, QuadroMACS Separator, cat#130-090-976) and the negative fraction was run through the column, while the positive fraction remained attached due to the magnetic field. Next, the column was removed from the MACS sorter and the positive fraction (population of interest) was eluted with MACS buffer. Cells were centrifuged for 5 min at 300 g and re-suspended in 500µL of MACS buffer. Isolated rod photoreceptor precursors were counted using a Neubauer chamber and re-suspended to a final concentration of 200000 cells/µL and kept on ice until transplantation.

3.2.4 Sub-retinal transplantation of photoreceptor precursors into host retinas

Animals were anaesthetised with 100 µL/ 10 g body weight with a solution containing Ketamin (Ratiopharm GmbH, cat#7538843) and Dormitor (Pfizer, cat#76579) in distilled water. 2.5% Phenylephrin – 0.5 % Tropicamid (TU Dresden Pharmacy) drops were used to dilate the pupils and Vidisic (Dr. Mann Pharma/Andreae-Noris Zahn AG) was used to keep the eyes hydrated and prevent cataract formation. Under a magnifying lens (Leica), a small hole was performed on the *ora serrata* of the eye to be transplanted using a 30 Gauge (30 G) sharp needle (BD, cat#304000). 1 µL of cell suspension (200000 cells/µL) was loaded into a Hamilton syringe, which was introduced to the previously generated hole. Then, the Hamilton syringe was introduced trans-vitreally to the sub-retinal space and a local retinal detachment was generated while slowly releasing the cell suspension. Then, the Hamilton syringe was slowly removed, avoiding reflux of the just transplanted cells. The same procedure was repeated to transplant the other eye. Then, the animal was woken up by an intraperitoneal injection of 100 µL/10 g

body weight of atipamozole hydrochloride (Antisedan, Pfizer, cat#GTIN08436529620160) solution.

3.2.5 Immunohistochemistry

Eyes were removed and shortly washed with PBS. Next, a 30 G needle was used to poke a hole in the cornea and then eyes were fixed in a 4 % paraformaldehyde (PFA, Merck, cat#1.04005.1000) solution for 1 h at 4 °C. The fixed eyes were then transferred to a cryoprotectant solution (30% sucrose, Interchim, cat#150695) overnight. Next day, extraocular muscles, cornea, iris and lens were removed, and the eyecup was embedded in Neg50 (ThermoScientific, cat#6502) freezing media. Embedded eyecups were then deep frozen in liquid Nitogen and kept at -80 °C until further processing.

20 µm thick sections were obtained using a Cryostat (ThermoScientific, NX70), air dried for 20 min at 37 °C and directly used or stored at -80 °C until further processing. Sections were then air dried for 1 h at room temperature (RT) and rehydrated for 20 min in PBS. Sections were then incubated in blocking solution (5 % donkey serum, [Uptima, cat#UP77719A], 1 % bovine serum albumin, BSA [Serva, cat#11926.04], 0.3 % Triton X-100 [Serva, cat#37240]) for 1 h at RT, and then incubated with the desired primary antibody (see Table 8) overnight at 4 °C. After washing, sections were incubated with the corresponding secondary antibody (see Table 8) and 4'6-diamidino-2-phenylindole (DAPI, 1:15000, AppliChem GmbH, cat#A1001) for 1h and 30 min at RT. Finally, sections were washed again and mounted using Aqua-Polymount (Aqua-Polysciences, cat#18606-20) mounting media. Slides were then air dried overnight at RT and imaged directly or stored at 4 °C. Images were taken using Zeiss Axio Imager Z1 with ApoTome (Zeiss).

Table 8. Antibodies used in this study. Secondary antibodies are all from Jackson IR and used at a dilution of 1:1000.

Antibody	Company	Catalogue #	Host	Dilution	Secondary
GFP	Abcam	ab13970	chicken	1:800	anti-ch AF488
RFP	Rockland	600-401-379	rabbit	1:2000	anti-rb Cy3
Tom20	Santa Cruz	sc-11415	rabbit	1:500	anti-rb Cy3

3.2.6 *In situ* hybridization

Tissue for *in situ* hybridization (ISH) was processed as described above (section 3.2.5), however, all the solutions were prepared with diethyl pyrocarbonate (DEPC)-treated

water/PBS, in order to inactivate RNase enzymes. Sections for ISH were 10 µm thick to allow better penetration of the probe to the tissue.

3.2.6.1 Chromosomal Fluorescent *in situ* hybridization

The protocol used was adapted from Solovei, 2010. Briefly, slides containing the sections were air dried for 1 h at RT and then rehydrated for 5 min in 10 mM sodium citrate (AppliChem, cat#A3901,0500) buffer. Slides were transferred to a Coplin jar containing pre-warmed 10 mM sodium citrate buffer and incubated at 80 °C for 25 min. Then, slides were let cool down at RT and incubated in 2X saline-sodium citrate (SSC, Invitrogen, cat#AM9763) buffer for 5 min. Previous to ISH, an IHC step was introduced. Slides were incubated for 5 min in PBS and incubated with primary antibody (see Table 8) in blocking solution (0.1 % BSA, 0.1 % Triton X-100 in PBS) overnight at RT. Slides were then washed three times, 15 min each, with pre-warmed 0.05 % Triton X-100 in PBS solution at 37 °C and incubated with secondary antibody (see Table 8) in blocking solution (0.1 % BSA in PBS) overnight at RT. Next, the ISH step was performed. Sections were post-fixed for 10 min in 2 % PFA solution and washed in PBS three times, 5 min each. Sections were then incubated for 5 min in 2X SSC and transferred into a 50 % formamide (Sigma, cat#47670)/ 2X SSC solution for at least 1 h. After this incubation, sections were air dried until no formamide was left and covered with the Y-chromosome probe (MetaSystems, cat#D-1421-050-OR). To prevent probe evaporation, slides were covered with parafilm. Then, slides were placed into the hybridization oven (HybEZ II Oven, ACD) for 3 h at 45 °C in order to allow infiltration of the section with the probe. Slides were then placed for 5 min at 80 °C for probe and DNA denaturation and then moved back to the HybEZ during 2 days at 37 °C for hybridization. Then, parafilm was carefully removed and slides were washed in 2X SSC three times, 15 min each, at 37 °C and in 0.1X SSC two times, 5 min each, at 60 °C. Slides were then incubated for 2 min in 2X SSC at RT and counterstained with DAPI (1:10000 into 2X SSC) for 5 min at RT. Finally, slides were washed three times, 5 min each, in 2X SSC at RT and mounted using PolyMount mounting media. Slides were then air dried overnight at RT and then directly imaged or stored at 4 °C until imaging. Slides were imaged using Zeiss Axio Imager Z1 with ApoTome (Zeiss).

3.2.6.2 RNAscope

RNAscope is a technology developed by Advance Cell Diagnostics (ACD) that allows to combine IHC and mRNA ISH protocols in the same sample. The general protocol developed by ACD was optimized for retinal tissue. Briefly, sections were pre-treated by blocking endogenous peroxidases and by protease treatment (Pretreat 1&3, ACD, cat#320037), which was optimised to allow the IHC step to be successful. The hybridisation step consisted on incubating the slides with the corresponding probes (DapB [negative control], ACD, cat#310043, Polr2a [positive control], ACD, cat#312471] and eGFP [target], ACD,

cat#400281) for 2 h at 40 °C in the HybEZ. After a washing step, the ISH signal was amplified through 6 amplification steps and finally detected (RNAscope2.5 HD Detection Reagents-RED, ACD, cat#322360). At last, an IHC step was performed, as described in section 3.2.5. Images were taken with Zeiss Axio Imager Z1 with ApoTome (Zeiss).

3.2.7 ImageStream

Retinas were isolated and enzymatically dissociated as described in section 3.2.3. The single cell suspension was then stained against CD73 using APC (allophycocyanin) anti-mouse CD73 clone TY/11.8 (BioLegend, cat#127209) antibody. Cells were then centrifuged for 5 min at 300 g and re-suspended to a minimal concentration of 1 million cells / 50 µL FACS buffer and filtered through a 50 µm mesh strainer. The cell population was then analysed and imaged by Amnis ImageStreamX. Data was later analysed using FlowJo software.

3.2.8 FACS sorting

Retinas were isolated from the eyecup and enzymatically dissociated to a single cell suspension in a similar way as described above (section 3.2.3). However, for adult retina the time needed for dissociation was only 20 min, and at the end, cells were re-suspended in FACS buffer. The cell suspension was then stained against CD73 (rod photoreceptors) using APC (allophycocyanin) anti-mouse CD73 clone TY/11.8 (BioLegend, cat#127209) antibody and filtered through a 35 µm cell strainer previous to FACS sorting. CD73-APC+ eGFP+ or eGFP-, depending on the purpose of the experiment, single cells were sorted into 8-tube strips or 96-well plates using FACSAria III (BD) sorter. Data was then analysed using FlowJo software.

3.2.9 Single Cell Analysis

Right after sorting, single cells were deep frozen with dry ice and kept at -80 °C until further use. For analysis, single cells were heat up at 65 °C for 2min and then the material was split in two, half for sex genotyping (see section 3.2.9.1) and half for RT-qPCR analysis (see section 3.2.9.2).

3.2.9.1 Sex Genotyping

The sample was treated with proteinase K (Panreac, cat# A3830,0100) at a final concentration of 50 µg/mL. Proteinase K treatment was performed using the Mastercycler epgradient/pro (Eppendorf) using the following program: 1 h at 37 °C, 10 min at 65 °C and 10 min at 95 °C. Then, two rounds of PCR amplification were performed using TaKaRa Ex Taq Hot Start (Clontech, cat#RR006A). For the first amplification (PCR1), the sample treated with proteinase

K was used as input material. For the second amplification (PCR2), a 1:5 dilution of the PCR1 product was used as input material. The PCRs were run using Mastercycler. The program for each PCR is specified in Table 9. The primers used (F: 5'-GATGATTTGAGTGGAAATGTGAGGTA-3', R: 5'-CTTATGTTTATAGGCATGCACCATGTA-3') were described by McFarlane et al., 2013. The same pair of primers allows to distinguish between male (single band around 280bp) and female (band around 685bp, but also might lead to additional bands of 480 and 660 bp). The PCR product was then loaded into a 1 % agarose (Serva, cat#11404.07) gel containing 0.01 % SYBR Safe DNA gel stain (Invitrogen, cat#S33102). The gel run at 110 V during 45 min and then was imaged using Quantum ST5 Multi-Imaging system.

Table 9. PCR programs used for sex genotyping.

Program	PCR1	PCR2	
94 °C	1 min	1 min	
57 °C	40 sec	40 sec	40x
72 °C	30 sec	2 min	
72 °C	6 sec	6 sec	
4 °C	∞	∞	

3.2.9.2 RT-qPCR

The sample was directly used for cDNA synthesis using the qScript cDNA Super Mix 5x (Quanta, cat#95048-100). This reaction was performed in the Mastercycler and the program was 10 min at 25 °C, 60 min at 42 °C, 5 min at 85 °C. Next, a pre-amplification reaction using the 2x Multiplex PCR Master Mix (Qiagen, cat#206143) was performed using the Mastercycler and using the program detailed in Table 10. The primers used for this reaction were: F: 5'-CACTACCAGCAGAACACCCC-3' and R: 5'-GTCCATGCCGAGAGTGATCC-3'.

Table 10. Pre-amplification PCR program

95 °C	5 min	
95 °C	45 sec	
60 °C	1 min	20x
72 °C	1 min 30 sec	
72 °C	10 min	
4 °C	∞	

Following the pre-amplification reaction, a quantitative PCR was performed, using the same primers. The master mix used was 2x SYBR Premix ExTaq (Clontech, cat#RR820W) and the reaction was run in a LightCycler480 (Roche) using the protocol described in Table 11.

Table 11. qPCR program used for single cell analysis

Step	Temperature	Time	Ramp rate:	
Initiation	95 ºC	30 sec	4.4	
Amplification	95 ºC	5 sec	4.4	40x
	60 ºC	30 sec	2.2	
Melting curve	95 ºC	5 sec	4.4	
	60 ºC	1min	2.2	
	95 ºC	-	0.11	
Cooling	50 ºC	30 sec	2.2	

3.3 Results

3.3.1 Donor and host photoreceptors exchange cytoplasmic material upon transplantation

In order to distinguish between photoreceptor integration and exchange of cytoplasmic material between donor and host photoreceptors, male Nrl-eGFP post-mitotic photoreceptor precursors were transplanted into adult wild-type female hosts. Three weeks post-transplantation, host retinas were analysed for the presence and localization of donor cells. For this purpose, the nuclei and cytoplasm of donor cells were independently labelled. To distinguish between donor and host nuclei, fluorescent *in situ* hybridization (FISH) for the Y-chromosome, which is only present in male donor cells, was used. To label the cytoplasm, IHC against the eGFP reporter, which is expressed by donor photoreceptors under the control of the rod-specific promoter *nrl* was performed.

Prior to analysing the transplanted retinas, chromosomal FISH had to be established. Figure 27 shows the specificity of the Y-chromosome probe, which labels all the nuclei in male retinas, while no signal is detected in female retinas. Moreover, due to the high temperatures required during the chromosomal FISH protocol, inherent eGFP fluorescence of the Nrl-eGFP reporter line was lost. Therefore, in order to be able to detect simultaneously cytoplasmic and nuclear labelling after transplantation, additional IHC for the eGFP combined with the Y-chromosome FISH was required. As seen in Figure 27, the combination of both, chromosomal FISH and

IHC was achieved and the eGFP staining was specific for rod photoreceptors, as eGFP signal was restricted to the ONL and not observed in other retinal layers of Nrl-eGFP animals.

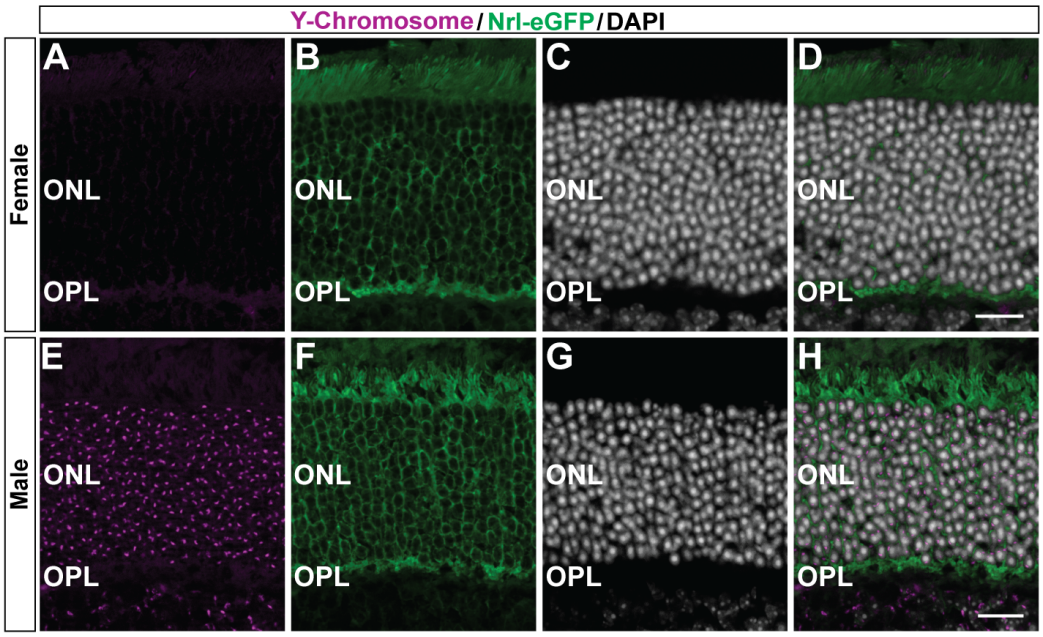

Figure 27. Y-chromosome FISH controls. Y-chromosomal FISH combined with IHC for eGFP was performed in both, female (A-D) and male (E-H) Nrl-eGFP retinas. Y-chromosome (magenta) was detected only in male retinas, while the eGFP reporter (green) was detected in both, male and female retinas, exclusively in the ONL, where rod photoreceptors are located. ONL: outer nuclear layer, OPL: outer plexiform layer. Scale bar: 20µm.

Once the Y-chromosome FISH combined with IHC for eGFP was established, the transplanted retinas were analysed. As can be seen in Figure 28, cells located in the SRS were positive for both, the Y-chromosome and the eGFP protein, identifying them as donor photoreceptors (98.24±0.77%). Only a small percentage (1.2±0.42%) of eGFP+ cells within the host ONL were also positive for the Y-chromosome. The rest of eGFP+ cells within the host ONL were negative for the Y-chromosome, indicating that most of the eGFP+ cells located in the host ONL are a result of cytoplasmic material exchange between donor and host photoreceptors, rather than structural integration.

These results showed, for the first time, that the underlying mechanism for visual function recovery might not be the structural integration of donor photoreceptors into the host retinas, as had been assumed in the field for more than a decade, but rather cytoplasmic material exchange between donor and host photoreceptors. This change of paradigm, which will be further discussed in section 3.4, opens many new questions such as: what is the mechanism by which donor and host photoreceptors exchange cytoplasmic material? what kind of cytoplasmic material can be transferred? how will this knowledge influence the development of new cell transplantation therapies for retinal degeneration diseases?

In the next two sections (3.3.2 and 3.3.3), the question regarding the kind of cytoplasmic material that can be transferred from donor to host photoreceptors is addressed.

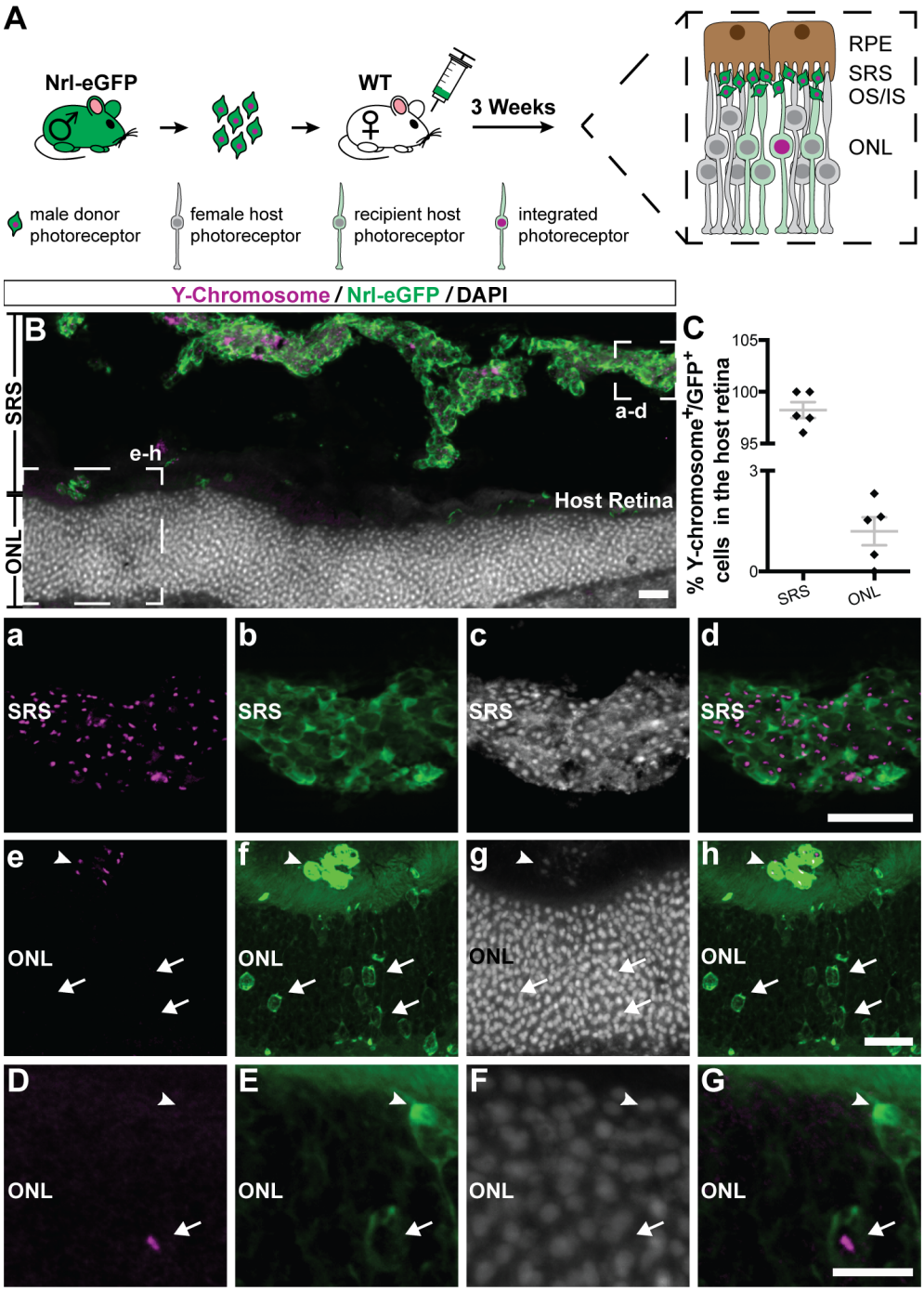

Figure 28. Donor cells engage in cytoplasmic material exchange with host retinas. A) Schematic representation of the experiment design. Briefly, male Nrl-eGFP post-mitotic photoreceptor precursors were transplanted into adult wild-type female animals. Three weeks after transplantation, host retinas (n=5) were analysed using chromosomal FISH and IHC. **B)** Overview of a host retina three weeks post-transplantation. **a-d)** Donor cells can be identified in the sub-retinal space by the presence of both, Y-chromosome (magenta) and eGFP protein (green). **e-h)** A clump of donor cells, identified by the presence of Y-chromosome and eGFP, is observed laying on top of the host retina (arrowhead). eGFP+ cells can be identified in the host ONL, however, these are negative for the Y-chromosome (arrows), identifying them as host cells GFP positive as a result of cytoplasmic

material exchange. **D-G)** Example of an integrated donor cell, identified by the presence of both Y-chromosome and GFP protein. **C)** Quantification of Y-chromosome+ cells per eGFP+ cells, in both the SRS and the ONL. In the SRS, the majority of the eGFP+ cells contained a Y-chromosome (98.24±0.77%), identifying them as donor cells, while only 1.2±0.42% of the eGFP+ cells within the ONL are also positive for the Y-chromosome, indicating that the majority of eGFP+ cells within the host retina are result of cytoplasmic material exchange. WT: wild-type, SRS: sub-retinal space, ONL: outer nuclear layer, OS/IS: outer segments/inner segments, RPE: retinal pigment epithelium. Scale bars: 20µm (B, d, h), 10µm (G).

3.3.2 mRNA is transferred from donor to host photoreceptors

Independent labelling of nuclei and cytoplasm exposed the existence of cytoplasmic material transfer between donor and host photoreceptors. As a cytoplasmic label the eGFP fluorescent reporter, i.e. a protein, was used and, therefore, the direct conclusion would be that proteins are transferred from donor to host photoreceptors. However, messenger RNA, which is also located in the cytoplasm and upon translation leads to protein synthesis, might also be transferred from donor to host photoreceptors. To test this hypothesis, the RNAscope technology (Advanced Cell Diagnostics) was established in the laboratory. This technique allows for high sensitive and specific RNA detection, however, similarly to the Y-chromosome FISH protocol, the RNAscope protocol led to loss of fluorescence of the eGFP protein, and therefore, an additional step of IHC for the eGFP protein was required.

After several steps of optimization of the RNAscope protocol combined with IHC for retinal tissue, it was possible to detect both, eGFP mRNA and protein, within the same retinal section. For the optimisation steps, Nrl-eGFP adult retinas were used (data not shown). Once the technology was optimized, the transplanted retinas could be analysed. As a negative control, a probe against the *Bacillus subtilis* gene dihydrodipicolinate reductase (dapB) was used and, as can be seen in Figure 29 (A-D), no signal despite minor background noise, was detected in the mouse retinal sections. As a positive control, the *Mus musculus* polymerase (RNA) II polypeptide A (Polr2a) was used, and as can be observed in Figure 29 (E-H), it was strongly detected across all the retinal sections analysed. Moreover, independently of the probe used, Figure 29 (A-H) shows that it was possible to detect eGFP+ cells within the host retina after transplantation of eGFP-expressing donor cells. The last control required for this experiment was to test the specificity of the probe for eGFP mRNA. As shown in Figure 29 (I-L), eGFP mRNA and protein were specifically detected and co-localised in the ONL of Nrl-eGFP adult retinas, while no signal for eGFP mRNA or protein was detected in the INL, indicating that the probe for eGFP mRNA is specific and no unspecific labelling is observed in cells which are negative for eGFP mRNA.

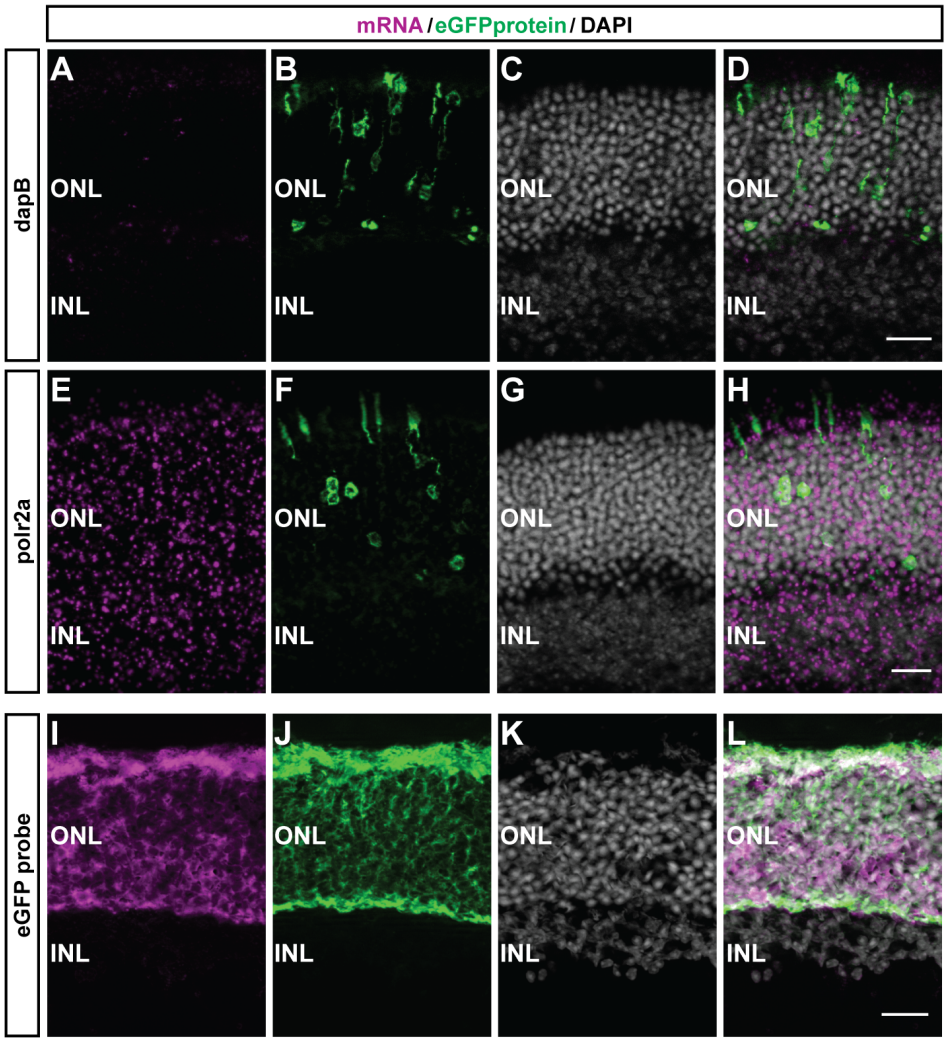

Figure 29. Controls for the RNAscope technology. DapB **(A-D)** and Polr2a **(E-H)** were used as negative and positive controls, respectively, on the transplanted retinas. DapB shows a slight background signal, but this is negligible compared to the strong signal detected for the Polr2a probe. **(I-J)** The specificity of the eGFP-mRNA probe was tested on Nrl-eGFP retinas. eGFP mRNA and protein co-localised in the ONL of the tested retinas, and showed no background in the INL, indicating specificity the eGFP-mRNA probe. DapB: dihydrodipicolinate reductase, *B. subtilis*, Polr2a: Polymerase RNA II polypeptide A, *M. musculus*, ONL: outer nuclear layer, INL: inner nuclear layer. Scale bars: 20μm.

To assess whether mRNA is also transferred to host photoreceptors, Nrl-eGFP post-mitotic photoreceptor precursors were transplanted into adult wild-type hosts. Three weeks post-transplantation, host retinas were analysed via RNAscope for eGFP mRNA in combination with IHC for eGFP protein detection. The transplanted cell mass was directly identifiable in the SRS (Figure 30, B) and, as expected, was positive for both, eGFP mRNA and protein (Figure 30, a-d). Within the host ONL, cells positive for eGFP protein were identified showing a photoreceptor morphology (Figure 30, B,f). However, the presence of eGFP mRNA was hardly distinguishable (Figure 30, B,e). A weak dotted signal was detected at the region of inner/outer segments (IS/OS), however it was difficult to assess whether this corresponded to specific or unspecific signal, since it did not seem to strongly co-localize with the eGFP+ IS/OS, and in

addition, in the negative control (DapB, see Figure 29, A-D) some background was also detectable. Thus, the cell bodies of the eGFP+ cells within the host ONL might contain no or very low amounts of eGFP mRNA.

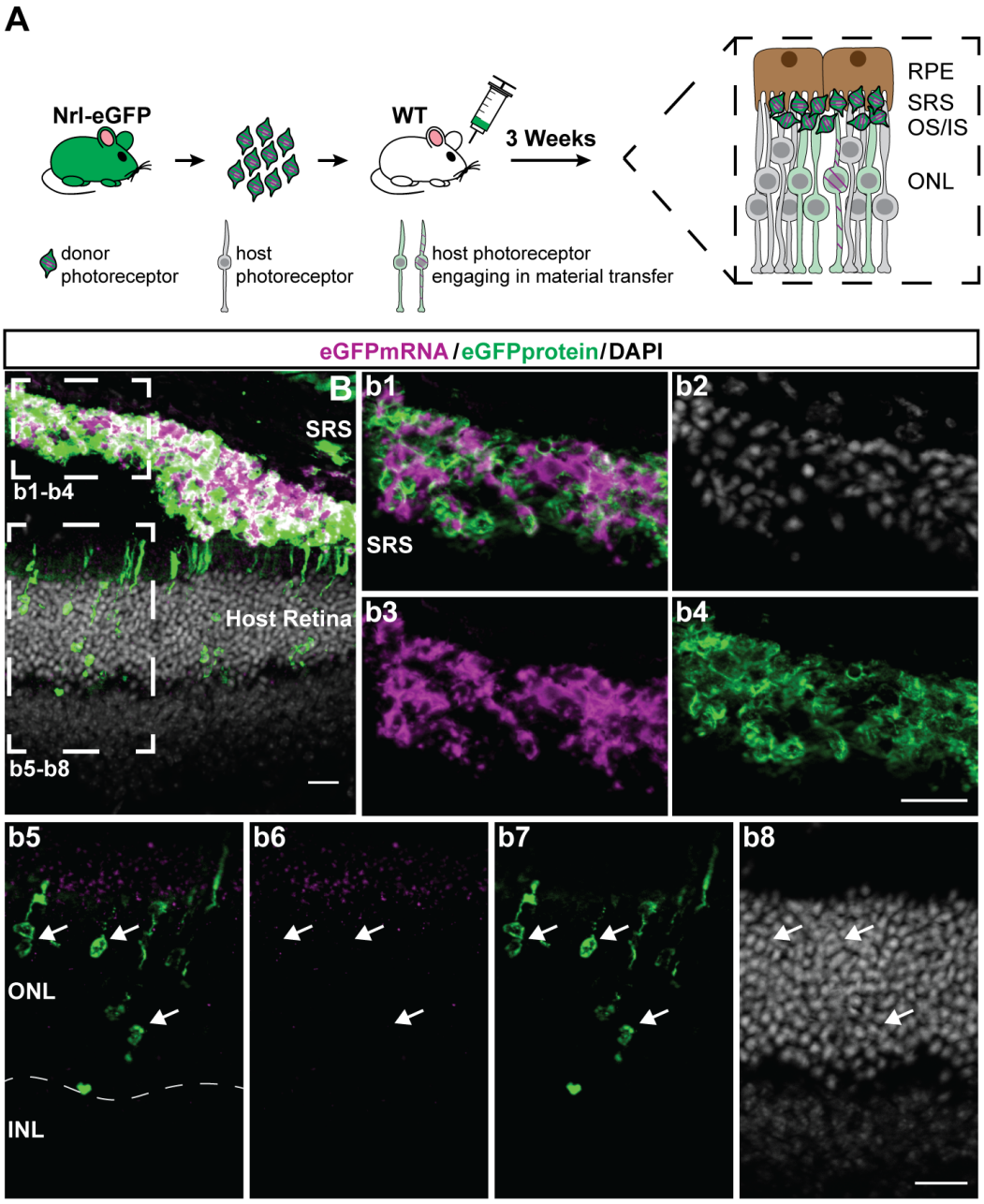

Figure 30. Detection of eGFP mRNA and protein in transplanted retinas. A) Schematic representation of the experimental approach. Nrl-eGFP post-mitotic photoreceptor precursors were transplanted into adult wild-type animals. Three weeks post-transplantation, host retinas were analysed via RNAscope combined with IHC for eGFP mRNA (magenta) and eGFP protein (green) detection, respectively. **B)** Overview of a transplanted retina. **(a-d)** The transplanted cell mass was localised in the SRS and was positive for both, eGFP mRNA and protein. **(e-h)** Cells containing eGFP protein were detected within the host ONL, however, it was hard to discriminate whether those cells were also positive for eGFP mRNA. RPE: retinal pigment epithelium, SRS: sub-retinal space, OS/IS: outer segments/inner segments, ONL: outer nuclear layer, INL: inner nuclear layer. Scale bars: 20µm.

Since the results obtained with the RNAscope combined with IHC were not fully conclusive, I designed another experiment to better assess whether mRNA can be transferred from donor to host cells. The experimental approach, schematically represented in Figure 33 (A) was the following: male Nrl-eGFP post-mitotic photoreceptor precursors were transplanted into adult wild-type females. Three weeks post-transplantation, host retinas were analysed using two different techniques. First, three transplanted retinas were analysed using the Y-chromosome FISH combined with IHC for eGFP protein detection. These samples served as controls for cytoplasmic material exchange as responsible for the presence of eGFP+ cells within the host retina rather than structural integration. Second, four transplanted retinas were individually dissociated to a single cell suspension and then single cells positive or negative (as control) for eGFP protein were sorted using flow cytometry (fluorescence activated cell sorting, FACS). Each single cell was then assessed for sex genotype using PCR and for the presence/absence of eGFP mRNA using RT-qPCR.

To test whether this approach is feasible, I set up a pilot experiment that allowed me to test the FACS sorting strategy as well as the single cell analysis. The purpose of this pilot experiment was i) to assess whether it was possible to obtain, for each single cell, information for sex genotyping and for the presence/absence of eGFP mRNA, ii) the efficiency of the procedure and iii) whether the information obtained was reliable or not (rate of false negatives/false positives). To set up the conditions for this pilot experiment, adult male Nrl-eGFP and adult female wild-type retinas, as well as a 50:50 mixed population of both, were used. Figure 31 shows the FACS gating strategy, in this case using as input a single cell suspension containing a 50:50 mixture of adult male Nrl-eGFP and female wild-type retinal cells.

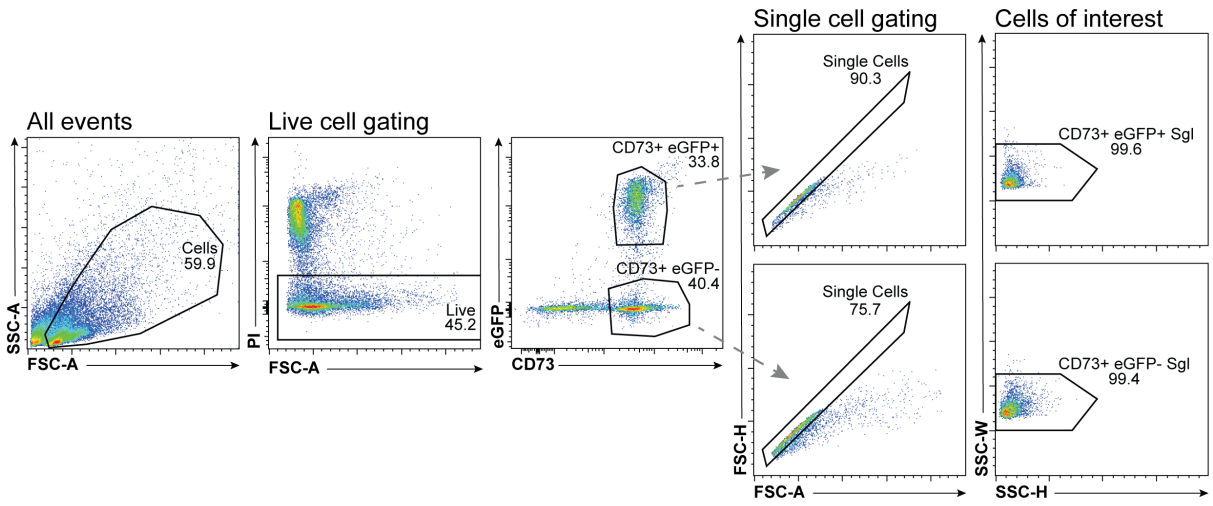

Figure 31. Gating strategy for single cell sorting. The first gate was used to select cells vs. debris. Then a second gate, based on the presence/absence of PI was used to distinguish live from dead cells. From the live cell

population, photoreceptors (CD73 positive) positive or negative for eGFP where discriminated. For each photoreceptor population (eGFP+ and eGFP-), two different gatings (FSC-H vs. FSC-A and SSC-W vs. SSC-H) where used to identify single cells, which were then sorted and used for sex genotyping and eGFP mRNA detection by RT-qPCR. SSC-A: Side Scatter Area, SSC-H: Side Scatter Height, SSC-W: Side Scatter Width, FSC-A: Forward Scatter Area, FSC-H: Forward Scatter Height, PI: Propidium Iodide, CD73: Cluster of Differentiation 73, APC: allophycocyanin.

After sorting the male Nrl-eGFP/female wild-type/mix retinal cell suspension using the represented gating strategy (Figure 31), 3 main populations were observed (Figure 32): i) CD73+/eGFP+ cells, which correspond to male Nrl-eGFP rod photoreceptors, ii) CD73+/eGFP- cells, which correspond to female wild-type rod photoreceptors and iii) CD73-/eGFP- cells, which correspond to the non-rod photoreceptor cell fraction of the retina.

For this pilot experiment, the populations of interest where the CD73+/eGFP+ cells (male rod photoreceptors) and the CD73+/eGFP- cells (female rod photoreceptors), which were sorted as single cells/10cells/100cells in 8-tube strips (n=3 strips/population). The single cells were used to test whether male/female sex genotype could be obtained and to test whether eGFP mRNA was detectable in male Nrl-eGFP cells, and non-detectable in female wild-type cells. The 10/100 cells wells were used to test whether single cells were enough starting material for such analysis or whether more starting material was required. Each strip had an additional well for positive (male/female genomic DNA for the sex genotyping or male Nrl-eGFP/female wild-type RNA for the RT-qPCR) control and one well for negative (water) control. Moreover, using the mix population, Nrl-eGFP rod photoreceptors (CD73+/eGFP+) vs. wild-type rod photoreceptors (CD73+/eGFP-) were sorted. Therefore, these strips were used to actually test whether FACS sorting for eGFP was accurate and if it was possible to distinguish male Nrl-eGFP+ from female wild-type cells in a mix population, which resembles the situation expected to encounter after dissociating transplanted retinas.

Figure 32, B shows that male Nrl-eGFP single cells were detected as male cells, while female wild-type cells were detected as female cells, and for the mix population, it was possible to distinguish single male from female cells. Moreover, for the mixed strips, in the 10/100 cells wells, a mixed genotype was also observed. However for the single cells, around 30% considering all the tests performed, did not show any sex genotyping result.

The corresponding RT-qPCR results are shown in Figure 32, C. For the single cell samples, which are the ones of interest, Cp (crossing point) values lower than 25 for male Nrl-eGFP cells were observed, while for female wild-type cells the Cp values were always over 25, almost reaching 30. Thus, there is a noticeable difference between cells positive for eGFP mRNA and those that are negative. Moreover, the melting curves (data not shown) obtained for male Nrl-

eGFP single cells are the same as those obtained in the positive control, whereas only melting curves resulting from primer-dimers can be observed for the female wild-type cells. However, it is important to consider that it is possible to obtain false negatives for the eGFP mRNA. For example, in the mix sample, the single cell 3 (Figure 32, B and C, SC-3) is a male cell according to sex genotyping, and therefore it should be positive for the eGFP mRNA, however, the Cp value obtained for this sample is over 30, which would be considered negative. Nonetheless, it is important to note that no false positives were detected among the single cells analysed during this pilot experiment.

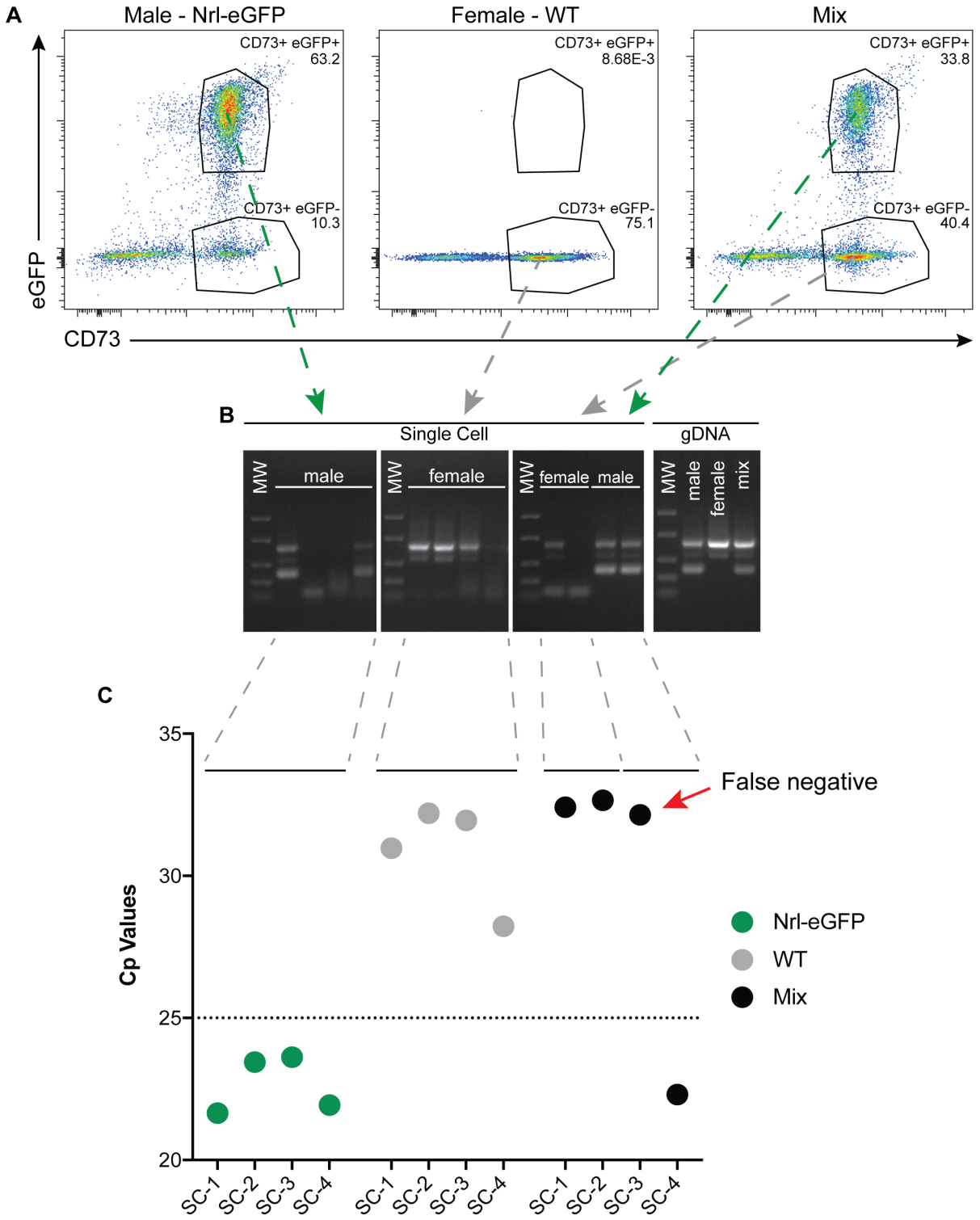

Figure 32. Pilot experiment to set up the single cell sex genotyping and RT-qPCR analysis. A) After dissociating male Nrl-eGFP retinas and staining them for CD73, the main population obtained was CD73+/eGFP+, which corresponds to rod photoreceptors. For dissociated female wild-type retinas stained for CD73, the main population obtained is CD73+/eGFP-, which corresponds also to rod photoreceptors. After mixing in a 50:50 ratio the dissociated retinas, two main populations (CD73+/eGFP+ and CD73+/eGFP-) were obtained. Such populations were then used to sort single cells for further **(B)** sex genotyping and **(C)** RT-qPCR analysis. **B)** Agarose gel showing the sex genotyping, which allows to distinguish male from female cells. **C)** RT-qPCR results, showing that there is a difference in the Cp values obtained from eGFP+ samples vs. eGFP- samples. A Cp value of 25 will be used in

the following experiment to distinguish between positive and negative cells for eGFP mRNA. CD73: cluster of Differentiation 73, SC: Single Cell, MW: molecular weight ladder (50, 200,400,850, 1500bp) (ThermoScientific, cat#SM1103).

Once the single cell analysis was set up, transplanted retinas were analysed in order to elucidate whether mRNA can be transferred between donor and host photoreceptors.

Prior to collecting the retinas, the fundus of the transplanted eyes was screened for the presence of an eGFP+ cell mass by a retina microscope (Micron IV). From the retinas with exemplary cell mass (see Figure 33, B-B'), three samples where used for Y-chromosome FISH and IHC for eGFP and four samples for single cell analysis. As expected, the eGFP+ cell mass present in the SRS of transplanted retinas was also positive for the Y-chromosome, identifying those cells as male Nrl-eGFP donor cells (Figure 33, C, c1-c3), while the eGFP+ cells located within the host ONL were negative for the Y-chromosome (Figure 33, C, c4-c6), identifying them as eGFP+ host cells resulting from cytoplasmic material exchange. Precisely those cells were the target cells for the single cell analysis of this experiment. The goal of this experiment was to discriminate whether these cells have eGFP mRNA or not. The sex genotyping was a requirement to be certain that the eGFP+ cells sorted via FACS are host (female) cells, and not donor (male) cells that remained attached to the host retina during isolation.

The retinas used for single cell analysis were carefully isolated from the rest of ocular tissue with the objective to remove as much eGFP+ sub-retinal cell mass (male donor cells) as possible. In this way the eGFP+ cells obtained by FACS sorting should be mainly host (female) cells resulting from cytoplasmic material exchange. Then, retinas were dissociated to a single cell suspension and stained for CD73. The gating strategy to select the desired cell fraction was the same as the one shown in Figure 31. As would be expected, in Figure 33, D, the population of interest (CD73+/eGFP+ cells) was significantly smaller, nonetheless, a total of 180 eGFP+ single cells were obtained for further sex genotyping (male vs. female, Figure 33, E) and RT-qPCR (Figure 33, F). Some eGFP- cells were also sorted as a negative control for RT-qPCR analysis. From the cells that a sex genotype was obtained (n=104), 48.08% were male, indicating that despite isolating the host retinas from the rest of ocular tissue, a portion of the donor cell mass remained attached to the host retina. The other remaining 51.92% of the eGFP+ cells were female. From the male cells, 48% were positive for eGFP mRNA, indicating a high rate of false negatives (since all the male cells (Nrl-eGFP) should be positive for eGFP mRNA). From the female cells, 22.22% were positive for eGFP mRNA, indicating that mRNA can be transferred from donor to host cells. Furthermore, considering the high rate of false negatives obtained (male Nrl-eGFP cells in which eGFP mRNA was not detected), most likely, the percentage of female cells containing eGFP mRNA is significantly higher than the number detected in this experiment.

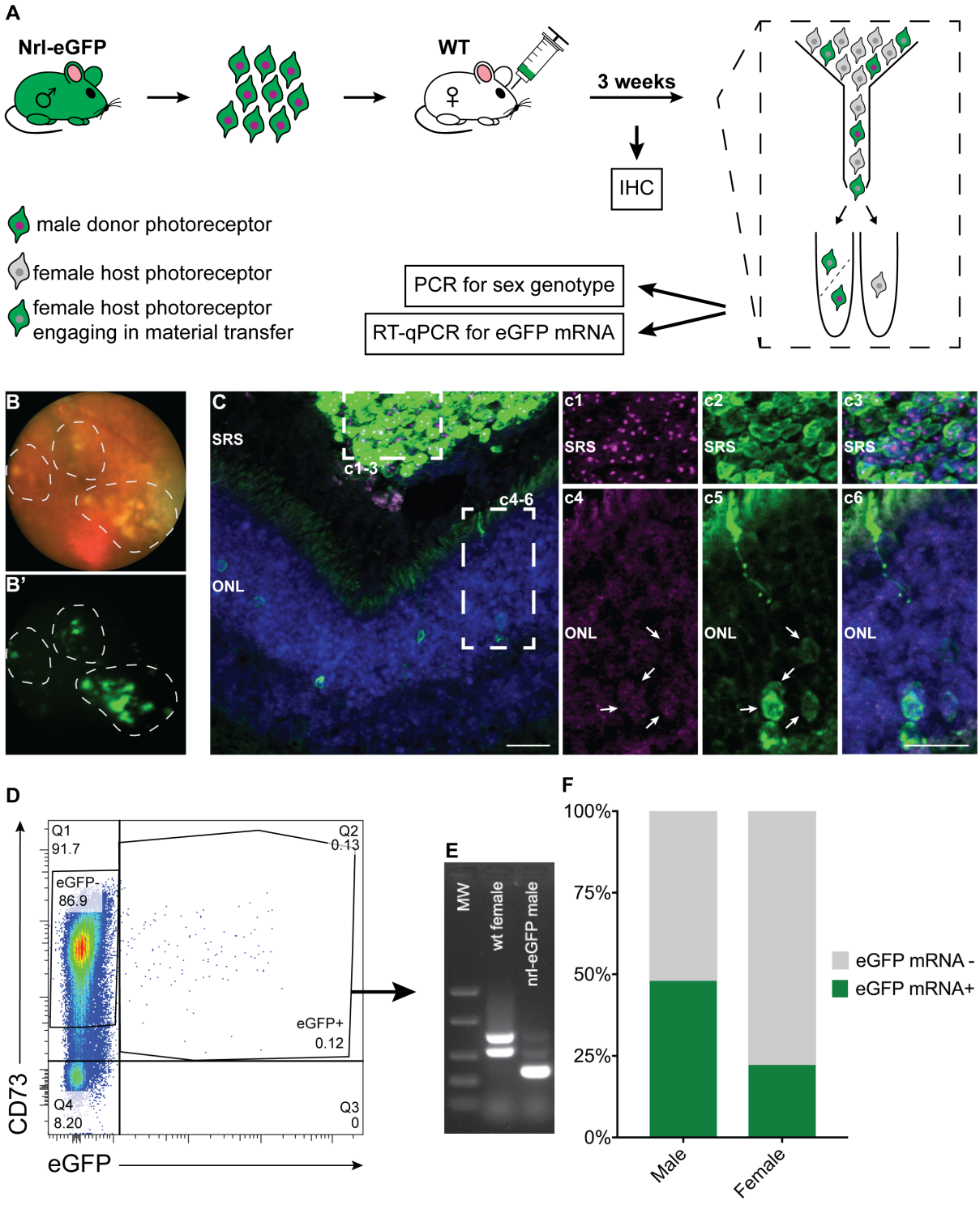

Figure 33. mRNA is transferred between donor and host cells. A) Schematic representation of the experimental design. Briefly, male Nrl-eGFP post-mitotic photoreceptor precursors were transplanted into adult wild-type female hosts. Three weeks post-transplantation, host retinas were analysed by Y-chromosome FISH and IHC for eGFP and by single cell sex genotyping and RT-qPCR. **B-B')** Representative eye fundus of a transplanted animal. In the green channel (B') is possible to identify the transplanted cell mass. **C)** Y-chromosome FISH and IHC for eEGFP. **c1-c3)** The cells located in the SRS are double positive for the Y-chromosome and the eGFP, identifying them as male donor cells. **c4-c5)** The eGFP+ cells located within the host retina are negative for the Y-chromosome, indicating that they are the result of cytoplasmic material exchange. **D)** Representative FACS plot obtained during

the analysis of the transplanted retinas. The biggest population (CD73+/eGFP-) corresponds to female wild-type host photoreceptors, while the minor population (CD73+/eGFP+, 0.12%) corresponds to a mixture of remaining male donor cells and female host cells that received cytoplasmic material from the donor cells. This is the population that was sorted into single cells for further analysis. **E)** Representative result of sex genotyping that was used to discriminate the single cells between male and female. **F)** Single cell RT-qPCR results for the eGFP mRNA. Only 48% of the male cells were detected as positive for the eGFP mRNA, indicating a high rate of false negatives. Nonetheless, up to 22.22% of the female cells were positive for eGFP mRNA, indicating that mRNA is transferred from donor to host cells. RT-qPCR: Reverse Transcription-quantitative Polymerase Chain Reaction, SRS: sub-retinal space, ONL: outer nuclear layer, CD73: Cluster of Differentiation 73, MW: molecular weight ladder (50, 200,400,850, 1500bp) (ThermoScientific, cat#SM1103). Scale bars: 20µm (C), 15µm (c1-c6).

3.3.3 Mitochondria are not transferred from donor to host photoreceptors

Another cytoplasmic component candidate that might be transferred between donor and host cells are organelles, for example mitochondria. In comparison to cytoplasmic macromolecules such as eGFP or mRNA, mitochondria are much bigger in size, and highly dynamic in terms of fission and fusion. They can be found individually or organized in linear networks or clumps (Chan and Marshall, 2010). Different studies have shown that mitochondria can be transferred between cells, and the hypothesised mechanisms by which this transport occurs are tunnelling nanotubes or microvesicles (Csordás, 2006; Spees et al., 2006). Even though the exact content of extracellular vesicles is unknown, they bear proteins, lipids and nucleic acids (Colombo et al., 2014), therefore, it is unlikely that they participate in mitochondrial transfer. On the contrary, mitochondria have been shown to be transferred between ARPE-19 cells in culture through tunnelling nanotubes (Wittig et al., 2012). Therefore, analysing mitochondrial transfer between donor and host photoreceptors could provide hints of the mechanism by which cytoplasmic material exchange takes place.

To analyse whether mitochondria can also engage in cytoplasmic material transfer, a reporter mouse line that expresses the photo-convertible protein Dendra2 specifically in mitochondria (PhAM mouse) (Pham et al., 2012) was used. To test the reliability of the reporter expression, adult retinas from this mouse line were stained with the mitochondrial marker Tom20 (complex of proteins involved in the translocation of proteins from the cytoplasm to the intermembrane space of the mitochondria). As can be observed in Figure 34, Dendra2 fluorescence is strong enough to be detected without any further staining (Figure 34, C). Moreover, in photoreceptors it localises mostly in the inner segments, as well as in their synaptic terminals. Dendra2 is also found in the dendrites of second order neurons and in the inner plexiform layer. Importantly, besides the strong co-localization of Dendra2 and Tom20 (Figure 34, E), Dendra2 signal is

detected where mitochondria are reported to be localized indicating that this is a good reporter for mitochondrial localization and detection.

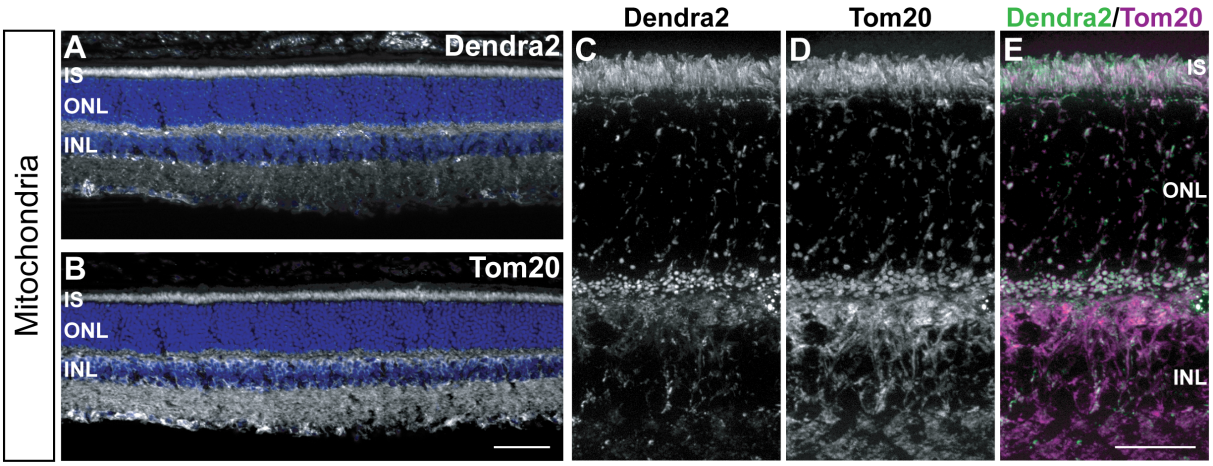

Figure 34. PhAM mouse line is a reliable reporter for mitochondria. A,B) Overview of Dendra2 and Tom20 localization. **C,D)** Closer view of of Dendra2 and Tom20 localization. **E)** Dendra2 and Tom20 co-localise perfectly and they are detected where mitochondria are expected to be localised across the mouse retina. IS: inner segments, ONL: outer nuclear layer, INL: inner nuclear layer. Scale bars: 50µm (A, B), 20µm (C-E).

The PhAM mouse line was crossed with a ubiquitous reporter line that expresses the tdTomato protein in the cell membrane (mTmG) (Muzumdar et al., 2007). The resulting progeny showed green mitochondria and red cell membranes and were used to isolate donor photoreceptor precursors for transplantation. This donor cell population was analysed by imaging flow cytometry prior to transplantation (Figure 35). This technique is similar to a flow cytometry analysis, with the particularity that each individual event can be imaged within different channels for analysis (bright field, fluorescence).

Considering that Dendra2 is an irreversible photo-convertible protein (green to red) and that the activating light required for the photo-conversion is of the same wavelength (460-500nm) required for visualization, the laser set up for the imaging flow cytometry was tested in each single reporter line prior to analysis of the double reporter labelled cells (Figure 35). As can be observed in Figure 35 (A, a1) no green to red photo-conversion was detected during imaging flow cytometry, and mitochondria could be detected within the cells. An additional control for false double positive detection was performed. For that purpose, a 50:50 mixed cell population from each single reporter was analysed. In this situation, 6.95% of the population was detected as double positive, however, the images of these events revealed that they were, in fact, false positives resulting from cell aggregation or cell debris attached to cells (Figure 35, B, b1). In contrast, post-mitotic photoreceptor precursors (CD73+) obtained from litters resulting from the crossing of both reporter lines (PhAM/mTmG) were real double positive, with green mitochondria and red membranes (96.1%) (Figure 35, B, b2).

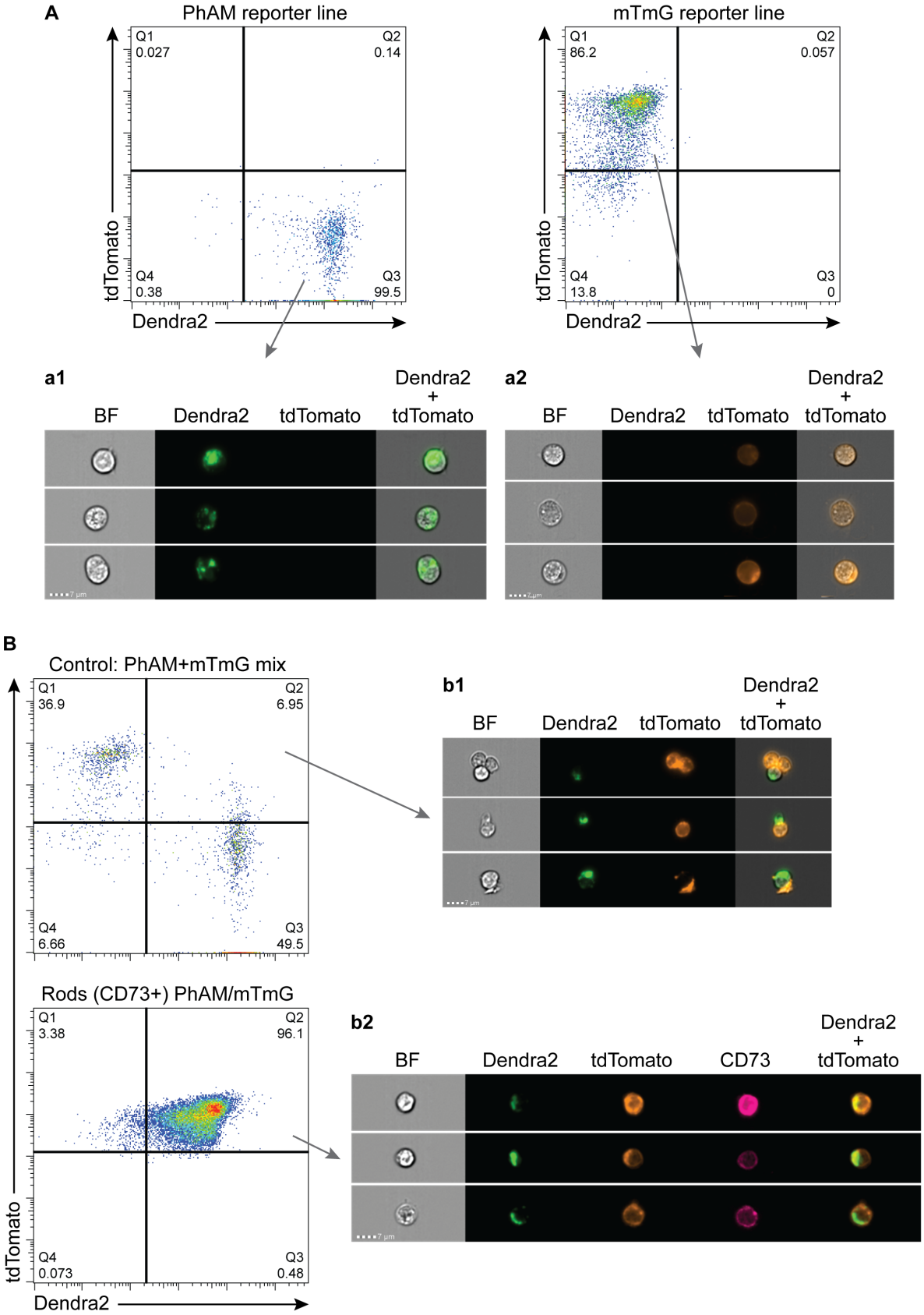

Figure 35. Analysis of the PhAM/mTmG donor post-mitotic photoreceptor precursors. A) ImageStreamX plots of the single reporter lines PhAM (Dendra2) and mTmG (tdTomato). **a1, a2)** Representative images for each of the events recorded for the PhAM and the mTmG mouse lines, respectively. **B)** ImageStreamX plots for the false

double positive control and the analysed donor cell population (double transgenic PhAM/mTmG). **b1, b2)** Representative images for each of the desired populations, false double positives and double transgenic cells (PhAM/mTmG), respectively. BF: bright field

To actually assess whether mitochondria can also be transferred from donor to host photoreceptors, post-mitotic photoreceptor precursors obtained from PhAM/mTmG mice were transplanted into adult wild-type hosts. Three weeks post-transplantation, host retinas were analysed by IHC. Cells located in the sub-retinal space were, as expected and in concordance to the ImageStream data, double positive for Dendra2 (mitochondria) and tdTomato (membrane) (Figure 36, B, b1-b3). On the contrary, Dendra2 signal (mitochondria) was not detected (Figure 36, b4-b6) either in the tdTomato positive cells (total of 978) observed within the host ONL (n=4) or in tdTomato negative host cells, indicating that mitochondria were not transferred from donor to host photoreceptors.

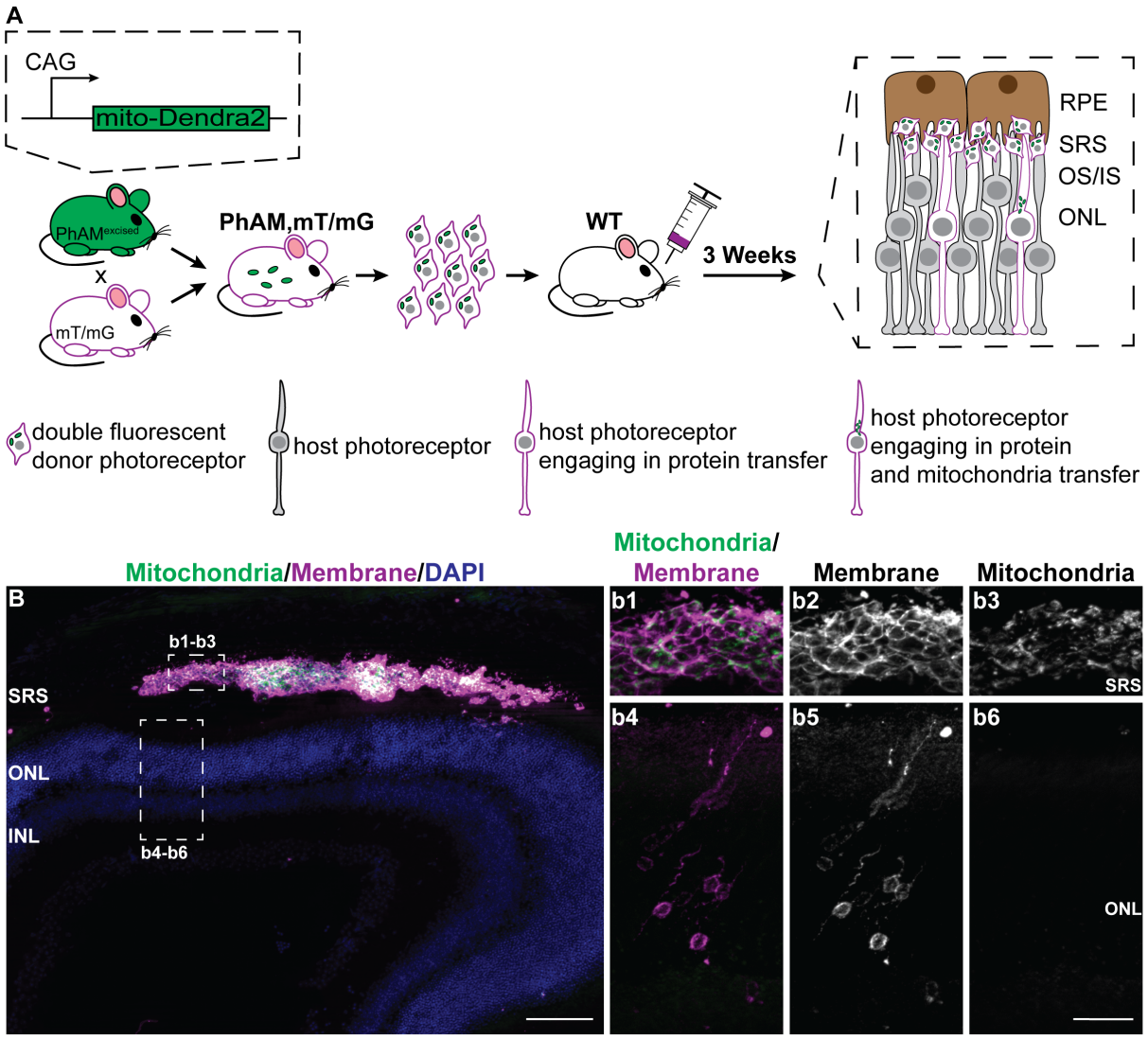

Figure 36. Mitochondria are not transferred from donor to host photoreceptors. A) Schematic representation of the experimental design. A mitochondria reporter mouse line (PhAM) was crossed with a membrane reporter (mTmG). Post-mitotic photoreceptor precursors from the resulting mouse line (PhAM/mTmG) were transplanted

into adult wild-type animals. Three weeks post-transplantation, host retinas were analysed by IHC. **B)** Overview of a transplanted retina. **b1-b3)** Donor cells located in the SRS were positive for both reporters, Dendra2 and tdTomato. **b4-b6)** tdTomato positive cells located in the host ONL were negative for Dendra2. SRS: sub-retinal space, ONL: outer nuclear layer, INL: inner nuclear layer, RPE: retinal pigment epithelium, OS: outer segments, IS: inner segments. Scale bars: 100µm (B), 20µm (b1-b6).

3.4 Discussion

In this study, a rigorous experiment to differentiate between structural integration of donor photoreceptors within the host retina and fusion between donor and host photoreceptors was performed. Here, we took advantage of an inherent nuclear difference between male donors and female hosts, the presence of a Y-chromosome. Male Nrl-GFP young post-mitotic photoreceptors were transplanted into female wild-type hosts. Three weeks later, the transplanted retinas were analysed for the presence of both, the cytoplasmic GFP protein, and the nuclear Y-chromosome. Unexpectedly, the vast majority of the GFP+ cells within the host retina were negative for the Y-chromosome, identifying them as female cells. In addition, an experiment performed by another researcher in the lab identified the presence of double fluorescent photoreceptors (98 ±17 GFP+/DsRED+ photoreceptors per 1 million cells) after transplanting GFP-expressing donor photoreceptors into hosts ubiquitously expressing DsRed. Furthermore, in another experiment conducted in our lab, Cre-dependent reporter donor photoreceptors (Ai9 mice, Madisen et al., 2010) were transplanted into hosts expressing Cre recombinase specifically in photoreceptors (B2-Cre mice, Le et al., 2006). Three weeks post-transplantation expression of the reporter was detected in both, donor and host photoreceptors. The results of the Y-chromosome experiment described in this study, together with these two other experiments performed by colleagues in the laboratory indicated that the exchange of cytoplasmic material between donor and host photoreceptors is the main underlying mechanism for the presence of reporter-positive cells within the host retina, and most likely, for the visual function recovery observed upon photoreceptor transplantation (Figure 37). Moreover, from the Cre-reporter experiment, we interpret that cytoplasmic material exchange is bi-directional, i.e. cytoplasmic material can be transferred from donor to host photoreceptors and vice-versa, and that nuclear proteins, such as Cre, can also be exchanged (Santos-Ferreira et al., 2016b).

The results of the experiments conducted in our laboratory, including the Y-chromosome experiment described here, together with similar experiments performed by other research groups, including: i) transplantations of GFP+ donor photoreceptors into sexually or fluorescently mismatched recipients (Pearson et al., 2016; Singh et al., 2016), ii) transplantation of healthy donor photoreceptors into hosts deficient for photoreceptor-specific

proteins (Pearson et al., 2016) and iii) transplantations of Cre-dependent/expressing donor photoreceptors into Cre-expressing/dependent (respectively) hosts (Pearson et al., 2016; Singh et al., 2016) led to a change of paradigm in the field of photoreceptor transplantation for the treatment of retinal degenerative diseases. Furthermore, a later publication reported host-reporter positive cells failing to exhibit the donor nuclear hetero/euchromatin architecture (Ortin- Martinez et al., 2017). The evidence presented supporting cytoplasmic material exchange as the underlying mechanism for visual function restoration requires a re-interpretation of the transplantation data published until now. Furthermore, considering that cytoplasmic reporters, such as GFP, can be transferred from donor to host, proper criteria to analyse transplantation outcome should be established in the field. Cytoplasmic labelling facilitates the detection of donor cells upon transplantation, however, does not allow to differentiate between cell integration and cytoplasmic material exchange. Combination with nuclear labelling might be an option to solve this issue. Nonetheless, experiments from other researchers in the laboratory indicate that nuclear proteins can also be transferred from donor to host cells. Moreover, experiments in which Cre-dependent reporters were transplanted into Cre-expressing hosts, or vice versa, reporter expression was detected in both, donor and host cells supporting the idea that nuclear proteins can also be transferred (Pearson et al., 2016; Santos-Ferreira et al., 2016b; Singh et al., 2016). Therefore, nuclear labelling should not be based on nuclear proteins, but rather on genomic DNA, and this could be achieved either by using intercalating thymidine analogues like EdU or BrdU, or, as shown in this study, transplanting donor cells into sexually mismatched hosts and assessing the presence of Y-chromosome. Actually, this last option is the more reliable one, since EdU or BrdU often fails to label 100% of the donor cell population, therefore, leading to in-conclusive results (Santos-Ferreira et al., 2016b).

Before photoreceptor cell transplantation can become a routinely applied therapy for retinal degenerative diseases, it is important to fully understand how the transplanted donor photoreceptors interact with the host retina. In that sense, the discovery of cytoplasmic material exchange between donor and host photoreceptors represents an advance in this direction. However, questions regarding the exact mechanism by which donor and host cells exchange material, which cells are actually able to engage in such phenomenon, and which cytoplasmic material can be exchanged remain open.

Here experiments addressing the kind of cytoplasmic material that can be engaged in this newly described phenomenon have been conducted. First, it was assessed whether mRNA could be transferred from donor to hosts. Evidence for mRNA transfer between RPC has been recently shown in an *in vitro* setting. After verifying that mRPC release extracellular vesicles

containing, among others, mRNA, mRPC expressing GFP were cultured in a transwell system together with hRPCs. After 96 h of culture the presence of GFP mRNA in the hRPCs was detected by RT-qPCR, indicating mRNA transfer from mRPCs via extracellular vesicles (Zhou et al., 2018).

In this thesis, the goal was to analyse, *in vivo*, whether mRNA could be transferred from donor to host photoreceptors. In a first experimental approach, GFP-expressing donor photoreceptors were transplanted into wild-type hosts. Transplanted retinas were analysed for the presence of GFP protein and mRNA three weeks post-transplantation using a combination of IHC and RNAscope ISH. According to Advanced Cell Diagnostics, the company that developed the RNAscope technology, this is supposed to be highly sensitive, i.e. allows the detection of single RNA molecules. In the experiment performed in this study, however, the detection of GFP mRNA in the cell body of cells expressing GFP protein within the host retina was not possible. Nonetheless, a dotted signal, hardly distinguishable from background, was observed in the region of IS/OS of the host retina. Considering that translation occurs in the IS of photoreceptors, this experiment was not enough to fully discard mRNA transfer between donor and host cells, and therefore, an alternative experimental approach was used. In this new experimental design, male GFP-positive donor cells were transplanted into wild-type females. Three weeks post-transplantation, host retinas were isolated and dissociated to a single cell suspension. GFP-positive cells were single-sorted and further sex genotyped by conventional PCR and analysed for the presence of mRNA by RT-qPCR.

Results obtained using this second experimental approach show, for the first time in the field of photoreceptor transplantation, strong evidence that mRNA can be transferred from donor to host in an *in vivo* setting. Considering the percentage of host cells that present donor-specific mRNA (around 22% of the GFP+ cells within the host ONL), it is reasonable to think that also protein is transferred between donor and host photoreceptors. However, it is also possible that the translation of the transferred mRNA within the host cell is responsible for the detection of donor proteins within the host photoreceptors, rather than actual protein transfer. The fact that the single cell analysis experiment described in this study shows a high rate of false negatives for the detection of GFP mRNA (around 50% of the GFP+ donor cells, which are obtained from an Nrl-GFP mouse reporter line, are detected as negative for the presence of GFP mRNA), together with the lack of an experiment that directly analyses for protein transfer, makes it hard to distinguish whether only mRNA or both mRNA and protein are being transferred. To elucidate whether only mRNA or also protein engages in cytoplasmic material transfer, one could consider to label the protein fraction of donor cells prior to transplantation, for example, by incubating donor photoreceptors with radioactive amino acids or chemical tags that

covalently bind to proteins. Transplanted retinas could then be analysed for the presence of radioactivity/chemical tag, and thus, conclude whether proteins are also able to engage in cytoplasmic material transfer.

Next, in this study the possible transference of larger cellular components, such as organelles, i.e. mitochondria, has been analysed. Taking advantage of a mitochondria-reporter line, evidence for the lack of transfer of such large cytoplasmic components is presented here.

Regarding the cell types able to engage in cytoplasmic material exchange, it appears to be that this is a photoreceptor-photoreceptor specific phenomenon. Evidence supporting this hypothesis is that very limited numbers or no GFP-positive cells have been observed in the host ONL after transplanting retinal progenitor cells (MacLaren et al., 2006), retinal cells other than photoreceptors, i.e. CD73-negative cells (Eberle et al., 2011), or fibroblasts (Pearson et al., 2016). Furthermore, results from a researcher in the laboratory show that the number of reporter-positive cells within the host ONL decrease when the non-photoreceptor fraction of retinal cells, cortical brain cells or bone marrow-derived cells are transplanted into the SRS of host mice, compared to the transplantation of young post-mitotic photoreceptor precursors (Borsch, 2017).

Most of the studies regarding material transfer have been performed using as donor cells young primary post-mitotic rod photoreceptor precursors. However, as already discussed in Chapter 2 of this thesis, PSC-derived photoreceptors are the preferred source when it comes to translate photoreceptor cell replacement towards clinical application. In this regard, studies directly addressing whether PSC-derived rod photoreceptor precursors integrate or engage in cytoplasmic material transfer are missing. Prior to the discovery of cytoplasmic material exchange, PSC-derived rod photoreceptor precursors were shown to “integrate” into the host ONL of wild type and retinal degeneration mouse models in similar numbers as when post-mitotic rod photoreceptors were used as donor cells (Gonzalez-Cordero et al., 2013; Decembrini et al., 2014; Santos-Ferreira et al., 2016a). With the change of paradigm, it would be interesting to reanalyse those results and properly assess whether the GFP+ cells detected in the ONL of the host retinas are a result of integration or of cytoplasmic material exchange. Two recent studies in which PSC-derived cone photoreceptor precursors were transplanted into mouse models of retina degeneration include methods to distinguish whether GFP+ cells located in the ONL of the host were structurally integrated or, instead, result from material exchange. Despite the observation that cone photoreceptor transplantation seems to be less efficient than rod transplantation, GFP+ cells detected in the host retinas were the result of both integration and cytoplasmic material exchange. Interestingly, after transplantation of

mESC-derived cone photoreceptor precursors, cytoplasmic material exchange seemed to predominate over integration (Waldron et al., 2018), however, when transplanting hESC-derived cone photoreceptor precursors into mouse models of retinal degeneration, it appeared that the few GFP+ cells identified within the host ONL were mostly the result of integration, and just occasionally, showed signs of cytoplasmic material exchange (Gonzalez-Cordero et al., 2017). This difference might be due to the effect of a xenotransplant, indicating that cytoplasmic material transfer might not only be photoreceptor- but also species-specific. In the case that cytoplasmic material transfer is species-specific, animal models will not be useful for assessing the ability of human photoreceptors to engage in this phenomenon. Therefore, alternative systems will need to be considered. A first approach, for example, could be to transplant reporter-positive hESC-derived photoreceptors into sexually mismatched hESC-derived retinal organoids, and analyse for the presence of donor cells in the host organoids. Alternatively, but maybe ethically and logistically more complicated, hESC-derived photoreceptors could be delivered on the photoreceptor side of human retinal explants derived from post-mortem tissue.

The mechanism by which donor and host photoreceptors exchange cytoplasmic material remains elusive. Possibilities including direct cell-cell connections by the establishment of nanotubular structures between donor and host photoreceptors, free uptake of cellular material present in the SRS after transplantation or vesicular transport between donor and host photoreceptors have been hypothesised (Figure 37) (Santos-Ferreira et al., 2017). Of these different mechanisms, due to the minimal uptake of purified GFP protein injected into the SRS of host animals, Pearson and colleagues discarded free molecule uptake as a mechanism playing a major role in cytoplasmic material exchange (Pearson et al., 2016). However, data obtained in our laboratory indicates that free molecule uptake might actually play a role in this phenomenon. After transplanting fluorescently labelled dextran of different sizes, we observed a size-dependent dextran uptake by host photoreceptors. Moreover, the injection of GFP mRNA (modified for stabilization) into the SRS of wild-type animals led to high numbers of GFP positive cells within the host ONL (Ebner, 2018). Taken together, these results indicate that free-molecule uptake might play a role in cytoplasmic material exchange, however, it depends on the size and nature of the transplanted molecules.

A physical connection between donor and host photoreceptors has also been hypothesised as a possible mechanism for cytoplasmic material exchange between donor and host photoreceptors. In fact, it is known that nanotubular structures exist in the retina and they connect cone pedicles and rod spherules (Rodieck, 1998). Their exact function is unknown; however, such structures could be involved in horizontal transfer of molecules between

photoreceptors and could explain why GFP+ cells within the host ONL are generally found in clusters, rather than as isolated cells. Nevertheless, the existence of nanotubes between donor and host photoreceptors has not yet been shown. The lack of evidence for nanotubular structures can be either because they do not exist between donor and host photoreceptors, or if they exist, they may either be transient (Pearson et al., 2016) or unable to resist tissue fixation and processing procedures (Nickerson et al., 2018). On the other side, it is known that mitochondria can be transferred between ARPE-19 cells in culture through tunnelling nanotubes (Wittig et al., 2012). Experiments presented in this study, however, in which donor cells containing fluorescent mitochondria were transplanted into wild-type hosts, indicate that these organelles do not engage in cytoplasmic material transfer. These results suggest that tunnelling nanotubes do not appear to be the underlying mechanism for cytoplasmic material exchange between donor and host photoreceptors. Nonetheless, further studies, ideally involving live imaging, should be performed to directly assess whether nanotubes play a role in cytoplasmic material exchange between donor and host photoreceptors.

Exosomes have been shown to mediate intercellular communication in both, normal and pathological conditions (Colombo et al., 2014), and therefore, vesicular transport has also been hypothesised as a possible mechanism for material transfer. Exosomes in particular are known to contain proteins, lipids and RNAs (Valadi et al., 2007; Colombo et al., 2014). It is therefore feasible that exosomes could transfer all of these cellular materials between donor and host cells. *In vitro* studies have shown that transcription factors (i.e. nuclear proteins), microRNAs and membrane proteins are encapsulated in extracellular vesicles released by retinal progenitor cells, and those can be transferred from mRPCs to hRPCs in transwell cultures (Zhou et al., 2018). Furthermore, in the present study, evidence for membrane proteins (tdTomato) and mRNA transfer between donor and host photoreceptors has been shown, as well as a lack of transfer of larger cytoplasmic structures such as mitochondria. Taken together, these results might indicate that exosomes do play a role in material transfer, however, direct evidence for such mechanism remains elusive.

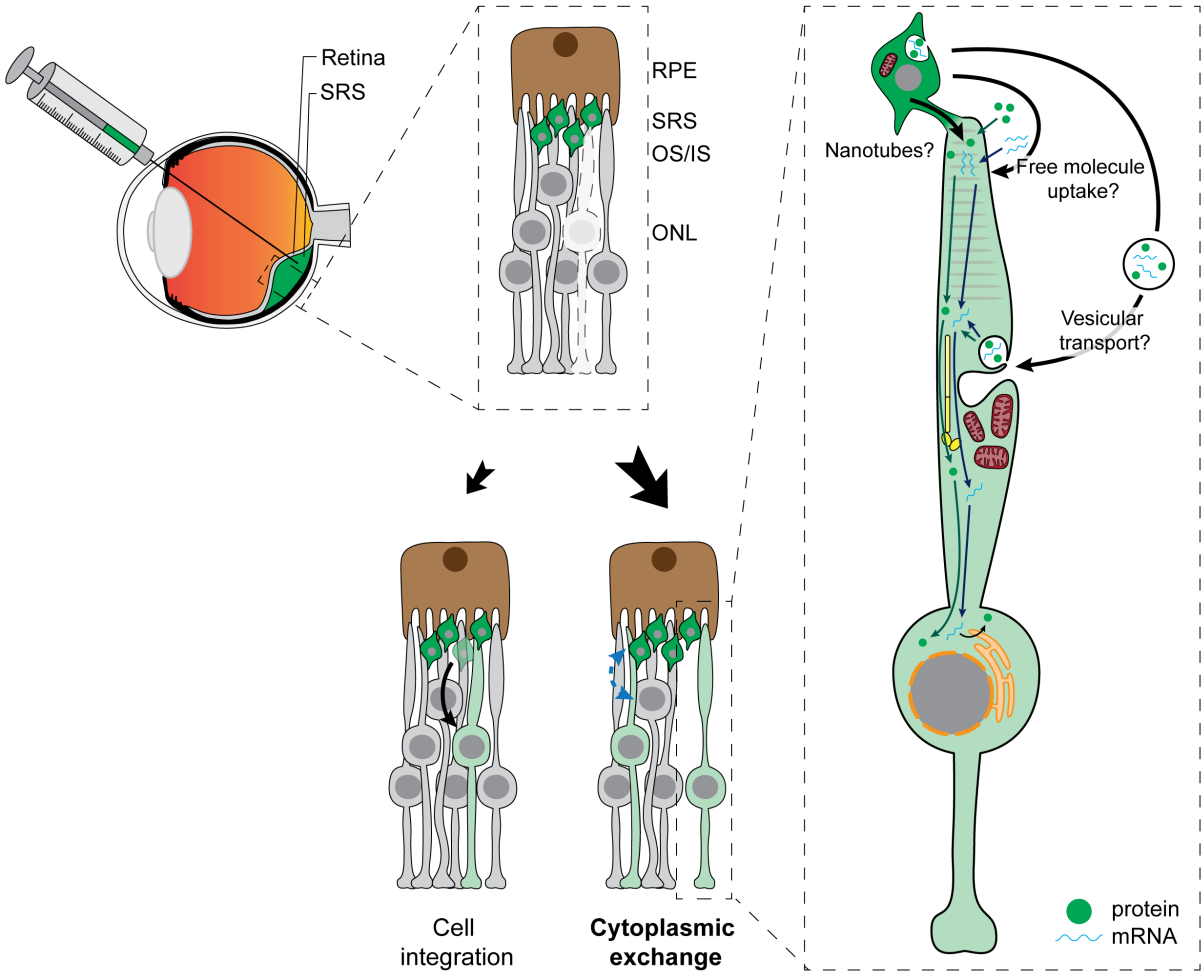

Figure 37. Summary of the photoreceptor transplantation outcome paradigm. Results presented in this study show that, following transplantation, the vast majority of GFP+ cells within the host ONL result from cytoplasmic material exchange between donor and host photoreceptors, rather than from structural integration of donor cells into the host retina. The mechanism by which this cytoplasmic material exchange occurs remains elusive, but results from our lab (Ebner, 2018) indicate that free molecule uptake plays a role in this phenomenon. Moreover, here evidence for mRNA transfer is shown, as well as for the absence of mitochondria transfer from donor to host cells. Such results would speak for a vesicular transport, however, experiments to directly address this issue need to be performed.

Despite this change of paradigm within the photoreceptor cell transplantation field, it was shown that visual function recovery has been achieved after transplanting primary young post-mitotic rod (MacLaren et al., 2006; Pearson et al., 2012) or cone-like (Santos-Ferreira et al., 2015) photoreceptor precursors into mouse models of retinal degeneration. The change of perspective regarding the underlying mechanism for such vision restoration calls for a distinction between potential cell support and cell replacement therapies. In early stages of retinal degeneration, in which endogenous but dysfunctional photoreceptors still remain, one could consider a cell support therapy. In this scenario, transplanted healthy photoreceptors stay in the host SRS for an extended period of time and supply the host photoreceptors with missing components for e.g. phototransduction and the subsequent downstream signalling

(Pearson et al., 2016; Santos-Ferreira et al., 2017). The advantage of a cell support therapy, compared to gene therapy, is that the same source of healthy donor photoreceptors can be used for patients with retinal degeneration diseases with different aetiologies. On the contrary, cell replacement therapy might be reserved for late-stages of retinal degeneration, in which the ONL has completely degenerated, and therefore, healthy donor photoreceptors can be delivered directly on top of the host's INL aiming to reconstitute the lost photoreceptor cell layer. In that case, considering that the host does not possess remaining photoreceptors, and therefore, cytoplasmic material exchange would be very unlikely, it is worth to re-consider whether a single cell suspension or a photoreceptor cell sheet have more possibilities to integrate with the INL and remaining host retinal circuit. Even though the surgical procedure to deliver a retinal sheet, compared to single cell suspension is more complicated, a retinal sheet contains the photoreceptor outer segments oriented towards the apical side, and the synaptic terminals oriented towards the basal side. Such structure might facilitate the establishment of synaptic connections, and therefore integration with the host's remaining retinal circuit. A disadvantage of such retinal sheet approach is that upon delivery massive rosette formation is reported in most of the current published studies. Therefore, an appropriate connection with the host RPE might not be established, circumventing proper OS phagocytosis and thus chromophore recycling. Nonetheless, it has been recently shown, that upon 9-*cis*-retinal supplementation of the hosts, visual function can be improved upon mESC-derived retinal sheet delivery into mouse models of end-stage retinal degeneration (Mandai et al., 2017). hESC-derived retinal sheets have also been reported to restore some visual function in rat models for advanced retinal degeneration, suggesting that human photoreceptors are able to form synapses with mouse bipolar cells (McLelland et al., 2018). On the other hand, single photoreceptor cell suspension transplanted into the end-stage *rd1* mouse model of retinal degeneration has also been shown to improve visual function, by means of pupil light response and laser speckle imaging of the blood flow in the visual cortex, indicating the integration of donor cells into the remaining host retinal circuit (Singh et al., 2013a).

In summary, in this part of the thesis evidence has been provided against structural integration and maturation of donor photoreceptors into the host retina as the underlying mechanism for visual function restoration. Instead, here it has been shown that donor photoreceptors exchange cytoplasmic material with remaining host photoreceptors upon integration. Furthermore, evidence for mRNA, but not mitochondria transfer has been provided, leading to the hypothesis that such cytoplasmic exchange might take place through extracellular vesicles, rather than tunnelling nanotubes.

Chapter 4:

Conclusion and future perspectives

Photoreceptor transplantation as a cell therapy for retinal degeneration has significantly evolved since the first pre-clinical studies performed three decades ago. Since then, a better understanding of retinal development in terms of the transcriptional networks required for neural retina and specific retinal cell types specification has been achieved. A combination of this knowledge and the advances in genetics, molecular biology and stem cell biology, as well as in the technological improvement of cell sorting devices has allowed the development of photoreceptor cell transplantation as we know it today.

Currently, the specific developmental stage of rod and cone photoreceptor precursors that leads to a best transplantation outcome, in terms of reporter-positive cells within the host retina, has been identified (MacLaren et al., 2006; Bartsch et al., 2008). Furthermore, reporter-free enrichment strategies for rod and cone photoreceptor precursors, obtained either from primary donors or from PSC-derived retinal organoids have been also described (Eberle et al., 2011; Lakowski Jorn et al., 2015; Santos-Ferreira et al., 2016a; Welby et al., 2017; Lakowski et al., 2018). Combining these tools, visual function recovery has been achieved after transplanting single cell suspensions of photoreceptor precursors (MacLaren et al., 2006; Pearson et al., 2012; Barber et al., 2013; Singh et al., 2013b; Santos-Ferreira et al., 2015) or PSC-derived retinal sheets (Mandai et al., 2017; McLelland et al., 2018) into mouse models of retinal degeneration.

Despite these encouraging results, photoreceptor cell transplantation as a cell therapy for retinal degeneration diseases remains in a pre-clinical phase. In order to reach clinical trials, several important remaining issues need to be addressed.

First, human vision relies mostly on cone photoreceptor cells, which are responsible for high acuity and daylight vision. However, most of the pre-clinical studies regarding photoreceptor cell transplantation are based on rodent models. Those are nocturnal animals, and so, their vision mainly relies on rod photoreceptors. Furthermore, rod photoreceptors represent around 97% of the photoreceptors within the rodent retina, and therefore, they are more accessible than cones, which represent only 3% of the total photoreceptors. For these reasons, the transcriptional networks that lead to rod photoreceptor cell fate specification are better understood than for cones. This translates to a better availability of tools, in terms of reporter lines, known surface markers, antibodies, etc, for the study of rod photoreceptor transplantation compared to cone transplantation. Nonetheless, in the last years the first studies in which cone photoreceptors have been isolated through viral labelling and transplanted have been published (Gonzalez-Cordero et al., 2017; Kruczek et al., 2017; Waldron et al., 2018). Furthermore, hESC-derived photoreceptors, isolated via CD73+ MACS

sorting, might have the potential to differentiate in high numbers towards cone photoreceptors four weeks post-transplantation (Gagliardi et al., 2018).

One of the main drawbacks of the mentioned studies is the poor cone enrichment achieved after sorting (Waldron et al., 2018). Furthermore, cone identification and labelling has been achieved after virally delivering GFP under the human L/M-opsin promoter, which is expressed in later stages of cone development. Early cone markers that could allow enrichment of cone photoreceptors at an equivalent developmental stage to P4 young post-mitotic rod photoreceptors are still missing. Therefore, in this study a new mESC line which expresses the GFP reporter in retinal progenitors, and later becomes restricted to cone photoreceptors, has been generated. An interesting characteristic of this line is that cone photoreceptors should start to express the GFP reporter from early stages. Thus, post-mitotic cone photoreceptors can potentially be isolated at the developmental stage which has been shown to result in better transplantation outcomes (Decembrini et al., 2017; Lakowski et al., 2010). Such a line might also be used as a tool to study cone development within the retinal organoids and may help to unravel the transcriptional program required to specify retinal progenitors into the cone cell fate. However, only preliminary results obtained with this mouse ESC line are presented in this study. Prior to any extensive use of this line, it has to be more thoroughly characterized.

Another aspect to consider for the advancement of cone replacement therapies is the animal model used in pre-clinical stages. As previously mentioned, rodents have a rod-dominated retina and, most importantly, they do not have a macula nor a fovea (Volland et al., 2015). In the primate retina however, cone density peaks in the fovea. The fovea is the region of the primate retina that not only contains the highest density of cones but also receives the highest amount of photons making this area indispensable for high acuity vision (Rodieck, 1998). In terms of cone photoreceptor replacement therefore, nocturnal rodents might not be the most adequate model. Thus, for study of cone dystrophies it might be interesting to consider other diurnal animals with retinas more structurally similar to the human retina for example chick, pigs, dogs or monkeys.

Second, before delivering any cell product to a patient it is important to understand how donor cells will interact with the host tissue, to both improve treatment outcomes and to avoid any detrimental effect of the transplanted cells into the host. In the field of photoreceptor transplantation, it was assumed that transplanted donor photoreceptor precursors could migrate and structurally integrate into the host outer nuclear layer where they would develop structures characteristic of mature photoreceptors, such as apically oriented outer segments and synaptic terminals projected towards the outer plexiform layer. This cellular integration

within the host retina, together with the establishment of synaptic connections with the host interneurons, was considered the underlying mechanism of the observed visual function recovery. Nevertheless, in this study, transplantation of donor photoreceptors into mismatched hosts represents strong evidence against such structural integration. These results, together with experiments from other researchers in the laboratory (Santos-Ferreira et al., 2016b) and results recently published by other groups (Pearson et al., 2016; Singh et al., 2016; Ortin-Martinez et al., 2017), have led to a change of paradigm in the field of photoreceptor transplantation. Currently, it is widely accepted that cytoplasmic material transfer, rather than integration, is responsible for the detection of reporter positive cells within the host ONL upon transplantation, and most likely, for the recovery of visual function.

Even though the mechanism for vision restoration is different than assumed, photoreceptor cell therapy remains as a potential therapeutic strategy to treat patients with retinal degeneration diseases. Actually, in early stages of retinal degeneration, when remaining host photoreceptors are still present, transplantation of healthy donor photoreceptors can deliver the required cytoplasmic components to the diseased cells, and therefore, rescue their phenotype. However, it is of crucial importance to understand the cause of the retinal degeneration, as results presented in this study clearly indicate that not all cytoplasmic components can be transferred. Here, it is shown that larger cellular structures, such as mitochondria, do not participate in such a phenomenon. In contrast, evidence for mRNA transfer between donor and host photoreceptors is presented. However, the mechanism by which cytoplasmic material is transferred between donor and host cells upon transplantation remains under investigation. Therefore, before photoreceptor transplantation can be used as a cell support therapy in early stages of retinal degeneration, a better understanding of the interaction between donor and host photoreceptors is required.

In later stages of retinal degeneration, in which there are no remaining host photoreceptors, visual function restoration upon photoreceptor cell replacement depends on the ability of the transplanted cells to establish synaptic connections with the host interneurons. In this situation, it is important to consider the remodelling that occurs within the remaining retinal circuit of the host, including retraction of axons and dendrites, and reactive gliosis (Marc et al., 2003; Strettoi, 2015). Both factors might incredibly complicate the establishment of synaptic connections between donor photoreceptors and host interneurons. In this regard, the window of opportunity for photoreceptor cell replacement therapy needs to be better defined, and therefore, appropriate timing of the treatment is of utmost importance (Strettoi, 2015).

Remaining milestones that need to be addressed before photoreceptor cell transplantation reaches clinical stages include the development of robust and reproducible protocols to differentiate PSC towards retinal organoids from which donor photoreceptors can be obtained. Results shown in this study reflect the high degree of variability and heterogeneity among retinal organoids. Moreover, the current protocols to obtain such organoids include many technically challenging steps that require intensive training of the professional staff. The development of automated protocols could potentially minimise variability among organoids as well as allow scale-up of production so as to be able to achieve the numbers of donor photoreceptors required in a clinical setting (DiStefano et al., 2018). Furthermore, it is known that long term cultures of PSCs can drive the accumulation of tumorigenic mutations (Laurent et al., 2011; Merkle et al., 2017), as well as chromosomal aberrations. This was indeed the case in this study for two of the four Chrnb4-GFP generated clones. Therefore, it is highly important to establish regular quality controls, including whole genome sequencing, epigenetic markers and X-chromosome inactivation status, for PSCs and their derived products prior to transplantation.

To summarize, the results presented in this study have contributed to a better understanding of the interaction between donor and host photoreceptor cells upon transplantation. Furthermore, for the first time a new mESC line with the potential to contribute to the study of cone photoreceptor transplantation has been generated. Resources like this early cone reporter mESC line are indispensable in the field of cell replacement therapies for retinal degeneration since human vision relies mainly on cone photoreceptors.

Bibliography

Akimoto, M., Cheng, H., Zhu, D., Brzezinski, J.A., Khanna, R., Filippova, E., Oh, E.C.T., Jing, Y., Linares, J.-L., Brooks, M., et al. (2006). Targeting of GFP to newborn rods by Nrl promoter and temporal expression profiling of flow-sorted photoreceptors. PNAS *103*, 3890–3895.

Ali, M.U., Rahman, M.S.U., Cao, J., and Yuan, P.X. (2017). Genetic characterization and disease mechanism of retinitis pigmentosa; current scenario. 3 Biotech *7*, 251.

Alvarez-Dolado, M., Pardal, R., Garcia-Verdugo, J.M., Fike, J.R., Lee, H.O., Pfeffer, K., Lois, C., Morrison, S.J., and Alvarez-Buylla, A. (2003). Fusion of bone-marrow-derived cells with Purkinje neurons, cardiomyocytes and hepatocytes. Nature *425*, 968–973.

Ambati, J., and Fowler, B.J. (2012). Mechanisms of Age-Related Macular Degeneration. Neuron *75*, 26–39.

Assawachananont, J., Mandai, M., Okamoto, S., Yamada, C., Eiraku, M., Yonemura, S., Sasai, Y., and Takahashi, M. (2014). Transplantation of Embryonic and Induced Pluripotent Stem Cell-Derived 3D Retinal Sheets into Retinal Degenerative Mice. Stem Cell Reports *2*, 662–674.

Baden, T., Berens, P., Franke, K., Rosón, M.R., Bethge, M., and Euler, T. (2016). The functional diversity of retinal ganglion cells in the mouse. Nature *529*, 345–350.

Bailey, C., N, J., Sobrin, L., Pericak-Vance, M.A., Haines, J.L., Hammond, C.J., and Wiggs, J.L. (2013). Advances in the genomics of common eye diseases. Hum Mol Genet *22*, R59–R65.

Bainbridge, J.W.B., Smith, A.J., Barker, S.S., Robbie, S., Henderson, R., Balaggan, K., Viswanathan, A., Holder, G.E., Stockman, A., Tyler, N., et al. (2008). Effect of Gene Therapy on Visual Function in Leber's Congenital Amaurosis. New England Journal of Medicine *358*, 2231–2239.

Bainbridge, J.W.B., Mehat, M.S., Sundaram, V., Robbie, S.J., Barker, S.E., Ripamonti, C., Georgiadis, A., Mowat, F.M., Beattie, S.G., Gardner, P.J., et al. (2015). Long-Term Effect of Gene Therapy on Leber's Congenital Amaurosis. New England Journal of Medicine *372*, 1887–1897.

Bakondi, B., Lv, W., Lu, B., Jones, M.K., Tsai, Y., Kim, K.J., Levy, R., Akhtar, A.A., Breunig, J.J., Svendsen, C.N., et al. (2016). In Vivo CRISPR/Cas9 Gene Editing Corrects Retinal

Dystrophy in the S334ter-3 Rat Model of Autosomal Dominant Retinitis Pigmentosa. Molecular Therapy *24*, 556–563.

Ballios, B.G., Cooke, M.J., van der Kooy, D., and Shoichet, M.S. (2010). A hydrogel-based stem cell delivery system to treat retinal degenerative diseases. Biomaterials *31*, 2555–2564.

Banin, E., Obolensky, A., Idelson, M., Hemo, I., Reinhardtz, E., Pikarsky, E., Ben-Hur, T., and Reubinoff, B. (2006). Retinal Incorporation and Differentiation of Neural Precursors Derived from Human Embryonic Stem Cells. STEM CELLS *24*, 246–257.

Barber, A.C., Hippert, C., Duran, Y., West, E.L., Bainbridge, J.W.B., Warre-Cornish, K., Luhmann, U.F.O., Lakowski, J., Sowden, J.C., Ali, R.R., et al. (2013). Repair of the degenerate retina by photoreceptor transplantation. PNAS *110*, 354–359.

Barnea-Cramer, A.O., Wang, W., Lu, S.-J., Singh, M.S., Luo, C., Huo, H., McClements, M.E., Barnard, A.R., MacLaren, R.E., and Lanza, R. (2016). Function of human pluripotent stem cell-derived photoreceptor progenitors in blind mice. Scientific Reports *6*, 29784.

Bartsch, U., Oriyakhel, W., Kenna, P.F., Linke, S., Richard, G., Petrowitz, B., Humphries, P., Farrar, G.J., and Ader, M. (2008). Retinal cells integrate into the outer nuclear layer and differentiate into mature photoreceptors after subretinal transplantation into adult mice. Experimental Eye Research *86*, 691–700.

Borsch, O. (2017). Donor and host photoreceptor cells engage in a novel mechanism resulting in long-term exchange of cytoplasmic material. Dissertation. Technische Universität Dresden, Fakultät Mathematik und Naturwissenschaften.

Boucherie, C., Mukherjee, S., Henckaerts, E., Thrasher, A.J., Sowden, J.C., and Ali, R.R. (2013). Brief Report: Self-Organizing Neuroepithelium from Human Pluripotent Stem Cells Facilitates Derivation of Photoreceptors. STEM CELLS *31*, 408–414.

Bringmann, A., Syrbe, S., Görner, K., Kacza, J., Francke, M., Wiedemann, P., and Reichenbach, A. (2018). The primate fovea: Structure, function and development. Progress in Retinal and Eye Research *66*, 49–84.

Brzezinski, J.A., and Reh, T.A. (2015). Photoreceptor cell fate specification in vertebrates. Development *142*, 3263–3273.

Cepko, C. (2014). Intrinsically different retinal progenitor cells produce specific types of progeny. Nature Reviews Neuroscience *15*, 615–627.

del Cerro, M. del, Gash, D.M., Rao, G.N., Notter, M.F., Wiegand, S.J., and Gupta, M. (1985). Intraocular retinal transplants. Invest. Ophthalmol. Vis. Sci. *26*, 1182–1185.

del Cerro, M., Notter, M.F.D., Wiegand, S.J., Jiang, L.Q., and del Cerro, C. (1988). Intraretinal transplantation of fluorescently labeled retinal cell suspensions. Neuroscience Letters *92*, 21–26.

del Cerro, M., Ison, J.R., Bowen, G.P., Lazar, E., and del Cerro, C. (1991). Intraretinal grafting restores visual function in light-blinded rats. NeuroReport *2*, 529.

del Cerro, M., Yeh, H.H., Marrero-Rodriguez, A., Lazar, E., and del Cerro, C. (1990). Intraocular transplantation of cell layers derived from neonatal rat retina. Brain Research *535*, 25–32.

Chan, Y.-H.M., and Marshall, W.F. (2010). Scaling properties of cell and organelle size. Organogenesis *6*, 88–96.

Chan, L., Mahajan, V.B., and Tsang, S.H. (2017). Genome Surgery and Gene Therapy in Retinal Disorders. Yale J Biol Med *90*, 523–532.

Chang, B., Hawes, N.L., Hurd, R.E., Davisson, M.T., Nusinowitz, S., and Heckenlively, J.R. (2002). Retinal degeneration mutants in the mouse. Vision Research *42*, 517–525.

Chen, H.Y., Kaya, K.D., Dong, L., and Swaroop, A. (2016b). Three-dimensional retinal organoids from mouse pluripotent stem cells mimic in vivo development with enhanced stratification and rod photoreceptor differentiation. Molecular Vision 18.

Cideciyan, A.V., Jacobson, S.G., Beltran, W.A., Sumaroka, A., Swider, M., Iwabe, S., Roman, A.J., Olivares, M.B., Schwartz, S.B., Komáromy, A.M., et al. (2013a). Human retinal gene therapy for Leber congenital amaurosis shows advancing retinal degeneration despite enduring visual improvement. PNAS *110*, E517–E525.

Cideciyan, A.V., Hufnagel, R.B., Carroll, J., Sumaroka, A., Luo, X., Schwartz, S.B., Dubra, A., Land, M., Michaelides, M., Gardner, J.C., et al. (2013b). Human Cone Visual Pigment Deletions Spare Sufficient Photoreceptors to Warrant Gene Therapy. Human Gene Therapy *24*, 993–1006.

Collin, J., Mellough, C.B., Dorgau, B., Przyborski, S., Moreno-Gimeno, I., and Lako, M. (2015). Using Zinc Finger Nuclease Technology to Generate CRX-Reporter Human Embryonic Stem Cells as a Tool to Identify and Study the Emergence of Photoreceptors Precursors During Pluripotent Stem Cell Differentiation. STEM CELLS *34*, 311–321.

Colombo, M., Raposo, G., and Théry, C. (2014). Biogenesis, Secretion, and Intercellular Interactions of Exosomes and Other Extracellular Vesicles. Annual Review of Cell and Developmental Biology *30*, 255–289.

Csordás, A. (2006). Mitochondrial Transfer Between Eukaryotic Animal Cells and Its Physiologic Role. Rejuvenation Research *9*, 450–454.

Curcio, C.A., and Johnson, M. (2013). Chapter 20 - Structure, Function, and Pathology of Bruch's Membrane. In Retina (Fifth Edition), S.J. Ryan, S.R. Sadda, D.R. Hinton, A.P. Schachat, S.R. Sadda, C.P. Wilkinson, P. Wiedemann, and A.P. Schachat, eds. (London: W.B. Saunders), pp. 465–481.

Dalkara, D., Duebel, J., and Sahel, J.-A. (2015). Gene therapy for the eye focus on mutation-independent approaches | Ovid. Curr. Opin. Neurol *60,* 28-51

Decembrini, S., Koch, U., Radtke, F., Moulin, A., and Arsenijevic, Y. (2014). Derivation of Traceable and Transplantable Photoreceptors from Mouse Embryonic Stem Cells. Stem Cell Reports *2*, 853–865.

Decembrini, S., Martin, C., Sennlaub, F., Chemtob, S., Biel, M., Samardzija, M., Moulin, A., Behar-Cohen, F., and Arsenijevic, Y. (2017). Cone Genesis Tracing by the Chrnb4-EGFP Mouse Line: Evidences of Cellular Material Fusion after Cone Precursor Transplantation. Molecular Therapy *25*, 634–653.

DiStefano, T., Chen, H.Y., Panebianco, C., Kaya, K.D., Brooks, M.J., Gieser, L., Morgan, N.Y., Pohida, T., and Swaroop, A. (2018). Accelerated and Improved Differentiation of Retinal Organoids from Pluripotent Stem Cells in Rotating-Wall Vessel Bioreactors. Stem Cell Reports *10*, 300–313.

Eberle, D., Schubert, S., Postel, K., Corbeil, D., and Ader, M. (2011). Increased Integration of Transplanted CD73-Positive Photoreceptor Precursors into Adult Mouse Retina. Invest. Ophthalmol. Vis. Sci. *52*, 6462–6471.

Eberle, D., Kurth, T., Santos-Ferreira, T., Wilson, J., Corbeil, D., and Ader, M. (2012). Outer Segment Formation of Transplanted Photoreceptor Precursor Cells. PLOS ONE *7*, e46305.

Eberle, D., Santos-Ferreira, T., Grahl, S., and Ader, M. (2014). Subretinal transplantation of MACS purified photoreceptor precursor cells into the adult mouse retina. J. Vis. Exp. *84*, e50932

Ebner, L.J.A. (2018). Characteristics of Photoreceptor Material Transfer After Sub-retinal Injections. Master Thesis. Technische Universität Dresden.

Ehinger, B., Bergström, A., Seiler, M., Aramant, R.B., Zucker, C.L., Gustavii, B., and Adolph, A.R. (1991). Ultrastructure of human retinal cell transplants with long survival times in rats. Exp. Eye Res. *53*, 447–460.

Ehlken, C., Jungmann, S., Böhringer, D., Agostini, H.T., Junker, B., and Pielen, A. (2014). Switch of anti-VEGF agents is an option for nonresponders in the treatment of AMD. Eye *28*, 538–545.

Eiraku, M., Takata, N., Ishibashi, H., Kawada, M., Sakakura, E., Okuda, S., Sekiguchi, K., Adachi, T., and Sasai, Y. (2011). Self-organizing optic-cup morphogenesis in three-dimensional culture. Nature *472*, 51–56.

Farrar, G.J., Millington-Ward, S., Chadderton, N., Humphries, P., and Kenna, P.F. (2012). Gene-based therapies for dominantly inherited retinopathies. Gene Therapy *19*, 137–144.

Fernandez, E. (2018). Development of visual Neuroprostheses: trends and challenges. Bioelectron Med *4*, 12.

Ferrari, S., Di Iorio, E., Barbaro, V., Ponzin, D., S. Sorrentino, F., and Parmeggiani, F. (2011). Retinitis Pigmentosa: Genes and Disease Mechanisms. Current Genomics *12*, 238–249.

Fritsche, L.G., Fariss, R.N., Stambolian, D., Abecasis, G.R., Curcio, C.A., and Swaroop, A. (2014). Age-Related Macular Degeneration: Genetics and Biology Coming Together. Annual Review of Genomics and Human Genetics *15*, 151–171.

Fuhrmann, S. (2010). Eye Morphogenesis and Patterning of the Optic Vesicle. Current Topics in Developmental Biology *93*, 61–84.

Gagliardi, G., Ben M'Barek, K., Chaffiol, A., Slembrouck-Brec, A., Conart, J.-B., Nanteau, C., Rabesandratana, O., Sahel, J.-A., Duebel, J., Orieux, G., et al. (2018). Characterization and Transplantation of CD73-Positive Photoreceptors Isolated from Human iPSC-Derived Retinal Organoids. Stem Cell Reports *11*, 665–680.

Gaillard, F., and Sauvé, Y. (2007). Cell-based therapy for retina degeneration: The promise of a cure. Vision Research *47*, 2815–2824.

Gelman, R., Stevenson, W., Prospero Ponce, C., Agarwal, D., and Christoforidis, J.B. (2015). Retinal Damage Induced by Internal Limiting Membrane Removal. Journal of Ophthalmology, http://dx.doi.org/10.1155/2015/939748

Ghosh, F., Bruun, A., and Ehinger, B. (1999). Graft-host connections in long-term full-thickness embryonic rabbit retinal transplants. Invest. Ophthalmol. Vis. Sci. *40*, 126–132.

Ghosh, F., Engelsberg, K., English, R.V., and Petters, R.M. (2007). Long-term neuroretinal full-thickness transplants in a large animal model of severe retinitis pigmentosa. Graefe's Archive for Clinical and Experimental Ophthalmology *245*, 835–846.

Gonzalez-Cordero, A., West, E.L., Pearson, R.A., Duran, Y., Carvalho, L.S., Chu, C.J., Naeem, A., Blackford, S.J.I., Georgiadis, A., Lakowski, J., et al. (2013). Photoreceptor precursors derived from three-dimensional embryonic stem cell cultures integrate and mature within adult degenerate retina. Nature Biotechnology *31*, 741–747.

Gonzalez-Cordero, A., Kruczek, K., Naeem, A., Fernando, M., Kloc, M., Ribeiro, J., Goh, D., Duran, Y., Blackford, S.J.I., Abelleira-Hervas, L., et al. (2017). Recapitulation of Human Retinal Development from Human Pluripotent Stem Cells Generates Transplantable Populations of Cone Photoreceptors. Stem Cell Reports *9*, 820–837.

Gordon, P.J., Yun, S., Clark, A.M., Monuki, E.S., Murtaugh, L.C., and Levine, E.M. (2013). Lhx2 Balances Progenitor Maintenance with Neurogenic Output and Promotes Competence State Progression in the Developing Retina. J Neurosci *33*, 12197–12207.

Gouras, P., Du, J., Gelanze, M., Lopez, R., Kwun, R., Kjeldbye, H., and Krebs, W. (1991a). Survival and Synapse Formation of Transplanted Rat Rods.

Gouras, P., Du, J., Gelanze, M., Kwun, R., Kjeldbye, H., and Lopez, R. (1991b). Transplantation of photoreceptors labeled with tritiated thymidine into RCS rats. Invest. Ophthalmol. Vis. Sci. *32*, 1704–1707.

Gouras, P., Du, J., Kjeldbye, H., Kwun, R., Lopez, R., and Zack, D.J. (1991c). Transplanted photoreceptors identified in dystrophic mouse retina by a transgenic reporter gene. Invest. Ophthalmol. Vis. Sci. *32*, 3167–3174.

Goureau, O., Monville, C., Chaffiol, A., Gauvain, G., Picaud, S., Duebel, J., and Sahel, J.-A. (2018). Retinal Prostheses: Other Therapies and Future Directions. In Retinal Prosthesis, (Springer, Cham), pp. 105–125.

Hartong, D.T., Berson, E.L., and Dryja, T.P. (2006). Retinitis pigmentosa. The Lancet *368*, 1795–1809.

Haverkamp, S., Grünert, U., and Wässle, H. (2000). The Cone Pedicle, a Complex Synapse in the Retina. Neuron *27*, 85–95.

Heavner, W., and Pevny, L. (2012). Eye Development and Retinogenesis. Cold Spring Harb Perspect Biol *4*, a008391.

Hiler, D., Chen, X., Hazen, J., Kupriyanov, S., Carroll, P.A., Qu, C., Xu, B., Johnson, D., Griffiths, L., Frase, S., et al. (2015). Quantification of Retinogenesis in 3D Cultures Reveals Epigenetic Memory and Higher Efficiency in iPSCs Derived from Rod Photoreceptors. Cell Stem Cell *17*, 101–115.

Hiler, D.J., Barabas, M.E., Griffiths, L.M., and Dyer, M.A. (2016). Reprogramming of mouse retinal neurons and standardized quantification of their differentiation in 3D retinal cultures. Nat. Protocols *11*, 1955–1976.

Hirami, Y., Osakada, F., Takahashi, K., Okita, K., Yamanaka, S., Ikeda, H., Yoshimura, N., and Takahashi, M. (2009). Generation of retinal cells from mouse and human induced pluripotent stem cells. Neuroscience Letters *458*, 126–131.

Hyer, J., Kuhlman, J., Afif, E., and Mikawa, T. (2003). Optic cup morphogenesis requires pre-lens ectoderm but not lens differentiation. Developmental Biology *259*, 351–363.

Ikeda, H., Osakada, F., Watanabe, K., Mizuseki, K., Haraguchi, T., Miyoshi, H., Kamiya, D., Honda, Y., Sasai, N., Yoshimura, N., et al. (2005). Generation of Rx+/Pax6+ neural retinal precursors from embryonic stem cells. PNAS *102*, 11331–11336.

Iraha, S., Tu, H.-Y., Yamasaki, S., Kagawa, T., Goto, M., Takahashi, R., Watanabe, T., Sugita, S., Yonemura, S., Sunagawa, G.A., et al. (2018). Establishment of Immunodeficient Retinal Degeneration Model Mice and Functional Maturation of Human ESC-Derived Retinal Sheets after Transplantation. Stem Cell Reports *10*, 1059–1074.

Jacobson, S.G., Cideciyan, A.V., Roman, A.J., Sumaroka, A., Schwartz, S.B., Heon, E., and Hauswirth, W.W. (2015). Improvement and Decline in Vision with Gene Therapy in Childhood Blindness. New England Journal of Medicine *372*, 1920–1926.

Jadhav, A.P., Mason, H.A., and Cepko, C.L. (2006). Notch 1 inhibits photoreceptor production in the developing mammalian retina. Development *133*, 913–923.

Jones, B.W., Kondo, M., Terasaki, H., Lin, Y., McCall, M., and Marc, R.E. (2012). Retinal remodeling. Jpn J Ophthalmol *56*, 289–306.

Jones, M.K., Lu, B., Girman, S., and Wang, S. (2017). Cell-based therapeutic strategies for replacement and preservation in retinal degenerative diseases. Progress in Retinal and Eye Research *58*, 1–27.

Joyal, J.-S., Sun, Y., Gantner, M.L., Shao, Z., Evans, L.P., Saba, N., Fredrick, T., Burnim, S., Kim, J.S., Patel, G., et al. (2016). Retinal lipid and glucose metabolism dictates angiogenesis through the lipid sensor Ffar1. Nature Medicine *22*, 439–445.

Kaewkhaw, R., Kaya, K.D., Brooks, M., Homma, K., Zou, J., Chaitankar, V., Rao, M., and Swaroop, A. (2015). Transcriptome Dynamics of Developing Photoreceptors in Three-Dimensional Retina Cultures Recapitulates Temporal Sequence of Human Cone and Rod Differentiation Revealing Cell Surface Markers and Gene Networks. Stem Cells *33*, 3504–3518.

Kaplan, H.J., Tezel, T.H., Berger, A.S., Wolf, M.L., and Priore, L.V.D. (1997). Human Photoreceptor Transplantation in Retinitis Pigmentosa: A Safety Study. Arch Ophthalmol *115*, 1168–1172.

Kemp, K., Wilkins, A., and Scolding, N. (2014). Cell fusion in the brain: two cells forward, one cell back. Acta Neuropathol *128*, 629–638.

Klassen, H.J., Ng, T.F., Kurimoto, Y., Kirov, I., Shatos, M., Coffey, P., and Young, M.J. (2004). Multipotent Retinal Progenitors Express Developmental Markers, Differentiate into Retinal Neurons, and Preserve Light-Mediated Behavior. Invest. Ophthalmol. Vis. Sci. *45*, 4167–4173.

Kolb, H., Nelson, R., Fernandez, E., and Jones, B. (1995). Webvision. [updated: 2018, accessed: 24.08.2018] URL: https://webvision.med.utah.edu/

Kruczek, K., Gonzalez-Cordero, A., Goh, D., Naeem, A., Jonikas, M., Blackford, S.J.I., Kloc, M., Duran, Y., Georgiadis, A., Sampson, R.D., et al. (2017). Differentiation and Transplantation of Embryonic Stem Cell-Derived Cone Photoreceptors into a Mouse Model of End-Stage Retinal Degeneration. Stem Cell Reports *8*, 1659–1674.

Ku, C.A., and Pennesi, M.E. (2015). Retinal gene therapy: current progress and future prospects. Expert Review of Ophthalmology *10*, 281–299.

Lakowski, J., Baron, M., Bainbridge, J., Barber, A.C., Pearson, R.A., Ali, R.R., and Sowden, J.C. (2010). Cone and rod photoreceptor transplantation in models of the childhood retinopathy Leber congenital amaurosis using flow-sorted Crx-positive donor cells. Hum Mol Genet *19*, 4545–4559.

Lakowski, J., Han, Y.-T., Pearson, R.A., Gonzalez-Cordero, A., West, E.L., Gualdoni, S., Barber, A.C., Hubank, M., Ali, R.R., and Sowden, J.C. (2011). Effective Transplantation of Photoreceptor Precursor Cells Selected Via Cell Surface Antigen Expression. Stem Cells *29*, 1391–1404.

Lakowski, J., Welby, E., Budinger, D., Marco, F.D., Foggia, V.D., Bainbridge, J.W.B., Wallace, K., Gamm, D.M., Ali, R.R., and Sowden, J.C. (2018). Isolation of Human Photoreceptor Precursors via a Cell Surface Marker Panel from Stem Cell-Derived Retinal Organoids and Fetal Retinae. STEM CELLS *36*, 709–722.

Lakowski J., Gonzalez-Cordero A., West E.L., Han Y.T., Welby E., Naeem A., Blackford S. J. I., Bainbridge J. W. B., Pearson R. A., Ali R. R. (2015). Transplantation of Photoreceptor Precursors Isolated via a Cell Surface Biomarker Panel from Embryonic Stem Cell-Derived Self-Forming Retina. STEM CELLS *33*, 2469–2482.

Lamb, T.D., Collin, S.P., and Jr, E.N.P. (2007). Evolution of the vertebrate eye: opsins, photoreceptors, retina and eye cup. Nature Reviews Neuroscience *8*, 960–976.

Lamba, D.A., Karl, M.O., Ware, C.B., and Reh, T.A. (2006). Efficient generation of retinal progenitor cells from human embryonic stem cells. PNAS *103*, 12769–12774.

Lamba, D.A., Gust, J., and Reh, T.A. (2009). Transplantation of Human Embryonic Stem Cell-Derived Photoreceptors Restores Some Visual Function in Crx-Deficient Mice. Cell Stem Cell *4*, 73–79.

Lamba, D.A., McUsic, A., Hirata, R.K., Wang, P.-R., Russell, D., and Reh, T.A. (2010). Generation, Purification and Transplantation of Photoreceptors Derived from Human Induced Pluripotent Stem Cells. PLoS ONE *5*, e8763.

Lancaster, M.A., and Knoblich, J.A. (2014). Generation of cerebral organoids from human pluripotent stem cells. Nature Protocols *9*, 2329–2340.

Laurent, L.C., Ulitsky, I., Slavin, I., Tran, H., Schork, A., Morey, R., Lynch, C., Harness, J.V., Lee, S., Barrero, M.J., et al. (2011). Dynamic Changes in the Copy Number of Pluripotency and Cell Proliferation Genes in Human ESCs and iPSCs during Reprogramming and Time in Culture. Cell Stem Cell *8*, 106–118.

Le, Y.-Z., Zheng, L., Zheng, W., Ash, J.D., Agbaga, M.-P., Zhu, M., and Anderson, R.E. (2006). Mouse opsin promoter-directed Cre recombinase expression in transgenic mice. Mol Vis *12*, 389–398.

Lin, K., and Xiao, A.Z. (2017). Quality control towards the application of induced pluripotent stem cells. Current Opinion in Genetics & Development *46*, 164–169.

Lin, B., McLelland, B.T., Mathur, A., Aramant, R.B., and Seiler, M.J. (2018). Sheets of human retinal progenitor transplants improve vision in rats with severe retinal degeneration. Experimental Eye Research *174*, 13–28.

Liu, I.S.C., Chen, J., Ploder, L., Vidgen, D., van der Kooy, D., Kalnins, V.I., and Mclnnes, R.R. (1994). Developmental expression of a novel murine homeobox gene (Chx10): Evidence for roles in determination of the neuroretina and inner nuclear layer. Neuron *13*, 377–393.

Llonch, S., Carido, M., and Ader, M. (2018). Organoid technology for retinal repair. Developmental Biology *433*, 132–143.

Lowe, A., Harris, R., Bhansali, P., Cvekl, A., and Liu, W. (2016). Intercellular Adhesion-Dependent Cell Survival and ROCK-Regulated Actomyosin-Driven Forces Mediate Self-Formation of a Retinal Organoid. Stem Cell Reports *6*, 743–756.

Lumen (2013). Vision | Boundless Biology. [updated: 2013, accessed: 05.10.2018] URL: https://courses.lumenlearning.com/boundless-biology/chapter/vision/

MacLaren, R.E., Pearson, R.A., MacNeil, A., Douglas, R.H., Salt, T.E., Akimoto, M., Swaroop, A., Sowden, J.C., and Ali, R.R. (2006). Retinal repair by transplantation of photoreceptor precursors. Nature *444*, 203–207.

Madisen, L., Zwingman, T.A., Sunkin, S.M., Oh, S.W., Zariwala, H.A., Gu, H., Ng, L.L., Palmiter, R.D., Hawrylycz, M.J., Jones, A.R., et al. (2010). A robust and high-throughput Cre reporting and characterization system for the whole mouse brain. Nature Neuroscience *13*, 133–140.

Mandai, M., Fujii, M., Hashiguchi, T., Sunagawa, G.A., Ito, S., Sun, J., Kaneko, J., Sho, J., Yamada, C., and Takahashi, M. (2017). iPSC-Derived Retina Transplants Improve Vision in rd1 End-Stage Retinal-Degeneration Mice. Stem Cell Reports *8*, 69–83.

Marc, R.E., Jones, B.W., Watt, C.B., and Strettoi, E. (2003). Neural remodeling in retinal degeneration. Progress in Retinal and Eye Research *22*, 607–655.

Masland, R.H. (2001). The fundamental plan of the retina. Nature Neuroscience *4*, 877–886.

Masland, R.H. (2012). The Neuronal Organization of the Retina. Neuron *76*, 266–280.

Mathers, P.H., Grinberg, A., Mahon, K.A., and Jamrich, M. (1997). The Rx homeobox gene is essential for vertebrate eye development. Nature *387*, 603–607.

M'Barek, K.B., Habeler, W., Plancheron, A., Jarraya, M., Regent, F., Terray, A., Yang, Y., Chatrousse, L., Domingues, S., Masson, Y., et al. (2017). Human ESC–derived retinal epithelial cell sheets potentiate rescue of photoreceptor cell loss in rats with retinal degeneration. Science Translational Medicine *9*, eaai7471.

McFarlane, L., Truong, V., Palmer, J.S., and Wilhelm, D. (2013). Novel PCR Assay for Determining the Genetic Sex of Mice. SXD *7*, 207–211.

McLelland, B.T., Lin, B., Mathur, A., Aramant, R.B., Thomas, B.B., Nistor, G., Keirstead, H.S., and Seiler, M.J. (2018). Transplanted hESC-Derived Retina Organoid Sheets Differentiate, Integrate, and Improve Visual Function in Retinal Degenerate Rats. Invest. Ophthalmol. Vis. Sci. *59*, 2586–2603.

Merkle, F.T., Ghosh, S., Kamitaki, N., Mitchell, J., Avior, Y., Mello, C., Kashin, S., Mekhoubad, S., Ilic, D., Charlton, M., et al. (2017). Human pluripotent stem cells recurrently acquire and expand dominant negative P53 mutations. Nature *545*, 229–233.

Meyer, J.S., Howden, S.E., Wallace, K.A., Verhoeven, A.D., Wright, L.S., Capowski, E.E., Pinilla, I., Martin, J.M., Tian, S., Stewart, R., et al. (2011). Optic Vesicle-like Structures Derived from Human Pluripotent Stem Cells Facilitate a Customized Approach to Retinal Disease Treatment. STEM CELLS *29*, 1206–1218.

Michaelides, M., Hunt, D.M., and Moore, A.T. (2004). The cone dysfunction syndromes. British Journal of Ophthalmology *88*, 291–297.

Michaelides, M., Hardcastle, A.J., Hunt, D.M., and Moore, A.T. (2006). Progressive Cone and Cone-Rod Dystrophies: Phenotypes and Underlying Molecular Genetic Basis. Survey of Ophthalmology *51*, 232–258.

Muranishi, Y., Terada, K., Inoue, T., Katoh, K., Tsujii, T., Sanuki, R., Kurokawa, D., Aizawa, S., Tamaki, Y., and Furukawa, T. (2011). An Essential Role for RAX Homeoprotein and NOTCH–HES Signaling in Otx2 Expression in Embryonic Retinal Photoreceptor Cell Fate Determination. J. Neurosci. *31*, 16792–16807.

Mustafi, D., Engel, A.H., and Palczewski, K. (2009). Structure of cone photoreceptors. Progress in Retinal and Eye Research *28*, 289–302.

Muzumdar, M.D., Tasic, B., Miyamichi, K., Li, L., and Luo, L. (2007). A global double-fluorescent Cre reporter mouse. Genesis *45*, 593–605.

Nakano, T., Ando, S., Takata, N., Kawada, M., Muguruma, K., Sekiguchi, K., Saito, K., Yonemura, S., Eiraku, M., and Sasai, Y. (2012). Self-Formation of Optic Cups and Storable Stratified Neural Retina from Human ESCs. Cell Stem Cell *10*, 771–785.

Nelson, B.R., Hartman, B.H., Georgi, S.A., Lan, M.S., and Reh, T.A. (2007). Transient inactivation of Notch signaling synchronizes differentiation of neural progenitor cells. Developmental Biology *304*, 479–498.

Nickerson, P.E.B., Ortin-Martinez, A., and Wallace, V.A. (2018). Material Exchange in Photoreceptor Transplantation: Updating Our Understanding of Donor/Host Communication and the Future of Cell Engraftment Science. Front. Neural Circuits *12*.

Nishida, A., Furukawa, A., Koike, C., Tano, Y., Aizawa, S., Matsuo, I., and Furukawa, T. (2003). *Otx2* homeobox gene controls retinal photoreceptor cell fate and pineal gland development. Nature Neuroscience *6*, 1255–1263.

Ohlemacher, S.K., Iglesias, C.L., Sridhar, A., Gamm, D.M., and Meyer, J.S. (2015). Generation of Highly Enriched Populations of Optic Vesicle−Like Retinal Cells from Human Pluripotent Stem Cells. In Current Protocols in Stem Cell Biology, (John Wiley & Sons, Inc.), p.

Okabe, M., Ikawa, M., Kominami, K., Nakanishi, T., and Nishimune, Y. (1997). `Green mice' as a source of ubiquitous green cells. FEBS Letters *407*, 313–319.

Ortín-Martínez, A., Nadal-Nicolás, F.M., Jiménez-López, M., Alburquerque-Béjar, J.J., Nieto-López, L., García-Ayuso, D., Villegas-Pérez, M.P., Vidal-Sanz, M., and Agudo-Barriuso, M. (2014). Number and Distribution of Mouse Retinal Cone Photoreceptors: Differences between an Albino (Swiss) and a Pigmented (C57/BL6) Strain. PLOS ONE *9*, e102392.

Ortin-Martinez, A., Tsai, E.L.S., Nickerson, P.E., Bergeret, M., Lu, Y., Smiley, S., Comanita, L., and Wallace, V.A. (2017). A Reinterpretation of Cell Transplantation: GFP Transfer From Donor to Host Photoreceptors. STEM CELLS *35*, 932–939.

Osakada, F., Ikeda, H., Mandai, M., Wataya, T., Watanabe, K., Yoshimura, N., Akaike, A., Sasai, Y., and Takahashi, M. (2008). Toward the generation of rod and cone

photoreceptors from mouse, monkey and human embryonic stem cells. Nature Biotechnology *26*, 215–224.

Otto, O., Rosendahl, P., Mietke, A., Golfier, S., Herold, C., Klaue, D., Girardo, S., Pagliara, S., Ekpenyong, A., Jacobi, A., et al. (2015). Real-time deformability cytometry: on-the-fly cell mechanical phenotyping. Nature Methods *12*, 199–202.

Ovando-Roche, P., West, E.L., Branch, M.J., Sampson, R.D., Fernando, M., Munro, P., Georgiadis, A., Rizzi, M., Kloc, M., Naeem, A., et al. (2018). Use of bioreactors for culturing human retinal organoids improves photoreceptor yields. Stem Cell Research & Therapy *9*, 156.

Pearson, R.A., Barber, A.C., Rizzi, M., Hippert, C., Xue, T., West, E.L., Duran, Y., Smith, A.J., Chuang, J.Z., Azam, S.A., et al. (2012). Restoration of vision after transplantation of photoreceptors. Nature *485*, 99–103.

Pearson, R.A., Gonzalez-Cordero, A., West, E.L., Ribeiro, J.R., Aghaizu, N., Goh, D., Sampson, R.D., Georgiadis, A., Waldron, P.V., Duran, Y., et al. (2016). Donor and host photoreceptors engage in material transfer following transplantation of post-mitotic photoreceptor precursors. Nature Communications *7*, 13029.

Pham, A.H., McCaffery, J.M., and Chan, D.C. (2012). Mouse lines with photo-activatable mitochondria to study mitochondrial dynamics. Genesis *50*, 833–843.

Phillips, M.J., Capowski, E.E., Petersen, A., Jansen, A.D., Barlow, K., Edwards, K.L., and Gamm, D.M. (2018). Generation of a rod-specific NRL reporter line in human pluripotent stem cells. Scientific Reports *8*, 2370.

Porter, F.D., Drago, J., Xu, Y., Cheema, S.S., Wassif, C., Huang, S.P., Lee, E., Grinberg, A., Massalas, J.S., Bodine, D., et al. (1997). Lhx2, a LIM homeobox gene, is required for eye, forebrain, and definitive erythrocyte development. Development *124*, 2935–2944.

Pritchard, C.D., Arnér, K.M., Langer, R.S., and Ghosh, F.K. (2010). Retinal transplantation using surface modified poly(glycerol-co-sebacic acid) membranes. Biomaterials *31*, 7978–7984.

Quadrato, G., Nguyen, T., Macosko, E.Z., Sherwood, J.L., Yang, S.M., Berger, D., Maria, N., Scholvin, J., Goldman, M., Kinney, J., et al. (2017). Cell diversity and network dynamics in photosensitive human brain organoids. Nature *545*, 48–53.

Radtke, N.D., Aramant, R.B., Seiler, M., and Petry, H.M. (1999). Preliminary report: indications of improved visual function after retinal sheet transplantation in retinitis pigmentosa patients11Norman D. Radtke, MD, Robert B. Aramant, PhD, and Magdalene Seiler, PhD, have a proprietary interest in the instrument and method (patent pending) discussed. American Journal of Ophthalmology *128*, 384–387.

Radtke, N.D., Seiler, M.J., Aramant, R.B., Petry, H.M., and Pidwell, D.J. (2002). Transplantation of intact sheets of fetal neural retina with its retinal pigment epithelium in retinitis pigmentosa patients. American Journal of Ophthalmology *133*, 544–550.

Radtke, N.D., Aramant, R.B., Seiler, M.J., Petry, H.M., and Pidwell, D. (2004). Vision Change After Sheet Transplant of Fetal Retina With Retinal PigmentEpithelium to a Patient With Retinitis Pigmentosa. Arch Ophthalmol *122*, 1159–1165.

Radtke, N.D., Aramant, R.B., Petry, H.M., Green, P.T., Pidwell, D.J., and Seiler, M.J. (2008). Vision Improvement in Retinal Degeneration Patients by Implantation of Retina Together with Retinal Pigment Epithelium. American Journal of Ophthalmology *146*, 172–182.e1.

Redenti, S., Tao, S., Yang, J., Gu, P., Klassen, H., Saigal, S., Desai, T., and Young, M.J. (2008). Retinal tissue engineering using mouse retinal progenitor cells and a novel biodegradable, thin-film poly(e-caprolactone) nanowire scaffold. J Ocul Biol Dis Inform *1*, 19–29.

Redenti, S., Neeley, W.L., Rompani, S., Saigal, S., Yang, J., Klassen, H., Langer, R., and Young, M.J. (2009). Engineering retinal progenitor cell and scrollable poly(glycerol-sebacate) composites for expansion and subretinal transplantation. Biomaterials *30*, 3405–3414.

Reh, T.A. (2013). Chapter 13 - The Development of the Retina. In Retina (Fifth Edition), S.J. Ryan, S.R. Sadda, D.R. Hinton, A.P. Schachat, S.R. Sadda, C.P. Wilkinson, P. Wiedemann, and A.P. Schachat, eds. (London: W.B. Saunders), pp. 330–341.

Reichman, S., Slembrouck Amélie, Gagliardi Giuliana, Chaffiol Antoine, Terray Angélique, Nanteau Céline, Potey Anais, Belle Morgane, Rabesandratana Oriane, Duebel Jens, et al. (2017). Generation of Storable Retinal Organoids and Retinal Pigmented Epithelium from Adherent Human iPS Cells in Xeno-Free and Feeder-Free Conditions. STEM CELLS *35*, 1176–1188.

RetNet (1996). RetNet: Summaries. [updated: 18.09.2018, accessed: 05.10.2018] URL: https://sph.uth.edu/retnet/sum-dis.htm#A-genes

Rodieck, R.W. (1998). The First Steps in Seeing (Sinauer Associates, Inc).

Rofagha, S., Bhisitkul, R.B., Boyer, D.S., Sadda, S.R., and Zhang, K. (2013). Seven-Year Outcomes in Ranibizumab-Treated Patients in ANCHOR, MARINA, and HORIZON: A Multicenter Cohort Study (SEVEN-UP). Ophthalmology *120*, 2292–2299.

Rowan, S., and Cepko, C.L. (2004). Genetic analysis of the homeodomain transcription factor Chx10 in the retina using a novel multifunctional BAC transgenic mouse reporter. Developmental Biology *271*, 388–402.

Saari, J.C. (2012). Vitamin A Metabolism in Rod and Cone Visual Cycles. Annu. Rev. Nutr. *32*, 125–145.

Samson, M., Emerson, M.M., and Cepko, C.L. (2009). Robust marking of photoreceptor cells and pinealocytes with several reporters under control of the Crx gene. Developmental Dynamics *238*, 3218–3225.

Sanes, J.R., and Masland, R.H. (2015). The Types of Retinal Ganglion Cells: Current Status and Implications for Neuronal Classification. Annual Review of Neuroscience *38*, 221–246.

Santos-Ferreira, T., Postel, K., Stutzki, H., Kurth, T., Zeck, G., and Ader, M. (2015). Daylight Vision Repair by Cell Transplantation. Stem Cells *33*, 79–90.

Santos-Ferreira, T., Völkner, M., Borsch, O., Haas, J., Cimalla, P., Vasudevan, P., Carmeliet, P., Corbeil, D., Michalakis, S., Koch, E., et al. (2016a). Stem Cell–Derived Photoreceptor Transplants Differentially Integrate Into Mouse Models of Cone-Rod Dystrophy. Invest. Ophthalmol. Vis. Sci. *57*, 3509–3520.

Santos-Ferreira, T., Llonch, S., Borsch, O., Postel, K., Haas, J., and Ader, M. (2016b). Retinal transplantation of photoreceptors results in donor–host cytoplasmic exchange. Nature Communications *7*, 13028.

Santos-Ferreira, T.F., Borsch, O., and Ader, M. (2017). Rebuilding the Missing Part—A Review on Photoreceptor Transplantation. Front. Syst. Neurosci. *10*.

Sato, S., Omori, Y., Katoh, K., Kondo, M., Kanagawa, M., Miyata, K., Funabiki, K., Koyasu, T., Kajimura, N., Miyoshi, T., et al. (2008). Pikachurin, a dystroglycan ligand, is essential for photoreceptor ribbon synapse formation. Nature Neuroscience *11*, 923–931.

Scholl, H.P.N., Strauss, R.W., Singh, M.S., Dalkara, D., Roska, B., Picaud, S., and Sahel, J.-A. (2016). Emerging therapies for inherited retinal degeneration. Science Translational Medicine *8*, 368rv6-368rv6.

Seiler, M.J., and Aramant, R.B. (1998). Intact sheets of fetal retina transplanted to restore damaged rat retinas. Invest. Ophthalmol. Vis. Sci. *39*, 2121–2131.

Seitz, I.P., Michalakis, S., Wilhelm, B., Reichel, F.F., Ochakovski, G.A., Zrenner, E., Ueffing, M., Biel, M., Wissinger, B., Bartz-Schmidt, K.U., et al. (2017). Superior Retinal Gene Transfer and Biodistribution Profile of Subretinal Versus Intravitreal Delivery of AAV8 in Nonhuman Primates. Invest. Ophthalmol. Vis. Sci. *58*, 5792–5801.

Shirai, H., Mandai, M., Matsushita, K., Kuwahara, A., Yonemura, S., Nakano, T., Assawachananont, J., Kimura, T., Saito, K., Terasaki, H., et al. (2016). Transplantation of human embryonic stem cell-derived retinal tissue in two primate models of retinal degeneration. PNAS *113*, E81–E90.

Siegert, S., Scherf, B.G., Del Punta, K., Didkovsky, N., Heintz, N., and Roska, B. (2009). Genetic address book for retinal cell types. Nature Neuroscience *12*, 1197–1204.

Silverman, M.S., and Hughes, S.E. (1989). Transplantation of photoreceptors to light-damaged retina. Invest. Ophthalmol. Vis. Sci. *30*, 1684–1690.

Singh, M.S., Issa, P.C., Butler, R., Martin, C., Lipinski, D.M., Sekaran, S., Barnard, A.R., and MacLaren, R.E. (2013a). Reversal of end-stage retinal degeneration and restoration of visual function by photoreceptor transplantation. PNAS *110*, 1101–1106.

Singh, M.S., Aslam, S.A., Duncan, I.L., Cramer, A.O., Barnard, A.R., and MacLaren, R.E. (2014). Cell fusion following photoreceptor transplantation into the non-degenerate retina. Invest. Ophthalmol. Vis. Sci. *55*, 3989–3989.

Singh, M.S., Balmer, J., Barnard, A.R., Aslam, S.A., Moralli, D., Green, C.M., Barnea-Cramer, A., Duncan, I., and MacLaren, R.E. (2016). Transplanted photoreceptor precursors transfer proteins to host photoreceptors by a mechanism of cytoplasmic fusion. Nature Communications *7*, 13537.

Singh, R., Phillips, M.J., Kuai, D., Meyer, J., Martin, J.M., Smith, M.A., Perez, E.T., Shen, W., Wallace, K.A., Capowski, E.E., et al. (2013b). Functional analysis of serially expanded human iPS cell-derived RPE cultures. Investigative Ophthalmology & Visual Science *54*, 6767–6778.

Smiley, S., Nickerson, P.E., Comanita, L., Daftarian, N., El-Sehemy, A., Tsai, E.L.S., Matan-Lithwick, S., Yan, K., Thurig, S., Touahri, Y., et al. (2016). Establishment of a cone photoreceptor transplantation platform based on a novel cone-GFP reporter mouse line. Scientific Reports *6*, 22867.

Solovei, I. (2010). Fluorescence in situ Hybridization (FISH) on Tissue Cryosections. In Fluorescence in Situ Hybridization (FISH), J.M. Bridger, and E.V. Volpi, eds. (Totowa, NJ: Humana Press), pp. 71–82.

Spees, J.L., Olson, S.D., Whitney, M.J., and Prockop, D.J. (2006). Mitochondrial transfer between cells can rescue aerobic respiration. PNAS *103*, 1283–1288.

Stanescu, D., Iseli, H.P., Schwerdtfeger, K., Ittner, L.M., Remé, C.E., and Hafezi, F. (2007). Continuous expression of the homeobox gene Pax6 in the ageing human retina. Eye *21*, 90–93.

Steedman, M.R., Tao, S.L., Klassen, H., and Desai, T.A. (2010). Enhanced differentiation of retinal progenitor cells using microfabricated topographical cues. Biomed Microdevices *12*, 363–369.

Stingl, K., Schippert, R., Bartz-Schmidt, K.U., Besch, D., Cottriall, C.L., Edwards, T.L., Gekeler, F., Greppmaier, U., Kiel, K., Koitschev, A., et al. (2017). Interim Results of a Multicenter Trial with the New Electronic Subretinal Implant Alpha AMS in 15 Patients Blind from Inherited Retinal Degenerations. Front. Neurosci. *11*.

Strettoi, E. (2015). A Survey of Retinal Remodeling. Front Cell Neurosci *9*.

Swaroop, A., Kim, D., and Forrest, D. (2010). Transcriptional regulation of photoreceptor development and homeostasis in the mammalian retina. Nature Reviews Neuroscience *11*, 563–576.

Takahashi, K., Tanabe, K., Ohnuki, M., Narita, M., Ichisaka, T., Tomoda, K., and Yamanaka, S. (2007). Induction of Pluripotent Stem Cells from Adult Human Fibroblasts by Defined Factors. Cell *131*, 861–872.

Takahashi, V.K.L., Takiuti, J.T., Jauregui, R., and Tsang, S.H. (2018). Gene therapy in inherited retinal degenerative diseases, a review. Ophthalmic Genetics *0*, 1–9.

Terada, N., Hamazaki, T., Oka, M., Hoki, M., Mastalerz, D.M., Nakano, Y., Meyer, E.M., Morel, L., Petersen, B.E., and Scott, E.W. (2002). Bone marrow cells adopt the phenotype of other cells by spontaneous cell fusion. Nature *416*, 542–545.

Thomson, J.A., Itskovitz-Eldor, J., Shapiro, S.S., Waknitz, M.A., Swiergiel, J.J., Marshall, V.S., and Jones, J.M. (1998). Embryonic Stem Cell Lines Derived from Human Blastocysts. Science *282*, 1145–1147.

Tikidji-Hamburyan, A., Reinhard, K., Storchi, R., Dietter, J., Seitter, H., Davis, K.E., Idrees, S., Mutter, M., Walmsley, L., Bedford, R.A., et al. (2017). Rods progressively escape saturation to drive visual responses in daylight conditions. Nature Communications *8*, 1813.

Tsin, A., Betts-Obregon, B., and Grigsby, J. (2018). Visual cycle proteins: Structure, function, and roles in human retinal disease. J. Biol. Chem. *293*, 13016–13021.

Tucker, B.A., Redenti, S.M., Jiang, C., Swift, J.S., Klassen, H.J., Smith, M.E., Wnek, G.E., and Young, M.J. (2010). The use of progenitor cell/biodegradable MMP2–PLGA polymer constructs to enhance cellular integration and retinal repopulation. Biomaterials *31*, 9–19.

Valadi, H., Ekström, K., Bossios, A., Sjöstrand, M., Lee, J.J., and Lötvall, J.O. (2007). Exosome-mediated transfer of mRNAs and microRNAs is a novel mechanism of genetic exchange between cells. Nature Cell Biology *9*, 654–659.

Veleri, S., Lazar, C.H., Chang, B., Sieving, P.A., Banin, E., and Swaroop, A. (2015). Biology and therapy of inherited retinal degenerative disease: insights from mouse models. Disease Models & Mechanisms *8*, 109–129.

Vergara, M.N., Flores-Bellver, M., Aparicio-Domingo, S., McNally, M., Wahlin, K.J., Saxena, M.T., Mumm, J.S., and Canto-Soler, M.V. (2017). Three-dimensional automated reporter quantification (3D-ARQ) technology enables quantitative screening in retinal organoids. Development *144*, 3698–3705.

Völkner, M., Zschätzsch, M., Rostovskaya, M., Overall, R.W., Busskamp, V., Anastassiadis, K., and Karl, M.O. (2016). Retinal Organoids from Pluripotent Stem Cells Efficiently Recapitulate Retinogenesis. Stem Cell Reports *6*, 525–538.

Volland, S., Esteve-Rudd, J., Hoo, J., Yee, C., and Williams, D.S. (2015). A Comparison of Some Organizational Characteristics of the Mouse Central Retina and the Human Macula. PLoS One *10*.

Wahlin, K.J., Maruotti, J.A., Sripathi, S.R., Ball, J., Angueyra, J.M., Kim, C., Grebe, R., Li, W., Jones, B.W., and Zack, D.J. (2017). Photoreceptor Outer Segment-like Structures in Long-Term 3D Retinas from Human Pluripotent Stem Cells. Scientific Reports *7*, 766.

Waldron, P.V., Di Marco, F., Kruczek, K., Ribeiro, J., Graca, A.B., Hippert, C., Aghaizu, N.D., Kalargyrou, A.A., Barber, A.C., Grimaldi, G., et al. (2018). Transplanted Donor- or Stem Cell-Derived Cone Photoreceptors Can Both Integrate and Undergo Material Transfer in an Environment-Dependent Manner. Stem Cell Reports.

Walther, C., and Gruss, P. (1991). Pax-6, a murine paired box gene, is expressed in the developing CNS. Development *113*, 1435–1449.

Wataya, T., Ando, S., Muguruma, K., Ikeda, H., Watanabe, K., Eiraku, M., Kawada, M., Takahashi, J., Hashimoto, N., and Sasai, Y. (2008). Minimization of exogenous signals in ES cell culture induces rostral hypothalamic differentiation. PNAS *105*, 11796–11801.

Welby, E., Lakowski, J., Foggia, V.D., Budinger, D., Gonzalez-Cordero, A., Lun, A.T.L., Epstein, M., Patel, A., Cuevas, E., Kruczek, K., et al. (2017). Isolation and Comparative Transcriptome Analysis of Human Fetal and iPSC-Derived Cone Photoreceptor Cells. Stem Cell Reports *0*.

West, E.L., Pearson Rachael A., Barker Susie E., Luhmann Ulrich F.O., Maclaren Robert E., Barber Amanda C., Duran Yanai, Smith Alexander J., Sowden Jane C., and Ali Robin R. (2010). Long-Term Survival of Photoreceptors Transplanted into the Adult Murine Neural Retina Requires Immune Modulation. STEM CELLS *28*, 1997–2007.

West, E.L., Gonzalez-Cordero Anai, Hippert Claire, Osakada Fumitaka, Martinez-Barbera Juan Pedro, Pearson Rachael A., Sowden Jane C., Takahashi Masayo, and Ali Robin R. (2012). Defining the Integration Capacity of Embryonic Stem Cell-Derived Photoreceptor Precursors. STEM CELLS *30*, 1424–1435.

WHO (2017). Blindness and visual impairment. [updated: 11.10.2017, accessed: 05.10.2018] URL: http://www.who.int/news-room/fact-sheets/detail/blindness-and-visual-impairment

Wiley, L.A., Burnight, E.R., DeLuca, A.P., Anfinson, K.R., Cranston, C.M., Kaalberg, E.E., Penticoff, J.A., Affatigato, L.M., Mullins, R.F., Stone, E.M., et al. (2016). cGMP production of patient-specific iPSCs and photoreceptor precursor cells to treat retinal degenerative blindness. Scientific Reports *6*, 30742.

Wittig, D., Wang, X., Walter, C., Gerdes, H.-H., Funk, R.H.W., and Roehlecke, C. (2012). Multi-Level Communication of Human Retinal Pigment Epithelial Cells via Tunneling Nanotubes. PLOS ONE *7*, e33195.

Ying, Q.-L., Nichols, J., Evans, E.P., and Smith, A.G. (2002). Changing potency by spontaneous fusion. Nature *416*, 545–548.

Yoshimatsu, T., Suzuki, S., and Wong, R.O.L. (2013). Circuit Assembly in the Developing Vertebrate Retina. In Cellular Migration and Formation of Neuronal Connections, (Elsevier), pp. 791–809.

Zagozewski, J.L., Zhang, Q., Pinto, V.I., Wigle, J.T., and Eisenstat, D.D. (2014). The role of homeobox genes in retinal development and disease. Developmental Biology *393*, 195–208.

Zhao, X., Liu, J., and Ahmad, I. (2002). Differentiation of embryonic stem cells into retinal neurons. Biochemical and Biophysical Research Communications *297*, 177–184.

Zhong, X., Gutierrez, C., Xue, T., Hampton, C., Vergara, M.N., Cao, L.-H., Peters, A., Park, T.S., Zambidis, E.T., Meyer, J.S., et al. (2014a). Generation of three-dimensional retinal tissue with functional photoreceptors from human iPSCs. Nature Communications *5*.

Zhong, X., Gutierrez, C., Xue, T., Hampton, C., Vergara, M.N., Cao, L.-H., Peters, A., Park, T.S., Zambidis, E.T., Meyer, J.S., et al. (2014b). Generation of three-dimensional retinal tissue with functional photoreceptors from human iPSCs. Nature Communications *5*, 4047.

Zhou, J., Benito-Martin, A., Mighty, J., Chang, L., Ghoroghi, S., Wu, H., Wong, M., Guariglia, S., Baranov, P., Young, M., et al. (2018). Retinal progenitor cells release extracellular vesicles containing developmental transcription factors, microRNA and membrane proteins. Scientific Reports *8*, 2823.

Zhou, S., Flamier, A., Abdouh, M., Tétreault, N., Barabino, A., Wadhwa, S., and Bernier, G. (2015). Differentiation of human embryonic stem cells into cone photoreceptors through simultaneous inhibition of BMP, TGFβ and Wnt signaling. Development *142*, 3294–3306.

Zhu, J., Reynolds, J., Garcia, T., Cifuentes, H., Chew, S., Zeng, X., and Lamba, D.A. (2018). Generation of Transplantable Retinal Photoreceptors from a Current Good Manufacturing Practice-Manufactured Human Induced Pluripotent Stem Cell Line. STEM CELLS Translational Medicine *7*, 210–219.

Zhu, X., Li, A., Brown, B., Weiss, E.R., Osawa, S., and Craft, C.M. (2002). Mouse cone arrestin expression pattern: Light induced transloca- tion in cone photoreceptors. Molecular Vision 10.

Appendix 1

Technische Univeristät Dresden
Medizinische Fakultät Carl Gustav Carus
Promotionsordnung vom 24. Juli 2011

Erklärungen zur Eröffnung des Promotionsverfahrens

1. Hiermit versichere ich, dass ich die vorliegende Arbeit ohne unzulässige Hilfe Dritter und ohne Benutzung anderer als der angegebenen Hilfsmittel angefertigt habe; die aus fremden Quellen direkt oder indirekt übernommenen Gedanken sind als solche kenntlich gemacht.

2. Bei der Auswahl und Auswertung des Materials sowie bei der Herstellung des Manuskripts habe ich Unterstützungsleistungen von folgenden Personen erhalten:

.....
.....
.....

3. Weitere Personen waren an der geistigen Herstellung der vorliegenden Arbeit nicht beteiligt. Insbesondere habe ich nicht die Hilfe eines kommerziellen Promotionsberaters in Anspruch genommen. Dritte haben von mir weder unmittelbar noch mittelbar geldwerte Leistungen für Arbeiten erhalten, die im Zusammenhang mit dem Inhalt der vorgelegten Dissertation stehen.

4. Die Arbeit wurde bisher weder im Inland noch im Ausland in gleicher oder ähnlicher Form einer anderen Prüfungsbehörde vorgelegt.

5. Die Inhalte dieser Dissertation wurden in folgender Form veröffentlicht:

Santos-Ferreira T*, **Llonch S***, Borsch O* et al. 2016. Retinal transplantation of photoreceptors results in donor-host cytoplasmic exchange. *Nat. Comms* 7:13028.

6. Ich bestätige, dass es keine zurückliegenden erfolglosen Promotionsverfahren gab.

.....

7. Ich bestätige, dass ich die Promotionsordnung der Medizinischen Fakultät der Technischen Universität Dresden anerkenne.

8. Ich habe die Zitierrichtlinien für Dissertationen an der Medizinischen Fakultät der Technischen Universität Dresden zur Kenntnis genommen und befolgt.

Ort, Datum

Unterschrift des Doktoranden

Appendix 2

Hiermit bestätige ich die Einhaltung der folgenden aktuellen gesetzlichen Vorgaben im Rahmen meiner Dissertation

Das zustimmende Votum der Ethikkommission bei Klinischen Studien, epidemiologischen Untersuchungen mit Personenbezug oder Sachverhalten, die das Medizinproduktegesetz betreffen

Aktenzeichen der zuständigen Ethikkommission:

.....

die Einhaltung der Bestimmungen des Tierschutzgesetzes

Aktenzeichen der Genehmigungsbehörde zum Vorhaben/zur Mitwirkung:

.....

die Einhaltung des Gentechnikgesetzes

Projektnummert number:

.....

die Einhaltung von Datenschutzbestimmungen der Medizinischen Fakultät und des Universitätsklinikums Carl Gustav Carus.

Ort, Datum

Unterschrift des Doktoranden